

Dear Editor,

We are grateful to for the thorough comments and helpful suggestions. We have responded in full to all comments, with the original comment show below and out reply and action shown in **bold**. Quoted line numbers refer to the line numbers in the tracked changes manuscript (appended to the bottom of this document).

Yours sincerely,
Tom Holding and co-authors.

Response to Mario Hoppema's comments

General Comments

My general comment to the manuscript is that in some places, the toolbox is kind of described as if the authors would like to sell something. Also, it sometimes feels as if reading a manual. I realize that the subject of the paper sometimes rather coerces to such writing, but possibly the authors can avoid it to some extent. Please go through the text and consider where such text can be improved. **All text has been reviewed for improvements (changes throughout the text). We have removed several links to the Github page and consolidated this information in 6 (Code Availability). Section 1 has been made more concise by considerably shortening the description of previous and on-going projects that utilise FluxEngine.**

Specific comments

L26 „the biogeochemical development“ I find this a strange combination. Any better wording?

Thank you, we have updated this sentence (line 26-27).

L27-28 “to monitor the health of the oceans” I think speaking of health in this context is not scientifically objective, and not necessary here. Please use other wording.

This sentence has been re-worded to be more explicit in our meaning (lines 28-29).

L31 delete: and the toolbox is already being used by scientists across multiple disciplines (this is not info for a scientific paper)

Done (line 31)

L74 Shutler et al. (2016) and Woolf et al. (2016). (format)

Done (line 78)

L76 ... by Woolf et al. (2016) and ... (format)

Done (line 80).

L86-87 (e.g., Ho et al., 2006; Nightingale et al., 2000; Wanninkhof, 2014).
(format)

Done (lines 98-99)

L110-111 “and broadened the range of possible applications to which it can be applied.” Delete “to which it can be applied” because this does not add any info.

Done (line 122).

L165 Suggested: ... with the reference data published in Holding et al. (2018).

Done, thank you (Appendix D, line 880).

§2.1 While I was reading this, it felt like reading a manual. Although this part of the manuscript contains important information, I think a large part should be transferred to the supplementary material or appendix, as this is not the kind of info for a scientific paper. Please consider how best to do this.

The technical details have been removed and placed in Appendix D. Section 2.1 now gives a short overview, with reader being directed to Section 10 (Appendix D) for the specific details on the location of installation scripts, the verification options (and datasets used) and benchmarking information.

L273 Goddijn-Murphy (typo)

Thank you, this has been corrected (line 375).

L354-356 “It is advisable to always use the most up-to-date version of FluxEngine which can be found via <http://github.com/oceanfluxghg/FluxEngine>.” This is not a sentence that belongs in a scientific paper.

We have removed this sentence as well as the link to the releases page. Instead we directed the reader to the code availability section (sect. 6) (lines 483-484).

L464-465 from 28 January 2015 to 9 September 2015 (format)

Done (line 607).

Fig.5 The units of xCO₂ and fCO₂ contain strange symbols, please correct.

Thank you. This has been corrected.

L531 ... of Nightingale et al. (2000) ... (format)

Done (line 677)

L532 from Pereira et al. (2018). (format)

Done (line 679)

L622 Zappa et al. (2007) (typo)

Done (line 718)

L685 Datasets used: SOCAT is not listed here. Is there any reason for that?

While the individual SOCAT cruises uses in case study one were listed, the entry for the interpolated collated SOCAT dataset used in case study 4 was missing. We have now added references to the methodology used to produce this dataset, the dataset download and original SOCAT dataset (see the last row of table 3, Appendix B).

L831 pages: 1937-1949
Done (line 1034).

The FluxEngine air-sea gas flux toolbox: simplified interface and extensions for *in situ* analyses and multiple sparingly soluble gases

5 Thomas Holding¹, Ian G. Ashton¹, Jamie D. Shutler¹, Peter E. Land², Philip D. Nightingale², Andrew P. Rees², Ian Brown², Jean-Francois Piolle³, Annette Kock⁴, Hermann W Bange⁴, David K. Woolf⁵, Lonneke Goddijn-Murphy⁶, Ryan Pereira⁷, Frederic Paul³, Fanny Girard-Ardhuin³, Bertrand Chapron³, Gregor Rehder⁸, Fabrice Ardhuin³, Craig J. Donlon⁹

- 10 ¹University of Exeter, Penryn Campus, Cornwall, TR10 9EZ, UK.
- ²Plymouth Marine Laboratory, Prospect Place, Plymouth, PL1 3DH, UK.
- ³Ifremer, Univ. Brest, CNRS, IRD, Laboratoire d’Oceanographie Physique et Spatiale (LOPS), IUEM, Brest, France.
- ⁴GEOMAR Helmholtz Centre for Ocean Research Kiel, Marine Biogeochemistry Research Division, 24105 Kiel, Germany.
- 15 ⁵International Centre for Island Technology, Heriot-Watt University, Stromness, Orkney, KW16 3AW, UK.
- ⁶Environmental Research Institute, University of the Highlands and Islands, Thurso, KW14 7EE, UK
- ⁷The Lyell Centre, Heriot-Watt University, Research Avenue South, Edinburgh, EH14 4AS, UK.
- ⁸Leibniz-Institute for Baltic Sea Research Warnemünde, 18119 Rostock, Germany.
- 20 ⁹European Space Agency, Noordwijk, The Netherlands.

Correspondence to: Thomas Holding (t.m.holding@exeter.ac.uk)

25 **Abstract.** The flow (flux) of climate critical gases, such as carbon dioxide (CO₂), between the ocean and the atmosphere is a fundamental component of our climate and [an important driver of the biogeochemical systems within the oceans](#). Therefore, the accurate calculation of these air-sea gas fluxes is critical if we are to monitor the oceans and [assess the impact that these gases are having on Earth’s climate and ecosystems](#). FluxEngine is an open source software toolbox that allows users to easily perform calculations of air-sea gas fluxes from model, *in-situ* and Earth observation data. The original development and verification of the toolbox was described in a previous publication. The toolbox has now been considerably updated to allow its use as a Python library, to enable simplified installation, verification of its installation, to enable the handling of multiple sparingly soluble gases and greatly expanded functionality for supporting *in situ* dataset analyses. This new functionality for supporting *in situ* analyses includes user-defined grids, time periods and projections, the ability to re-analyse *in situ* CO₂ data to a common temperature dataset and the ability to easily calculate gas fluxes using *in situ* data from drifting buoys, fixed moorings and research cruises. Here we describe these new capabilities and then demonstrate their application through illustrative case studies. The first case study demonstrates the workflow for accurately calculating CO₂ fluxes using *in situ* data from four research cruises from the Surface Ocean CO₂ Atlas (SOCAT) database. The second case study calculates air-sea CO₂ fluxes using *in situ* data from a fixed monitoring station in the Baltic Sea. The third case study focuses on nitrous oxide (N₂O) and through a user defined gas transfer parameterisation identifies that

Revision 5/11/2019 10:49

Deleted: development of

Revision 5/11/2019 10:49

Deleted: health of the

Revision 5/11/2019 10:49

Deleted: changes to the

Revision 5/11/2019 10:49

Deleted: and the toolbox is already being used by scientists across multiple disciplines.

Revision 5/11/2019 10:49

Formatted: Font:Italic

biological surfactants in the North Atlantic could suppress individual N₂O sea-air gas fluxes by up to 13%. The fourth and final case study illustrates how a dissipation-based gas transfer parameterisation can be implemented and used. The updated version of the toolbox (version 3) and all documentation is now freely available.

1. Introduction

The exchange of climate relevant gases between the oceans and atmosphere including that of carbon dioxide (CO₂), nitrous oxide (N₂O) and methane (CH₄) is a major component of the climate system, and the ability of the oceans to absorb and desorb these gases varies both temporally and spatially. The need to monitor this exchange has been the driver for international data collation initiatives such as the Surface Ocean CO₂ Atlas (SOCAT, (Bakker *et al.*, 2016)) and the MarinE MethanE and NiTrous Oxide database (MEMENTO, (Kock and Bange, 2015)). These collaborative efforts are now routinely collecting, quality controlling and collating over a million new *in situ* data points each year. FluxEngine complements these initiatives by providing a standardised tool, which can robustly calculate air-sea gas fluxes from such *in situ* data, with the flexibility to incorporate new data sources and methodologies. The use of common tools and methods simplifies collaborations and accelerates advancements, both within and between scientific disciplines, through eliminating methodological or implementation-driven differences and the duplication of effort.

1.0 Overview of FluxEngine

FluxEngine is a flexible open source toolbox that allows users to easily exploit Earth observation and model data, in combination with *in situ* data, to calculate air-sea gas fluxes (Shutler *et al.*, 2016). It is available to download from <http://github.com/oceanflux-ghg/FluxEngine>. The toolbox uses plain text-format configuration files allowing the user to configure the input data sources, [random noise or bias on input data](#), the temporal period for the analysis, the structure of the air-sea gas flux calculation and user-defined gas transfer velocity parameterisations. The calculation itself can be performed using fugacity, partial pressure or concentration data, via a user defined bulk formulation, including formulations that can account for vertical temperature gradients across the mass boundary layer, the very small layer at the surface over which gas exchange occurs. A full description of the differences between the different flux formulations is provided in [Shutler *et al.* \(2016\)](#) and [Woolf *et al.* \(2016\)](#). The formulation that enables vertical temperature and salinity gradients to be included allowing a more accurate gas flux calculation is described in detail by [Woolf *et al.* \(2016\)](#) and takes the generalised form of

$$F = k(\alpha_w f_{G_w} - \alpha_s f_{G_a}) \quad (1)$$

where F is the sea-to-air flux of a sparingly soluble gas G, k is the gas transfer velocity, α_s and α_w are the solubilities of the gas above and below the surface water interface and f_{G_a} and f_{G_w} are the respective fugacities. Here we use ‘p’ and ‘f’ prefixes to refer to partial pressure and fugacity of a gas, respectively. Gas transfer velocity is driven by turbulence at ocean surface, caused by wind stress and wave breaking, amongst other processes. Because of the wide availability of high quality wind data products and the relative difficulty of directly measuring turbulence, it is commonplace to estimate k

Revision 5/11/2019 10:49
Deleted: (Shutler *et al.*, 2016)

Revision 5/11/2019 10:49
Deleted: Further optional features include the addition of random noise or bias to the input data.

Revision 5/11/2019 10:49
Deleted: (Shutler *et al.*, 2016) and (Woolf *et al.*, 2016).

Revision 5/11/2019 10:49
Deleted: (Woolf *et al.*, 2016)

using a statistical relationship with wind speed, (e.g. Ho *et al.*, 2006; Nightingale *et al.*, 2000; Wanninkhof, 2014).

Revision 5/11/2019 10:49

Deleted: e.g. (Ho *et al.*, 2006; Nightingale *et al.*, 2000; Wanninkhof, 2014)

Concentration of the gas is determined by its solubility and fugacity (or partial pressure). Equation (1) can therefore be rewritten as a product of the gas transfer velocity and the difference in gas concentrations,

$$F = k(G_W - G_S) \quad (2)$$

where G_S and G_W are the concentration of the gas above and below the interface. The FluxEngine configuration file allows users to choose the structure of the gas flux calculation, the inputs and the gas transfer velocity (either by choosing an already implemented published algorithm or through parameterising their own). The user can then perform calculations across their chosen input data and the outputs are Climate Forecast (CF) standard netCDF 4.0 files that contain data layers for each of the stages of the calculation, along with process indicator layers to aid the interpretation of the calculated gas fluxes (such as surface chlorophyll-a concentrations, the climatological position of temperature fronts and error indicator layers). A summary of the main features of the toolbox is given in Table 4 (appendix C).

Revision 5/11/2019 10:49

Deleted: (Shutler *et al.*, 2016)

Revision 5/11/2019 10:49

Deleted: Since

Revision 5/11/2019 10:49

Deleted: the toolbox has continued to be developed and extended based on feedback

Revision 5/11/2019 10:49

Deleted:). These

Revision 5/11/2019 10:49

Deleted: have considerably

Revision 5/11/2019 10:49

Deleted: of the toolbox and broadened the

Revision 5/11/2019 10:49

Deleted: to which it can be applied.

Revision 5/11/2019 10:49

Deleted: ; Woolf *et al.*, 2019), evaluate the impact of gas transfer processes on regional and global gas exchange (e.g.

Revision 5/11/2019 10:49

Deleted: (Shutler *et al.*, 2016)

Revision 5/11/2019 10:49

Deleted: and it is currently being used within two pan-European carbon monitoring research infrastructure projects (EU RINGO and EU BONUS INTEGRAL) which are part of the Integrated Carbon Observing System, ICOS.

Revision 5/11/2019 10:49

Deleted: (e.g.

Revision 5/11/2019 10:49

Deleted:). Most recently the toolbox is being used by two European Space Agency (ESA) projects to support preliminary studies for a new satellite concept (the Sea Surface Kinematics Multiscale Monitoring, SKIM, satellite mission (Ardhuin *et al.*, 2018)) and to verify the theoretical understanding of vertical temperature profiles and concentration gradients (as presented by Woolf *et al.*, 2016) through the analysis of a novel fiducial reference dataset. The results from these studies will be reported elsewhere, but their needs have driven some of the advancements presented here

Version 1.0 of FluxEngine was introduced and described by (Shutler *et al.*, 2016), which included a full description of the calculations, the flexibility of the toolbox, and the extensive verification of the different calculations along with examples of its use. With the aim to provide a standardised community tool, development has continued since its original release. Feedback from the user communities and the needs of specific scientific studies (e.g. Ashton *et al.*, 2016) have guided these developments and considerable extended the functionality and range of possible applications.

At the time of writing, the toolbox and resulting data have been used to quantify regional and global uncertainties (e.g. Wrobel and Piskozub, 2016; Wrobel, 2017; Woolf *et al.*, 2019; Shutler *et al.*, 2019), evaluate the impact of gas transfer processes on regional and global gas exchange (e.g. Ashton *et al.*, 2016; Pereira *et al.*, 2018), evaluate the European shelf sea CO₂ gas-fluxes and sink (Shutler *et al.*, 2016) and investigate biological and physical controls of air-sea exchange (Henson *et al.*, 2018). FluxEngine has also been used to identify shortfalls of current modelling approaches through the inclusion of FluxEngine outputs within an international inter-comparison (Rödenbeck *et al.*, 2015). The toolbox has also been incorporated within undergraduate and postgraduate teaching at the University of Exeter within geography, environmental science and marine biology degrees, and at Utrecht University for computer science.

This paper uses four case studies to illustrate key developments and the extended capabilities now contained within version 3.0 of the FluxEngine toolbox. Collectively, the case studies illustrate user selectable grids, support for calculating sea-to-air gas fluxes from time series data collected by fixed monitoring stations and research cruises (and how to incorporate the flux outputs into the original dataset to create a coherent time series), and the ability to calculate nitrous oxide (N₂O) sea-to-air gas fluxes, the addition of a new forcing variable (kinetic energy dissipation rate). The extensive support for *in situ* data contained within version 3 of FluxEngine means that it can now be fully exploited by

three different scientific communities in isolation: *in situ*, model and Earth observation; whilst the original capability to enable gas fluxes to be calculated from combinations of *in situ*, model and Earth observation data is retained.

180

Section 2 of this paper describes the structural extensions and changes, and explains how the toolbox can now be used as a command line tool or as a Python library. Section 3 then presents the case studies, while section 4 outlines the future direction and developments for the toolbox and section 5 gives conclusions. To aid the user the Appendices of this paper provide a list all of the toolbox utilities (Sect. 7), details of all data sets used in the case studies (Sect. 8), an overview of the main toolbox features and options (Sect. 9) and a description of the automatic software installers and verification tools (Sect. 10).

185

2. New capabilities

190

The following sections describe the extensions to the FluxEngine toolbox that are now contained within version 3.

2.1. Installation, verification and use

195

FluxEngine has now been optimised for use on a standalone desktop or laptop computer, removing the previous requirement for specialist computing facilities. Installation tools or instructions are provided for Microsoft Windows, Apple MacOS and Ubuntu/Debian based Linux operating systems. Separate utilities can then be used to verify that FluxEngine has been successfully installed. Details of the installation, verification process and execution times are provided in Sect. 10.

200

FluxEngine is now implemented as a Python module, which means that FluxEngine and its accompanying utilities can be imported as a Python module and easily integrated with other software, or used as stand-alone tools that are called from the command line. This approach offers a larger degree of flexibility than offered by version 1 of the toolbox and supports advanced exploitation. For example, a simple Python script can be written to run a sensitivity analysis where ensembles of flux calculations are required without any need to modify the underlying FluxEngine software.

205

2.2. Flexible input data specification

210

Previous versions of FluxEngine required the user to make changes to the underlying software in order to use new or differently formatted sources of input data. This required additional (and time consuming) testing and verification after modifications were made, making FluxEngine less accessible to those unfamiliar to Python programming. Two features have been added in version 3.0 to address this issue: i) file pattern matching (through standard Unix glob patterns and custom date/time tokens, described fully in *FluxEngineV3_instructions.pdf*) allows input file name format and directory structure to be customised using the plain text configuration file, ii) optional pre-processing functions can be used to manipulate input data after the data have been read into memory. These features can be specified for each input variable in the configuration file and FluxEngine contains a selection of common pre-processing functions, such as unit conversions or matrix transformation of the input data. Additional custom pre-processing functions can be added and tested easily by the user without the need to modify the core FluxEngine software, through copying and then completing the Python template function provided within the source code (*data_preprocessing.py*). Storing the completed function into

220

Revision 5/11/2019 10:49
Deleted: , including the automatic software installers and verification tools (allowing users to verify the integrity of their installation). It also

Revision 5/11/2019 10:49

Deleted: 6

Revision 5/11/2019 10:49

Deleted: 7) and

Revision 5/11/2019 10:49

Deleted: 8).

Revision 5/11/2019 10:49

Moved down [2]: (2019) Surface Ocean CO₂ Atlas (SOCAT, Bakker *et al.*, 2016) derived sea-to-air CO₂ flux reference dataset for year 2010.

Revision 5/11/2019 10:49

Moved down [3]: The installation is deemed successful if all results are identical to the reference dataset within a precision of 5 decimal places. An additional utility (*run_full_verification.py*) enables the user to perform a more detailed verification of different user defined options

Revision 5/11/2019 10:49

Deleted: Installation tools or instructions are provided for the following operating systems: Ubuntu/Debian based Linux (*install_dependencies_ubuntu.sh*), Apple Mac (*install_dependencies_macos.sh*) and Windows (instructions are within *FluxEngineV3_instructions.pdf*). Separate utilities (*verify_takahashi09.py* and *verify_socatv4_sst_salinity_gradients_N00.py*) can then be used to verify that FluxEng ... [1]

Revision 5/11/2019 10:49

Moved down [1]: standard global sea-to-air CO₂ gas flux calculations and net ... [2]

Revision 5/11/2019 10:49

Deleted: .,

Revision 5/11/2019 10:49

Deleted: Both of these datasets are contained within Holding *et al.*, (2018) and the ... [3]

Revision 5/11/2019 10:49

Deleted: which exploits the Woolf *et al.*, (2019) reference dataset. This executes ... [4]

Revision 5/11/2019 10:49

Deleted: available on a creative commons license via <http://github.com/oceanflux> ... [5]

Revision 5/11/2019 10:49

Deleted: used as command line tools (stand-alone tools or called from another piece ... [6]

Revision 5/11/2019 10:49

Deleted: .

Revision 5/11/2019 10:49

Moved down [4]: .

Revision 5/11/2019 10:49

Deleted: .,

Revision 5/11/2019 10:49

Moved down [5]: (2019) reference dataset (involving a global one year analysis of ... [7]

Revision 5/11/2019 10:49

Formatted: Font:Bold

320 the `data_preprocessing.py` file will then result in the custom-pre-processing function being automatically available for use in any configuration files.

These features make it possible to use any observational netCDF dataset by specifying the file path and, if required, appropriate pre-processing functions. For example a custom pre-processing function
325 could resample the input files, followed by a transformation to change the projection. This flexibility is conceptualised by the diagram in Fig. 1.

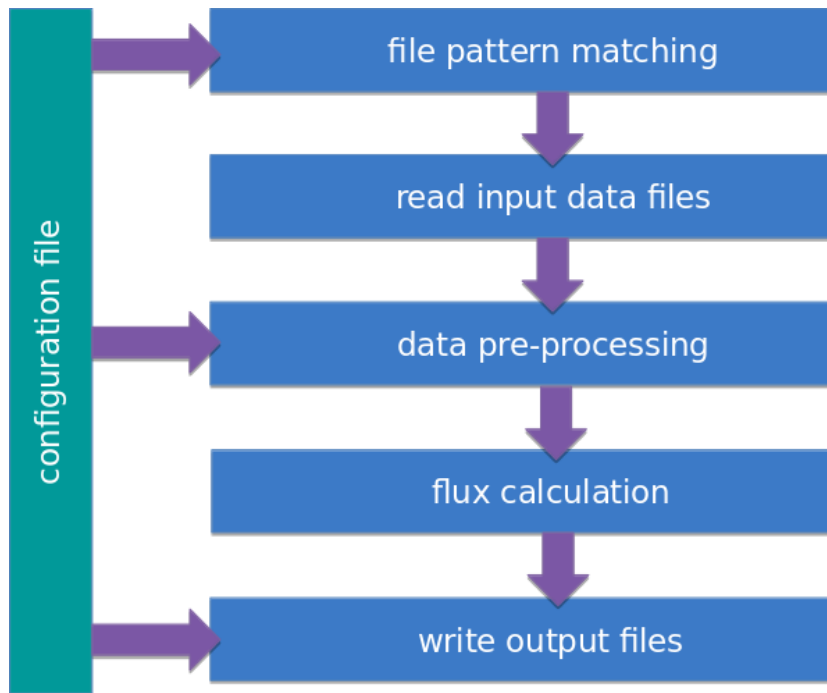


Figure 1: Conceptual diagram showing the way that input data are imported and used by FluxEngine. Single or groups of files are specified using a plain text configuration file. File names are interpreted using a subset of regular expression matching syntax (Unix glob patterns) and additional tokens are used to substitute time and date. The data pre-processing steps occur after input files are read into memory. Pre-processing functions are specified in the configuration file. Finally, the netCDF output files follow a user-specified filename and directory structure (as specified in the configuration file).

330 2.3. Extensive support for *in situ* data analyses

Version 1 of FluxEngine required that all input data be supplied as monthly $1^\circ \times 1^\circ$ global grids. These constraints restricted its relevance to regional analyses and *in situ* analyses, where sub-daily or sub-km resolutions are often more appropriate. The spatial resolution and extent can now be fully specified by the user and regional masks can be used in conjunction with the `ofluxghg_flux_budgets.py` tool to
335 calculate regional net integrated fluxes. In addition, flexible start and stop times and user-specified temporal resolution allows gas fluxes to be calculated for specific time intervals, e.g. the calculation can be configured to match the temporal resolution of the *in situ* data. Furthermore, a new

340 configuration option allows output from multiple time points to be grouped into a single netCDF file (rather than multiple files, one for each time point). This [enables](#) the calculation of gas fluxes from fixed research stations and other scenarios in which it is more convenient to provide results as a time-series.

Revision 5/11/2019 10:49

Deleted: feature is designed to enable

Revision 5/11/2019 10:49

Deleted: single

345 Improvements have been made to the bundled file conversion utilities, which convert between plain text data formats and the netCDF format used by FluxEngine. By default, these tools use the SOCAT format (Bakker *et al.*, 2016) for convenience, but now offer a high degree of flexibility to reflect the variety of data formats and conventions used for storing *in situ* data. This means that the tools can be used with virtually any text formatted *in situ* data files, avoiding the need for the user to convert their data to a fixed format with predefined column names.

350 The new utility, *append2insitu.py*, is designed specifically for use with *in situ* data and appends FluxEngine output as new columns within the original *in situ* data (achieved by matching spatial and temporal coordinates). For example, this means that users can use SOCAT (or custom) formatted *in situ* data as input to FluxEngine and then the results can be placed into a copy of the original input file, allowing the user to study the calculated fluxes, gas transfer rates, gas concentrations etc. alongside
355 (and aligned with) their original *in situ* data. This functionality is demonstrated in case studies one and three within this paper.

2.4. Reanalysis of *in situ* CO₂ fugacity data to a consistent temperature and depth

360 A new utility, *reanalyse_socat_driver.py*, is CO₂ specific and exploits a reference SST dataset (e.g. climate quality Earth observation SST data) and the original paired *in situ* measurements of CO₂ fugacity ([fCO₂](#)) and temperature to re-calculate the fCO₂ for the reference temperature dataset (and thus a consistent depth). The reasoning for the reanalysis is to reduce uncertainty and unknown biases that arise due to the fCO₂ measurements being collected using different instrumentation at some unknown and potentially variable depth below the surface. A detailed justification of the method and a full
365 description of the approach are described in [Goddijn-Murphy *et al.* \(2015\)](#).

Revision 5/11/2019 10:49

Deleted: ,

Revision 5/11/2019 10:49

Deleted: Goddijn-Murphy *et al.*, (2015

The reanalysis step is especially important if *in situ* data consisting of a collated dataset (originating from different instruments, sampling strategies or sources) is being used to calculate temporally averaged gas fluxes (e.g. monthly mean values). In this situation the *in situ* measurements are highly
370 likely to be collected from a range of different depths and unlikely to fully capture the monthly mean conditions of temperature and fCO₂ (due to aliasing). Whereas temporally averaged (mean) satellite observations are likely to provide a better representation (reference) of the mean temperature conditions. Therefore re-analysing the collated fCO₂ dataset to this reference temperature enables the calculation of the equivalent mean fCO₂ data.

375

380 It is worth noting that ship draught, and thus underway measurement intake depth, can even vary on a single research cruise due to changes in sea state, ballasting or cargo. So the method can also be important for data collected during a single research cruise.

385 For the case studies presented here the satellite observed SST data used for the reanalysis are valid for a depth of ~1 m (Reynolds *et al.* 2007). So the re-calculated fCO₂ are therefore also valid for this depth, and are used to represent the conditions at the bottom of the mass boundary layer or sub-skin temperature. The reanalysis to a consistent depth also enables a more accurate calculation of the gas fluxes, as it is then possible to accurately calculate two solubilities and thus two concentrations, one at the bottom, and one at the top of the mass boundary layer.

390 The [Goddijn-Murphy *et al.* \(2015\)](#) re-analysis method relies upon variations in fCO₂ being purely isochemical. This assumes that the total dissolved inorganic carbon is approximately constant throughout the surface waters over the temporal period and spatial scale being studied, and that differences in fCO₂ are solely due to temperature differences altering the equilibria of the carbonate system. Therefore caution should be used when applying the reanalysis method to data where these assumptions are not valid.

400 The slow re-equilibrium time of CO₂ in seawater (i.e. on the order of months for CO₂ to equilibrate with the atmosphere) ensure that monthly mean, or rolling monthly mean (centred on the day of interest) skin or sub-skin sea surface temperature (SST) values are suitable for re-analysing the *in situ* data. Arguably for re-analysing individual *in situ* datasets (e.g. to calculate gas fluxes for a single cruise dataset) a robust daily skin or sub-skin SST value would be better, even if that is obtained by a seasonal curve fitted to the monthly values and interpolated to the day of interest. Another solution would be to collect paired measurements of skin SST, and fCO₂ and SST at depth, all *in situ*, as has been done on a recent research cruise (Tarran, 2018) as ship-ready instruments are available, e.g. the Infrared Sea surface Autonomous Radiometer (ISAR, [Donlon *et al.*, 2008](#)). This enables the paired measurements at depth to be re-analysed using the *in situ* skin SST. However in the majority of cases ships collecting fCO₂ data do not collect skin data. Where *in situ* skin temperature data are not available and satellite temperature data are not appropriate, a regional model could be used to estimate skin temperature from the SST a few metres below the surface. An example model capable of this is the US National Oceanic and Atmospheric Administration (NOAA) Coupled Ocean-Atmosphere Response Experiment (COARE) model (e.g. see Fairall *et al.*, 1996).

Revision 5/11/2019 10:49
Formatted: Font:Italic

Revision 5/11/2019 10:49
Deleted: Goodijn

Revision 5/11/2019 10:49
Deleted: ., (2016

Revision 5/11/2019 10:49
Formatted: Font:Italic

Revision 5/11/2019 10:49
Deleted: Donlon *et al.*, 2008)

Whilst the reanalysis method and utility is CO₂ specific, its applicability to alternative gases (including unreactive N₂O and CH₄) is discussed and shown in Table 1 of (Woolf *et al.*, 2016). The impact on the net gas fluxes of not performing this reanalysis on a relatively large time series of CO₂ measurements through the north and south Atlantic is demonstrated within case study one (Sect. 3.1), whereas the impact on global net integrated gas fluxes has been analysed by [Woolf *et al.* \(2019\)](#).

Revision 5/11/2019 10:49
Deleted: Woolf *et al.*, (2019)

A typical workflow for calculating sea-to-air gas fluxes from *in situ* data using FluxEngine, and the tools used at each step, is illustrated in Fig. 2. All of the *in situ* analysis utilities, including the use of the *reanalyse_socat_driver.py* tool, are demonstrated in case studies one to three (Sect. 3).

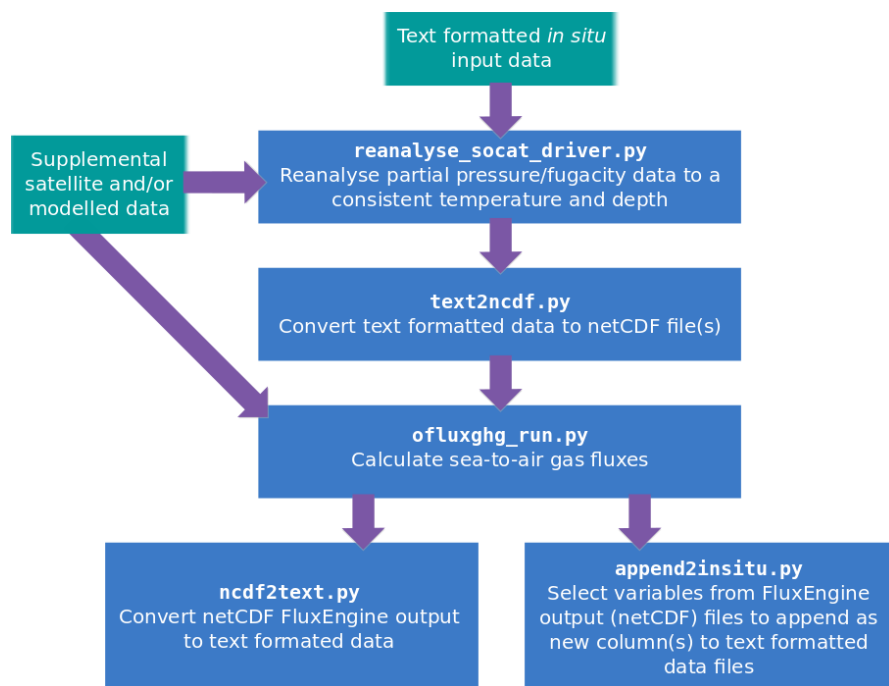


Figure 2: A typical CO₂ workflow for using FluxEngine with *in situ* data, showing the different utilities (blue boxes) and input data (green boxes) used at each stage.

2.5. Custom gas transfer velocity parameterisation

The processes that govern exchange, their relative importance and how gas exchange should be parameterised are all active areas of research ([e.g. Pereira *et al.* \(2018\)](#); [Wrobel and Piskozub, \(2016\)](#)).

Revision 5/11/2019 10:49
Deleted: e.g. Pereira *et al.*, (2018); Wrobel and Piskozub, (2016)

FluxEngine has always allowed users to select or define different gas transfer velocity parameterisations. However, version 3.0 adopts a modular approach to specifying the flux calculation, which makes it simpler for the user to extend the functionality and incorporate new gas transfer parameterisations. Custom parameterisations can be implemented as separate Python classes without

440 modifying the core FluxEngine software. This is achieved by copying and modifying the template class
provided in *rate_parameterisation.py*. Storing the new class within *rate_parameterisation.py* means
that the new parameterisation will be automatically available for inclusion in the configuration file.
These custom parameterisations can define new input variables and therefore make use of additional
445 input data sources. These custom parameterisations can also produce new data layers in the final
netCDF output, such as the results from intermediate calculation steps, which may be useful for testing
or subsequent analysis outside of FluxEngine. Examples of how to use this functionality are provided
in the source code. The toolbox documentation describes the process of, and best practices for,
extending FluxEngine in this way (see Sect. 9.1 and 9.2 within *FluxEngineV3_instructions.pdf*).

450 This increased flexibility means that users can define and use region-specific gas transfer
parameterisations or incorporate new transfer processes into existing gas transfer parameterisations
(such as the impact of biological surfactants as discussed by [Pereira et al. \(2018\)](#). Case studies one
(Sect. 3.1) and two (Sect. 3.2) demonstrate the use of different well known wind speed based gas
transfer parameterisations, while case study three (Sect. 3.3) demonstrates the use of a custom gas
455 transfer velocity parameterisation, which is used to assess the impact of biological surfactants on the
N₂O gas fluxes. Case study four (Sect 3.4) utilises a gas transfer velocity parameterisation that is based
on turbulent kinetic energy dissipation and provides an example of using additional input data.

2.6. Extensions for other sparingly soluble gases

460 The toolbox now supports the handling of two other sparingly soluble gases, (CH₄ and N₂O), and so
gas specific data can be substituted into Eq. (1) or Eq. (2) (dependent upon the choice of setup).
FluxEngine can calculate dissolved gas concentration from these gas input data, which can be supplied
as either partial pressure or mean molar fraction of a gas in the dry atmosphere. Alternatively, dissolved
gas concentrations can be provided directly as an input. Gas specific parameterisations for Schmidt
465 number (Sc) and solubility (α) are automatically chosen from those provided in Wanninkhof, (2014).
The option to use the older Sc and α parameterisations from Wanninkhof, (1992) is also included for
compatibility with previous versions and to aid comparative analysis. It is worth noting that both sets of
Sc parameterisations are only valid for saline water, and care should be taken when using them for
analysis of freshwater data, or regions with low salinity (e.g. the Baltic Sea, see case study two, Sect.
470 3.2). Support for additional and user-defined Schmidt number parameterisations are likely to be added
in the future.

3. Case study examples of the new capabilities

475 The following sections describe the application and results from four case studies that illustrate the new
capabilities. Table 1 summarises the new features that are demonstrated in each case study. These case
studies were run using FluxEngine version 3.0 which can be accessed via the GitHub [repository](#) (see
[code availability in Sect. 6](#)). The configuration files for each case study are included as examples in the
configs sub-directory of the GitHub repository and these will be updated to maintain compatibility as
new versions of the toolbox are released. In addition, interactive iPython Jupyter notebook tutorials for
480 the first three case studies are included in the *tutorials* sub-directory of the repository. Section 4 of this
paper provides more information about these tutorials.

Revision 5/11/2019 10:49

Deleted: Pereira et al., (2018).

Revision 5/11/2019 10:49

Deleted: .

Revision 5/11/2019 10:49

Deleted: repository's releases page:
<http://github.com/oceanflux-ghg/FluxEngine/releases/>. It is advisable to
always use the most up-to-date version of
FluxEngine which can be found via
<http://github.com/oceanflux-ghg/FluxEngine>.

	New features utilised
<p>Case study 1: Calculating sea to air CO₂ gas fluxes from ship research cruise data and using SOCAT data.</p>	<p>Flexible input data specification to select <i>in situ</i> data files and unit conversion using pre-processing functions (Sect. 2.2).</p> <p>Utilises new support for <i>in situ</i> data analysis, including the use of the <i>text2ncdf.py</i> and <i>append2insitu.py</i> tools, custom temporal resolution, reanalysis of fCO₂ to a consistent temperature field.</p>
<p>Case study 2: Calculating sea to air CO₂ gas fluxes from the Östergarnsholm fixed monitoring station data.</p>	<p>Flexible input data specification to select <i>in situ</i> data files and unit conversion using pre-processing functions (Sect. 2.2).</p> <p>Utilises new support for <i>in situ</i> data analysis, including use of <i>text2ncdf.py</i>, daily temporal resolution and output formatted as time-series (Sect. 2.3).</p>
<p>Case study 3: Surfactant suppression of sea to air N₂O gas fluxes using the MEMENTO data.</p>	<p>Flexible input data specification and unit conversion using pre-processing functions (Sect. 2.2).</p> <p>Utilises new support for <i>in situ</i> data analysis, including use of the <i>text2netcdf.py</i> and <i>append2insit.py</i> tools, custom temporal resolution and cruise-specific time interval (Sect. 2.3).</p> <p>Custom gas transfer parameterisation (Sect. 2.5).</p> <p>Calculation of N₂O gas fluxes (Sect. 2.6).</p>
<p>Case study 4: Gas transfer velocity parameterisation using turbulent kinetic energy dissipation rate.</p>	<p>Unit conversion and use of custom pre-processing functions to calculate the dissipation rate from the input data. This uses the pre-processing functions to perform a non-trivial computation (Sect. 2.2).</p> <p>Use of a custom gas transfer parameterisation which includes the specification of an additional input data layer (Sect. 2.5).</p>

Table 1: Summary of the new functionality demonstrated in each case study.

3.1 Case study 1: Calculating CO₂ fluxes from research cruise data

Revision 5/11/2019 10:49
Deleted:

Revision 5/11/2019 10:49
Deleted: .

495 Each year over 1 million new *in situ* data points are included within the annual updates to the SOCAT dataset. Field scientists collecting these data often need to calculate the coincident sea-to-air gas fluxes, either using solely *in situ* measurements or through combining them with satellite Earth observation and/or model data.

500 Here we illustrate the procedure for calculating sea-to-air gas fluxes from *in situ* data collected during four different sampling campaigns. These *in situ* data (Kitidis and Brown, 2017; Schuster, 2016; Steinhoff *et al.*, 2016; Wanninkhof *et al.*, 2016) were all collected in the north Atlantic during October 2013. These are hereafter referred to as cruises 1-4, respectively. The *in situ* data were first downloaded from PANGAEA (an open access data publishing and archiving repository, <http://www.pangaea.de>) in
505 tab-delimited format. The datasets follow the standard SOCAT structure and content (see Bakker *et al.*, 2016 table 9).

The majority of the measurements needed for the sea-to-air CO₂ gas flux calculation were included within the downloaded datasets. The aqueous fCO₂, salinity, SST and air pressure were measured *in*
510 *situ* and the molar fraction of CO₂ in dry air (xCO₂) had been extracted from the GLOBALVIEW-CO₂ dataset (GLOBALVIEW-CO₂, 2013). However, wind speed (needed for calculating the gas transfer velocity) was missing in all cases. Therefore, to complement these *in situ* data, multi-sensor merged wind speed data at 10 m were downloaded (Cross-Calibrated Multi-Platform, CCMPv2, 6 hour temporal resolution, 0.25° × 0.25° spatial grid (Atlas, *et al.*, 2011)). These wind speed data were
515 appended to the *in situ* data by matching each *in situ* measurement to the closest temporal and spatial grid point. This same process was used to add columns for the second and third moments of wind speed, which were estimated by taking the second and third power of wind speed, respectively.

Two datasets (Schuster, 2016; Steinhoff *et al.*, 2016) were missing xCO₂ data, and so the same method
520 of matching temporal and spatial grid points was used to fill in these fields using the GLOBALVIEW CO₂ dataset from the US National Oceanic and Atmospheric Administration (NOAA) Earth System Research Laboratory (ESRL) (GLOBALVIEW-CO₂, 2013). For ease, these additional wind speed and xCO₂ data were downloaded, extracted and then inserted into the tab delimited *in situ* file using some simple custom Python scripts but the same process could be performed manually. These scripts are not
525 part of FluxEngine.

Collectively the *in situ* data from these cruises were collected from different ships and underway systems, all sampling water at different and unknown depths. These measurements are typically collected from a few metres below the water surface, whereas the CO₂ concentration (combination of
530 fCO₂ and solubility) on either side of the mass boundary layer is required for an accurate gas flux calculation. Before these data from multiple sources can be used for an accurate gas flux calculation, they need to be reanalysed to a common temperature dataset and depth (Goddijn-Murphy *et al.*, 2015; Woolf *et al.*, 2016). Therefore, the *reanalyse_socat_driver.py* tool was first used to reanalyse all fCO₂ data to a consistent temperature and depth.

535 Monthly mean sea surface temperatures from the Reynolds Optimally Interpolated Sea Surface Temperature dataset (OISST, Reynolds *et al.*, 2007) were used as the reference sub-skin temperature

Revision 5/11/2019 10:49

Deleted: (Schuster, 2016; Steinhoff, *et al.*, 2016)

Revision 5/11/2019 10:49

Deleted: (Goddijn-Murphy *et al.*, 2015; Woolf *et al.*, 2016)

dataset, resulting in reanalysed $f\text{CO}_2$ that are valid for ~ 1 m and used to represent the bottom of the mass boundary layer (termed sub-skin within Woolf *et al.*, 2016).

545 The reanalysed $f\text{CO}_2$ were then inserted into the tab-delimited *in situ* dataset producing a single dataset. The tab-delimited file was then converted into a netCDF format file using the *text2ncdf.py* tool. This tool groups all data according to a user-specified spatial sampling grid, calculating the mean value and standard deviation for each cell within the grid as well as the number of data that were used to calculate these statistics. The spatial resolution was defined as $1^\circ \times 1^\circ$ grid and FluxEngine was then configured
550 to use each of the variables in the resulting netCDF file as input, with a pre-processing function applied to convert Reynolds OISST from Celsius to Kelvin (as all SST data within the main flux calculation use Kelvin). In order to produce a single netCDF output file for the entire 35 day period the temporal resolution for the flux calculation was set to 35 days. This allows the cruise tracks from all four cruises (1-4) to be easily visualised at the same time.

555 The sea-to-air CO_2 fluxes were then calculated using the rapid model (see Eq. (1) and Woolf *et al.*, 2016) and was run using a quadratic wind speed based gas transfer velocity parameterisation (Ho *et al.*, 2007). To identify the impact of the $f\text{CO}_2$ reanalysis stage, the sea-to-air CO_2 flux calculation was repeated using the original *in situ* SST and $f\text{CO}_2$.

560 Figure 3a shows the resultant calculated CO_2 flux along each of the cruises (1-4). The southern subtropical part of the cruise track 1 represents an area of the ocean that is a sink of CO_2 (negative sea-to-air flux). The northern sub-tropical section of cruise 1 shows an overall positive CO_2 flux into the atmosphere, while south of 15°N the net fluxes are smaller and in variable direction. Interestingly, there
565 are also examples (e.g. along the equatorial part of cruise track 1 and the western part of cruise track 2) where the direction of the flux has changed as a result of re-analysing the $f\text{CO}_2$ data. The highest magnitude fluxes were seen around the European continental shelf in cruise track 3, with a strong ocean sink west of Ireland and an intermittent source of CO_2 in the North Sea. Figure 3b shows the difference in calculated net flux between use of the original $f\text{CO}_2$ data and the reanalysed $f\text{CO}_2$. Whilst
570 very little difference is seen over large lengths of cruise tracks 1, 2 and 4, there are substantial differences in net flux of up to $0.1 \text{ C m}^{-2} \text{ day}^{-1}$ in some regions, for example within the frontal regions at the edge of the European shelf seas (cruise track 3) or in the southern section of cruise track 1. These are regions where temporally and spatially dynamic temperature gradients can exist that are likely under sampled (aliased) by both the *in situ* measurements and the satellite observations used to re-
575 analyse the $f\text{CO}_2$ data. In this case, reanalysis using an estimated or modelled skin temperature (based on the *in situ* SST at depth) may be more appropriate (see the discussion in Sect 2.4).

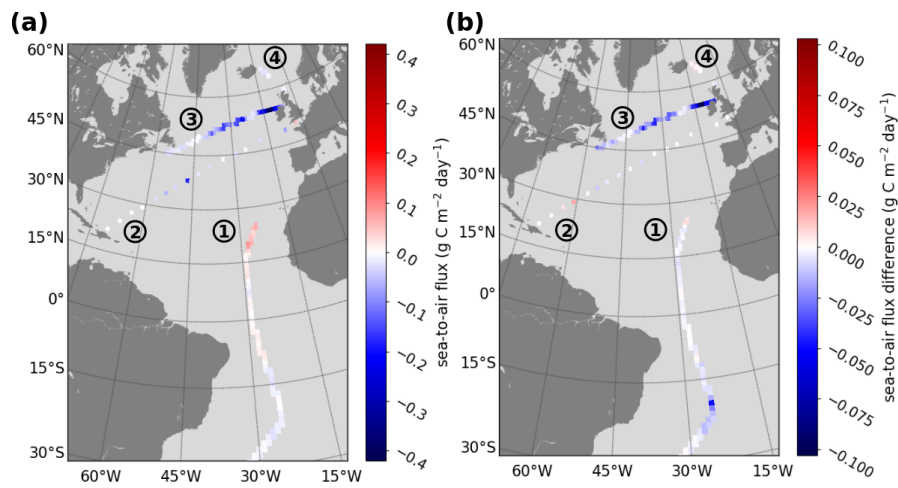


Figure 3: Example sea-to-air CO₂ fluxes calculated using *in situ* data and the gas transfer velocity detailed in [Ho et al. \(2006\)](#) (a) fluxes calculated for four sampling cruises in the North Atlantic during October and November 2013 (Kitidis and Brown, 2017; Schuster, 2016; Steinhoff et al., 2016; Wanninkhof et al., 2016) labelled 1-4, respectively. (b) The difference in the calculated flux resulting from using the reanalysed fCO₂ compared to the original *in situ* fCO₂ data (reanalysed minus original).

Revision 5/11/2019 10:49
Deleted: Ho et al., (2006)

580 The `append2insitu.py` tool was then used to append FluxEngine output to the original input data file for the Kitidis and Brown (2017) dataset. The output from this tool enables the user to visualise FluxEngine output (including any additional input data such as the CCMP wind speed data) as a time series alongside all other *in situ* data. Figure 4 shows the time series of SST, fCO₂, and xCO₂ (from the downloaded cruise data). Plotted alongside these are the corresponding CCMP wind speed and the calculated concentrations and fluxes using the original and reanalysed fCO₂ data.

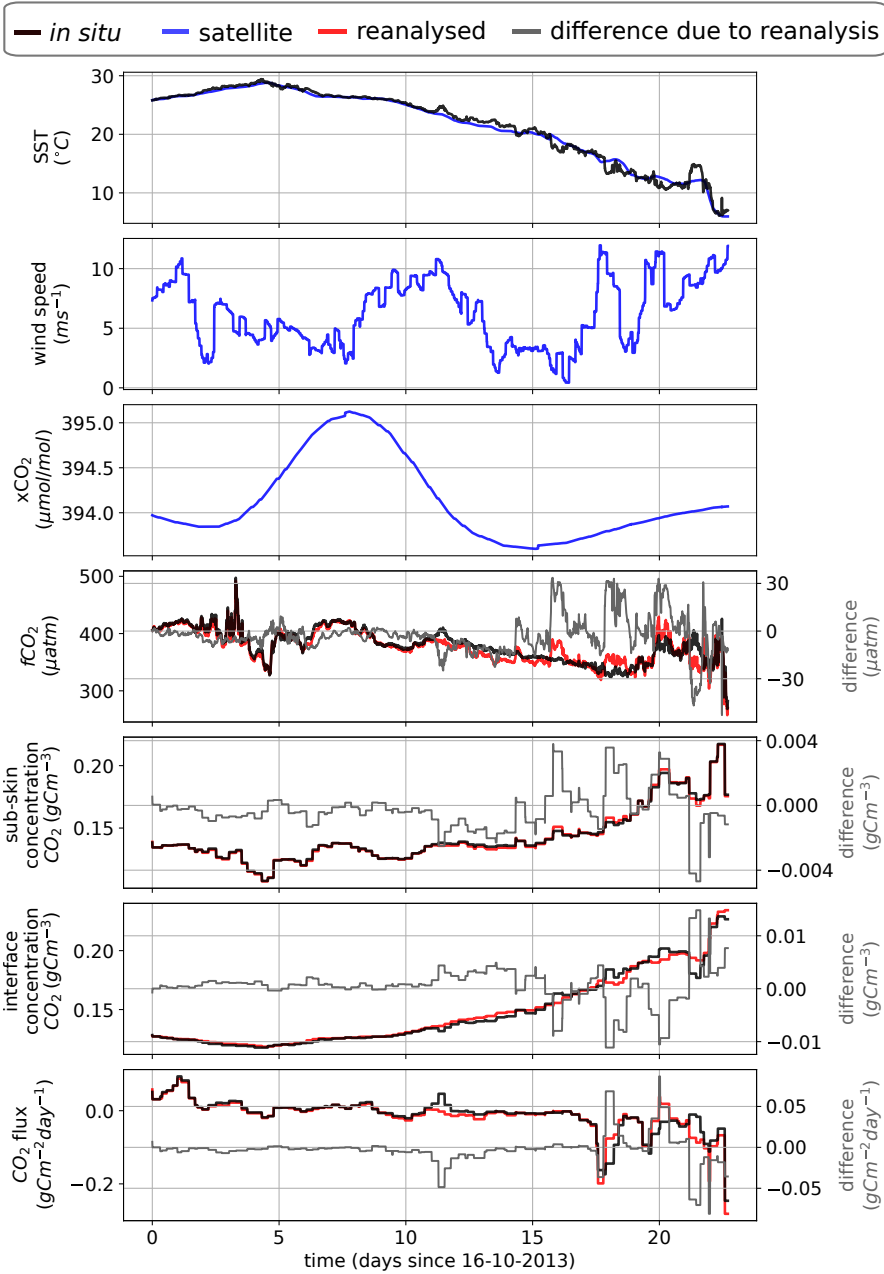


Figure 4: Time series of the (Kitidis and Brown, 2017) *in situ* campaign data with the sea-to-air CO₂ flux as calculated by FluxEngine using the [Ho et al. \(2006\)](#) gas transfer velocity parameterisation. The results from the reanalysed fCO₂ values are shown in red to distinguish them from the original data. The differences in fCO₂, sub-skin and interface CO₂ concentration and sea-to-air CO₂ flux, resulting from the reanalysis, are shown in grey (reanalysed minus original).

Revision 5/11/2019 10:49

Deleted: Ho et al., (2006)

3.2 Case study 2: Calculating CO₂ fluxes from Östergarnsholm fixed station data

590 In this section the new capabilities for calculating gas fluxes from fixed stations is demonstrated using
data from the long term monitoring station at Östergarnsholm. The Östergarnsholm station is situated
in the Baltic Sea (57.42N, 18.99E) and is part of the Integrated Carbon Observation System (ICOS)
infrastructure. The station was originally established in 1995 with the aim of collecting data on the
marine atmospheric boundary layer to support research on the exchange of heat, momentum and CO₂
595 between the atmosphere and ocean. It is equipped with instruments to measure (amongst other
parameters) profiles of wind speed, water temperature and aqueous fCO₂.

The new FluxEngine support for calculating gas fluxes from fixed stations uses the temporal dimension
of the input files, creating output files of the same dimension that can be easily visualised as a time
600 series. Data for the Östergarnsholm monitoring station covering a period from 28 January 2015 to 9
September 2015 were downloaded from the data repository (Rutgersson, 2017). These data contain *in
situ* measurements for fCO₂, salinity and temperature, model reanalysis air pressure at sea level from
the National Center for Environmental Prediction and National Center for Atmospheric Research
(NCEP/NCAR) dataset (Kalnay *et al.*, 1996), xCO₂ from the NOAA ESRL GLOBALVIEW dataset
605 (GLOBALVIEW-CO2, 2013) and World Ocean Atlas salinity data (Boyer *et al.*, 2013). CCMP wind
speed data were extracted and added to the tab delimited *in situ* dataset using the same method as used
in case study 1 (Sect. 3.1). For gridded input data values were extracted from the single grid point
containing the Östergarnsholm station location was selected from a global 1° × 1° projected grid.

610 The *text2ncdf.py* tool was configured to convert the text formatted data file into a single netCDF file
using a temporal resolution of one day. This produced a netCDF file with a temporal dimension size of
246 (days), containing the daily mean value for each of the 246 days covered by the dataset. For this
case study FluxEngine was configured to use this file as input.

615 The flux calculation used the rapid model (Woolf *et al.*, 2016) with the Nightingale *et al.* (2000) wind
based gas transfer velocity parameterisation and was performed using the original *in situ* fCO₂ and SST
data. The temporal resolution was set to provide daily calculations for each of the 246 days allowing
seasonal variations to be observed. FluxEngine supports arbitrary temporal resolutions to within minute
precision and the choice predominantly depends on the resolution of the available data and the
620 particular research questions to be addressed. FluxEngine was configured to write output into a single
netCDF file as a time series. The *in situ* fCO₂ and SST measurements were assumed to represent the
conditions at the bottom of the mass boundary layer and the concentrations at the top of the mass
boundary layer were estimated by configuring the FluxEngine to estimate the skin temperature using
the *in situ* SST - 0.17 (which is based on the work of Donlon *et al.*, 2002).

625 Figure 5 shows the time series of SST, wind speed, xCO₂, fCO₂, concentration of CO₂ and calculated
sea-to-air CO₂ flux. There is a moderate negative flux (ocean sink of CO₂) throughout most of the
sampled period, which switched to a positive flux (outgassing to the atmosphere) during winter months.
At approximately day 130 there is a local upwelling event which results in an incursion of CO₂ rich
630 cold water. This results in an increase in fCO₂ of approximately 250 µatm, however coincident low
wind speed means that there was little change in the flux during this event.

Revision 5/11/2019 10:49

Deleted: 28th

Revision 5/11/2019 10:49

Deleted: the 9th

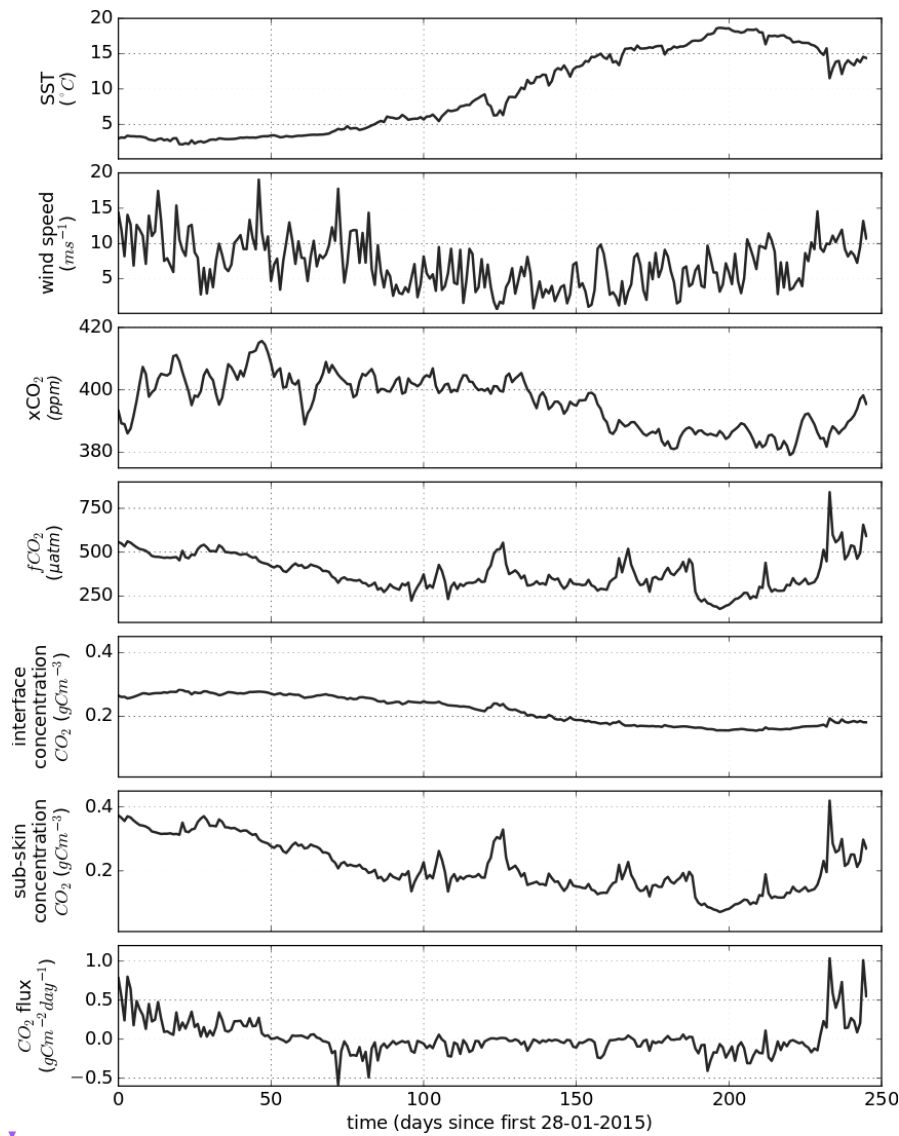
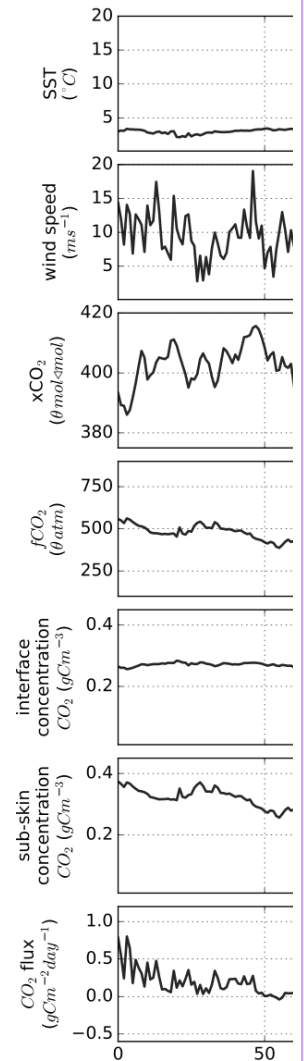


Figure 5: FluxEngine output file using data from Östergarnsholm station over the 246 day period. Example components of the sea-to-air flux calculation are shown alongside the calculated CO₂ flux.

Revision 5/11/2019 10:49



Deleted:

635

3.3 Case study 3: Surfactant suppression of N₂O gas fluxes using the MEMENTO database

Nitrous oxide (N₂O) and methane (CH₄) are both climatically important gases. In the troposphere, they act as greenhouse gases (IPCC, 2013), whereas stratospheric N₂O is the major source for nitric oxide radicals which are involved in one of the main ozone reaction cycles (Ravishankara *et al.*, 2009).

640

Source estimates indicate that the world's oceans play a major role in the global budget of atmospheric N₂O and a minor role in the case of CH₄ (IPCC, 2013). Oligotrophic ocean areas are near equilibrium with the atmosphere and, consequently, make only a relatively small contribution to overall oceanic emissions, whereas biologically productive regions (e.g., estuaries, shelf and coastal upwelling areas) appear to be responsible for the major fraction of the N₂O and CH₄ emissions (Bakker *et al.*, 2014).

645

650 Surfactants are surface-active compounds that can suppress turbulence at the sea surface thus altering air-sea gas exchange (McKenna and Bock, 2006; Pereira *et al.*, 2016; Salter *et al.*, 2011). There is growing evidence from field and laboratory studies that naturally occurring surfactants can significantly reduce the flux of N₂O across the water/atmosphere interface (Kock *et al.*, 2012; Mesarchaki *et al.*, 2015).

655 Previous work, which studied CO₂ fluxes, found that surfactants potentially reduce the annual net integrated CO₂ flux by up to 9% in the Atlantic Ocean (Pereira *et al.*, 2018). Here, we use FluxEngine to apply the methodology of Pereira *et al.* (2018) to *in situ* data from the MEMENTO (Marine MethanE and NiTrous Oxide) database (Kock and Bange, 2015) in order to estimate the equivalent suppression effect on the exchange of N₂O between ocean and atmosphere.

660 While FluxEngine is able to calculate sea-to-air fluxes of both N₂O and CH₄, we confined our analysis to N₂O because of the sparsity of CH₄ data. *In situ* and 1° x 1° gridded monthly mean atmospheric and ocean partial pressure of N₂O, sea surface temperature and salinity were obtained from the MEMENTO database for the Atlantic Meridional Transect (AMT) cruise (AMT-24, JR303), which took place between September and November 2014 (Brown and Rees, 2018). These data were supplemented with Earth observation wind speed, *U*₁₀, from the CCMP dataset and modelled air pressure from the European Centre for Medium-Range Weather Forecasts (ECMWF). All input data were gridded to 665 monthly means with a 1° x 1° resolution.

670 A custom gas transfer velocity parameterisation was implemented following the template provided in the toolbox to calculate the gas transfer suppression due to biological surfactants in surface waters. This parameterisation uses the gas transfer velocity of Nightingale *et al.* (2000) combined with an estimate of the degree of surfactant suppression from (Pereira *et al.*, 2018). The method described by Pereira *et al.* (2018) used sea surface temperature to estimate surfactant suppression meaning that no additional input data fields were needed. FluxEngine was configured to use the rapid flux model (Woolf *et al.*, 2016) and run once with the standard Nightingale *et al.* (2000) gas transfer parameterisation (no 675 suppression case) and then again using the Pereira *et al.* (2018) parameterisation (suppression case). This new gas transfer parameterisation is now freely available within the FluxEngine (and can be selected by specifying *k_Nightingale2000_with_surfactant_suppression* for the *k_parameterisation* option).

680 After calculating the air-to-sea N₂O fluxes we removed negative (atmosphere to ocean) fluxes. The fluxes for each grid cell (within which at least one *in situ* measurement exists) are shown in Fig. 6a, while the difference in sea-to-air flux due to surfactant suppression is shown in Fig. 6b. The largest fluxes occur in the tropics and sub-tropical part of the AMT cruise track (Fig. 6a). Suppression of the gas transfer reduces the magnitude of the air-sea flux and the largest absolute suppression is also seen 685 in the tropics and sub-tropical regions (Fig. 6a and Fig. 6b).

The *append2insitu.py* utility was used to combine FluxEngine output with the original *in situ* data. The time series are shown in Fig. 6c for SST, wind speed, atmospheric and aqueous N₂O, and sea-to-air N₂O flux. The net fluxes along the transect are generally small and in both directions. The overall mean 690 (and standard deviation) flux was 5.7×10^{-2} ($\pm 5.7 \times 10^{-2}$) g N₂O m⁻² day⁻¹ (no suppression) and 5.0×10^{-2}

Revision 5/11/2019 10:49

Deleted: ..

Revision 5/11/2019 10:49

Deleted: (Nightingale *et al.*, 2000) combined with an estimate of the degree of surfactant suppression from

Revision 5/11/2019 10:49

Deleted: ..

Revision 5/11/2019 10:49

Deleted: ..

($\pm 4.8 \times 10^{-3}$) $\text{g N}_2\text{O m}^{-2} \text{day}^{-1}$ (suppression), indicating in both cases a small net flux into the ocean. There was a mean flux suppression due to surfactants of 13% for the entire dataset.

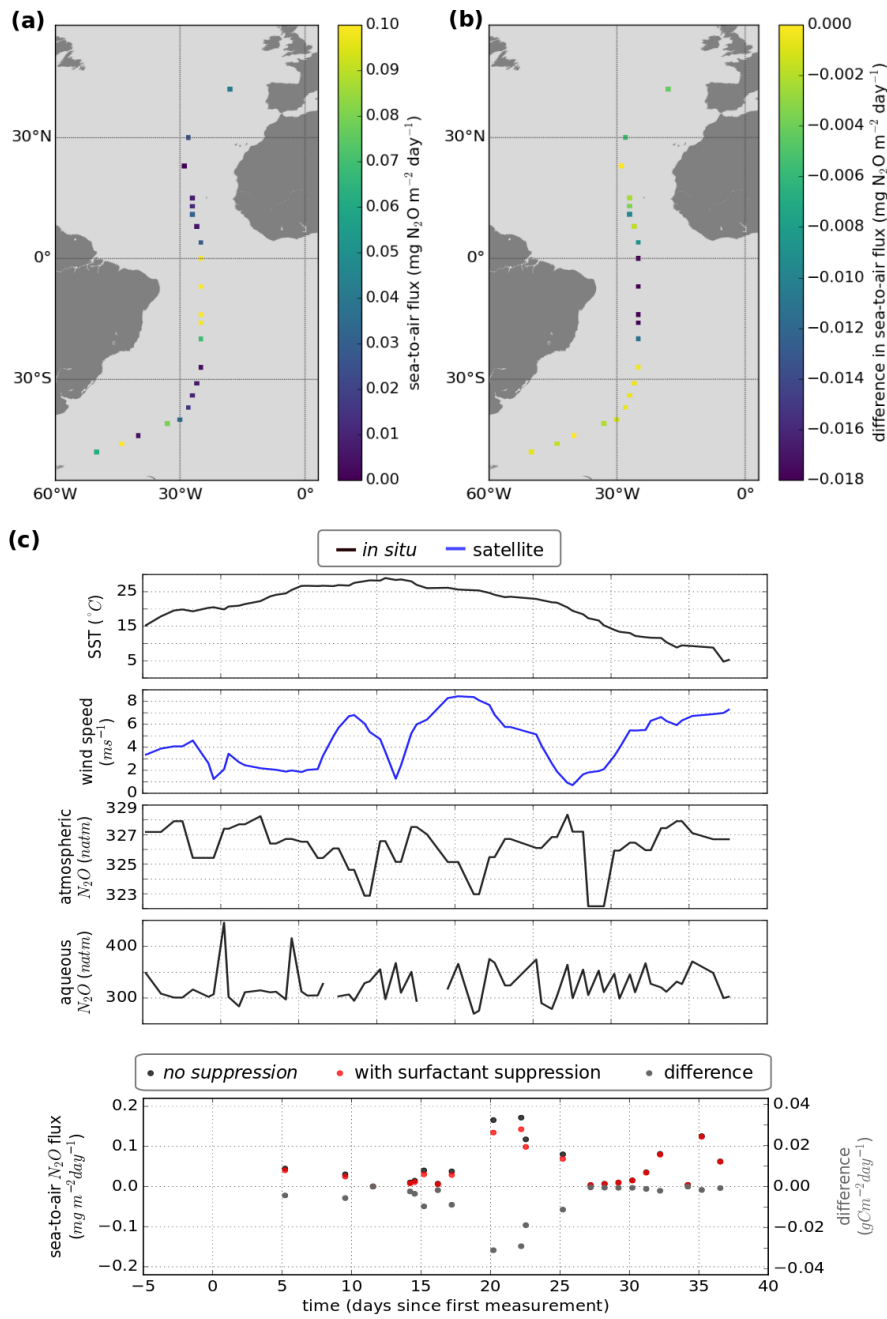


Figure 6: (a) Sea-to-air N_2O flux taking into account surfactant suppression. (b) Change in N_2O flux resulting from surfactant suppression. (c) Time series of SST, wind speed, atmospheric N_2O , aqueous N_2O and sea-to-air flux.

700 3.4 Case study 4: Gas transfer velocity parameterisation using turbulent kinetic energy dissipation rate

The gas transfer velocity, k in equation 1 and 2, is determined by the turbulent mixing near the ocean surface (Jähne *et al.*, 1987). While it is common to estimate gas transfer using a polynomial relationship with wind speed, turbulence in the upper ocean is influenced by additional physical processes that are independent, or not solely dependent, on the wind. These include wave breaking, shear stress due to geostrophic currents, wind-wave-current interactions, bottom-generated turbulence, tidal forces and precipitation (Villas Boas *et al.*, 2019; Zappa *et al.*, 2007; Zhao *et al.*, 2018).

710 In this case study we apply a turbulent kinetic energy dissipation rate (ϵ) based gas transfer velocity parameterisation, as developed by Zappa *et al.* (2007), to quantify the impact of wind- and wave-driven turbulence on sea-to-air CO₂. Zappa *et al.* (2007) used direct measurements of k and ϵ in aquatic and shallow marine regions to derive the following relationship

$$k = 0.419Sc^{-0.5}(\epsilon\nu)^{0.25} \quad (3)$$

715 where k is the gas transfer velocity (m s⁻¹), Sc is the Schmidt number, ϵ is the turbulent kinetic energy dissipation rate (W kg⁻¹) and ν is the kinematic viscosity of water (m² s⁻¹). We calculate the monthly mean ϵ using the monthly mean wave (swell, secondary swell and wind waves) to ocean turbulent kinetic energy flux (FOC) provided by the WAVEWATCH III model re-analysis (WAVEWATCH III development group, 2016). The mean dissipation rate of turbulent kinetic energy, ϵ_{mean} , is calculated using $\epsilon_{\text{mean}} = \text{FOC} / (\rho z_{\text{max}})$, where ρ is the density of sea water (taken to be 1026 kg m⁻³) and z_{max} is the maximum depth over which dissipation is assumed to occur (taken as 10 m from Fig. 8 of Craig and Banner, 1994). This provides the mean total dissipation rate through the volume of water. Equation 3 is valid for ϵ measurements near the surface (of the order of 0.1 to 0.2 m) and ϵ is known to decrease exponentially with depth. To estimate ϵ at a depth of 0.2 m we first fit an exponential function to the curve of ϵ from Fig. 8 of Craig and Banner (1994) which gave:

$$\epsilon = \beta \exp(0.20z + 0.78) \quad (4)$$

730 where z is depth and $\beta = 1.86 \times 10^{-3}$. Normalising this function to have a mean ϵ equal to ϵ_{mean} allows ϵ at any depth to be determined. This was done by fitting β to minimise the difference between ϵ_{mean} calculated from FOC and ϵ_{mean} calculated from equation 4 to produce separate depth relationships with ϵ for each individual grid cell. Finally, the dissipation rate at 0.2 m was calculated by substituting $z=0.2$ into the final depth relationship. The process of fitting of the depth relationship and calculating ϵ at depth $z=0.2$ was implemented using a custom pre-processing function that is included as an example in the FluxEngine download. This demonstrates how pre-processing functions can be used to perform complex data processing.

740 FluxEngine was then used to calculate monthly sea-to-air CO₂ fluxes, globally, for 2010. All inputs to FluxEngine were provided as monthly averages with a 1° x 1° resolution. The additional input data were wind speed data from WAVEWATCH III re-analysis forcing field (WAVEWATCH III development group, 2016), sea surface temperature from Reynolds Optimally Interpolated Sea Surface Temperature dataset (OISST, Reynolds *et al.*, 2007), salinity data from the NOAA World Ocean Atlas

Revision 5/11/2019 10:49

Deleted: (Jähne *et al.*, 1987)

Revision 5/11/2019 10:49

Formatted: Font:Italic

745 (Zweng *et al.*, 2018), xCO₂ from the GLOBALVIEW CO₂ dataset (GLOBALVIEW-CO₂, 2013), and fCO₂ data from the SOCAT derived sea-to-air CO₂ flux reference dataset for 2010 (Woolf *et al.*, 2019).

750 Since the Zappa *et al.* (2007) relationship was parameterised in low to moderate wind speeds and in shallow marine environments, a mask was set in the configuration file to constrain the calculation to grid cells with wind speeds less than 10 m s⁻¹ and shelf sea water depths between 20 and 200 m, and then the analysis repeated with depths between 20 and 500 m. These depth ranges were chosen to be consistent with previous studies (e.g. Laruelle *et al.*, 2018; Shutler *et al.*, 2016), and the General Bathymetric Chart of the Oceans (GEBCO) Digital Atlas bathymetry was used for this masking (GEBCO, 2003).

755 The *ofluxhg_flux_budgets.py* tool was used to compute the annual integrated net sea-to-air flux in all shelf sea regions. Collectively, the global shelf seas result in a net integrated flux into the ocean (sink) of 0.57 to 0.78 Pg C for 2010, where the range is due to the two shelf definitions. These results are within the bounds of those determined by previous studies (0.2 – 1 PgC yr⁻¹ from Laruelle *et al.*, 2018; Laruelle *et al.*, 2016). However we note that all previous studies have used wind speed for calculating gas exchange. Repeating the analysis with a wind speed based gas transfer velocity (Wanninkhof *et al.*, 2014) instead of equation 4 gives an ~8% smaller net integrated flux of 0.53 to 0.72 Pg C. This result could suggest that published values of the global shelf sea CO₂ sink (calculated using wind speed gas transfer) are underestimated, as they do not fully account for wind-wave-current interactions and whitecapping. Figure 7 shows the resulting mean annual sea-to-air CO₂ flux in 2010 for global shelf seas. The FluxEngine has the capability to use non-wind driven gas transfer parameterisations allowing more physically based approaches to be evaluated such as the use of ϵ . The first synoptic-scale observation-based estimates of ϵ could soon be possible from space using Doppler techniques (e.g. Ardhuin *et al.*, 2019).

770

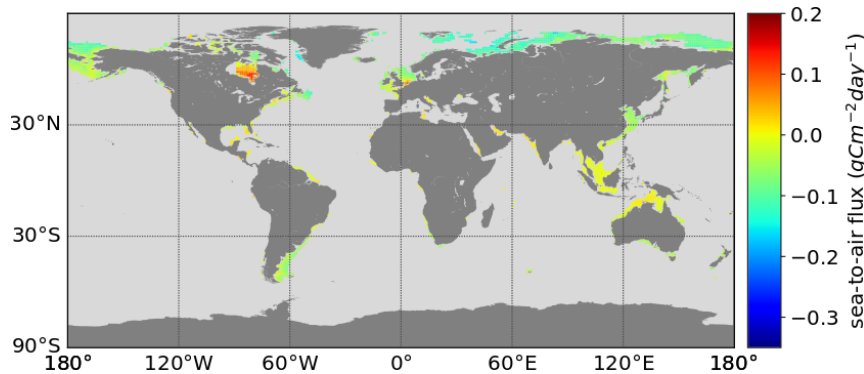


Figure 7: Mean annual sea-to-air CO₂ flux of shelf seas in 2010 using the Zappa *et al.* (2007) gas transfer relationship for all regions and months with wind speeds 0 to 10 m s⁻¹. Shelf regions are defined as having depth between 20 m and 200 m.

4. Future developments

775 The FluxEngine toolbox will continue to be developed in response to new advances in research and further user-uptake will be encouraged through the provision of iPython Jupyter notebooks. There are currently four interactive Jupyter notebooks (tutorials) available within the FluxEngine v3.0 download

Revision 5/11/2019 10:49
Deleted: ..

Revision 5/11/2019 10:49
Deleted:

Revision 5/11/2019 10:49
Formatted: Font:Italic

Revision 5/11/2019 10:49
Formatted: Font:Italic

Revision 5/11/2019 10:49
Deleted: a

Revision 5/11/2019 10:49
Formatted: Font:Italic

Revision 5/11/2019 10:49
Deleted: ..

780 and these correspond to the first three case studies presented in this paper as well as an additional
introductory tutorial. These interactive notebooks allow users to investigate the toolbox without the
need to install any additional software. Users are able to modify and re-run the notebook and
immediately see the impact of any changes. This approach has been previously used by the authors for
supporting collaborative research and summer school teaching. Additional Jupyter notebooks could be
785 written to provide worked examples of: i) driving FluxEngine with a custom Python script to perform a
sensitivity or ensemble analysis, ii) using the FluxEngine to study a freshwater environment or iii)
using the verification tools module to verify custom changes and extensions to the toolbox. All
notebooks will be maintained so that they remain available and relevant to future versions of the
FluxEngine.

790

5. Conclusions

The FluxEngine is an open-source and freely available software toolbox that provides standardised and
verified calculations of gas exchange and net integrated fluxes between the ocean and atmosphere, and
the toolbox is now being used by *in situ*, Earth observation and modelling scientific communities. The
795 development of the toolbox was driven by the desire to reduce duplication of effort, to facilitate
collaboration between different research communities, and thus to accelerate advancements in air-sea
gas flux research and monitoring.

800 Building on [Shutler et al. \(2016\)](#), which demonstrated the toolbox and verified the accuracy of the
calculations, this paper demonstrates new capabilities that considerably broadens the scope of research
questions that can be addressed using FluxEngine. Version 3.0 can now be easily installed and
executed on a desktop or laptop computer and does not require specialist hardware or software
libraries. It can be used as a Python library or as a set of stand-alone command line utilities. The
toolbox now includes an extensive suite of tools for calculating gas fluxes directly from *in situ* data.
805 Collectively, these improvements have streamlined the process for extending the toolbox and will allow
users to easily take advantage of newly developed gas transfer velocity parameterisations and/or new
sources of input data. These new tools and the toolbox are fully compatible with the internationally
established data structures being used by the SOCAT and the MEMENTO communities.

810 The inclusion of the handling of CH₄ and N₂O sea-air gas fluxes is intended to directly support those
communities studying these gases. Significant international research focus and effort is now being
directed to collating data on these gases towards monitoring and understanding their spatial distribution
and variability.

815 The FluxEngine toolbox will continue to be updated as new approaches become available. Further
development will be guided by the needs of the international research and monitoring communities,
and so we welcome feedback from users on all aspects of the toolbox.

820 6. Code availability

The FluxEngine software is open source and available on a creative commons license via
<http://github.com/oceanflux-ghg/FluxEngine>. FluxEngine is in constant development and historic
versions are available via GitHub. To access the specific version used to conduct the case studies in

Revision 5/11/2019 10:49
Deleted: Shutler et al., (2016)

825 section 3, please access the v3.0 release via: <https://github.com/oceanflux-ghg/FluxEngine/releases/tag/v3.0>

7. Appendix A: Utility names and descriptions

Several additional utilities are provided as Python scripts to support the installation, verification, execution and processing of output and these are listed in table 2.

Utility	Description
<i>append2insitu.py</i>	Appends netCDF data (e.g. FluxEngine output) to text formatted data files as new columns. Matching rows by longitude, latitude and time.
<i>install_dependencies_macos.py</i> , <i>install_dependencies_ubuntu.py</i>	Installation scripts. Installation instructions are provided for Windows users in <i>FluxEngineV3_instructions.pdf</i>
<i>ncdf2text.py</i>	Converts netCDF output files to text formatted files.
<i>ofluxghg_flux_budgets.py</i>	Calculates total monthly and annual gas flux from FluxEngine output. Supports global and regional analysis.
<i>ofluxghg_run.py</i> <i>reanalyse_socat_driver.py</i>	Commandline tool used to run FluxEngine Uses satellite sea surface temperature to reanalyse CO ₂ fugacity and partial pressure data to a consistent temperature and depth (see Goddijn-Murphy <i>et al.</i> , 2015)
<i>run_full_verification.py</i>	Runs an extended verification procedure. Required additional data from (Holding <i>et al.</i> , 2018)
<i>text2ncdf.py</i>	Converts text formatted data files into FluxEngine compatible netCDF format.
<i>validation_tools.py</i> , <i>compare_net_budgets.py</i>	Contains Python functions to aid verification of FluxEngine output to a reference dataset.
<i>verify_socatv4_sst_salinity_gradients_N00.py</i> , <i>verify_takahashi09.py</i>	Verifies that FluxEngine has been installed correctly by comparing output with a reference data from SOCAT-derived or Takahashi climatologies, respectively.

Table 2: Description of the bundled tools and scripts that are included in FluxEngine. Each tool can be used as a stand-alone command line tool or used as a Python package.

8. Appendix B: Datasets used

Table 3 provides details of each of the data sets that were used in the case studies.

Name	Parameter(s)	Reference/source
CCMP v2 (Cross-Calibrated Multi-Platform)	U ₁₀ (wind speed at 10m)	Atlas <i>et al.</i> , 2011 http://www.remss.com/measurements/ccmp/
OISST (Optimally-Interpolated Seas Surface Temperature)	Sea surface temperature (SST)	Reynolds <i>et al.</i> , 2007 https://www.ncdc.noaa.gov/oisst
GLOBALVIEW CO ₂	xCO ₂ (molar fraction of CO ₂ in dry air)	GLOBALVIEW-CO ₂ , 2013 https://www.esrl.noaa.gov/gmd/ccgg/globalview/co2/co2_intro.html
National Centers for Environmental Prediction, National Center for	Air pressure	Kalnay <i>et al.</i> , 1996 https://www.esrl.noaa.gov/psd/data/gridded/data.ncep.reanalysis.pressure.html

Atmospheric Research (NCEP/NCAR)		
Underway data from the James Clark cruise (74JC20131009)	SST, salinity, air pressure, fCO ₂	Kitidis and Brown, 2017 https://doi.pangaea.de/10.1594/PANGAEA.878492
Underway data from the Belguela Stream cruise (642B20131005)	SST, salinity, air pressure, fCO ₂	Schuster, 2016 https://doi.org/10.1594/PANGAEA.852980
Underway data from the Atlantic Companion cruise (77CN20131004)	SST, salinity, air pressure, fCO ₂	Steinhoff <i>et al.</i> , 2016 https://doi.org/10.1594/PANGAEA.852786
Underway data from the REYJAFOSS cruise (64RJ20131017)	SST, salinity, air pressure, fCO ₂ , xCO ₂	Wanninkhof <i>et al.</i> , 2016 https://doi.org/10.1594/PANGAEA.866092
Östergarnsholm station (77FS20150128)	Air pressure, salinity, SST, xCO ₂ (air), fCO ₂ (water)	Rutgersson, 2017 https://doi.pangaea.de/10.1594/PANGAEA.878531
MarinE MethanE and NiTrous Oxide database (MEMENTO)	SST, pN ₂ O _{air} , pN ₂ O _{water}	Kock and Bange, 2015 https://memento.geomar.de/
National Oceanic and Atmospheric Administration, US (NOAA) WAVEWATCH III	U ₁₀ (wind speed at 10m), FOC (wave to turbulent kinetic energy)	WAVEWATCH III development group, 2016
Interpolated and reanalysed fCO₂ field originating from the SOCAT dataset	fCO₂ (interpolated)	Dataset methodology: Woolf <i>et al.</i>, 2019 Resultant fCO₂ data: (Holding <i>et al.</i>, 2018) https://doi.pangaea.de/10.1594/PANGAEA.890118 Original SOCAT dataset: Bakker <i>et al.</i>, 2016 https://www.socat.info/

Table 3: The Earth observation *in situ*, model and climatology data used in this research.

Revision 5/11/2019 10:49
Formatted Table

9. Appendix C: Summary of main toolbox features

Table 4 lists the main features of the FluxEngine toolbox with summaries of their impact for the accurate calculation of atmosphere-ocean gas fluxes.

Revision 5/11/2019 10:49
Deleted: 8

845

Feature or option	Description	Example impact or use
Ability to choose the structure of the bulk gas flux calculation or formulation	The user can choose their bulk formulation, but a formulation based on concentration differences (i.e. containing two solubilities) is advised. This advised formulation enables near-surface temperature and salinity gradients to be included. For reasoning and examples of this advice please see Woolf <i>et al.</i> (2016), Woolf <i>et al.</i> (2019), and Section 1b of Shutler <i>et al.</i> (2016).	Woolf <i>et al.</i> (2019) shows that ignoring vertical temperature and salinity gradients for 2010 results in a 0.35 PgC (12%) bias or underestimate in the oceanic sink of CO ₂ .

Revision 5/11/2019 10:49
Formatted: Font:Italic

Revision 5/11/2019 10:49
Deleted: ..

Revision 5/11/2019 10:49
Deleted: ..

User selectable gas transfer velocity parameterisations	The toolbox includes 14 published wind speed parameterisations and one mean square slope parameterisation, along with a generic user-configurable wind speed parameterisation (see section 7 of the FluxEngine manual). Custom user parameterisations can be added using a Python template (section 9.2 of the FluxEngine manual).	Wrobel and Piskozub (2016) showed that the (model) uncertainty due to the choice of quadratic gas transfer parameterisation led to 9% difference in the gas transfer velocity for the North Atlantic and sub polar waters. This uncertainty increased to 65% when all parameterisations were considered.
Reanalyse fCO₂ data to a reference temperature and depth	The user can reanalyse paired <i>in situ</i> fCO ₂ and SST measurements to a consistent depth using a reference temperature dataset as described by Goddijn-Murphy <i>et al.</i> (2015).	This removes unknown biases due to paired data originating from multiple depths. The depth of <i>in situ</i> data can vary during a single research cruise (e.g. due to sea state or ballasting) and measurements from varying depths becomes a more significant problem when using large collated datasets collected using different measurement systems.
User selectable gas input data types	The user can input atmospheric and marine gas data as partial pressures, fugacities or concentrations.	Allows a wider range of poorly soluble gases to be analysed.
Flexibility to calculate air-sea gas fluxes of multiple poorly soluble gases	The toolbox supports user definable sea-to-air gas flux calculations for CO ₂ , CH ₄ and N ₂ O.	This paper estimates that surfactants can suppress N ₂ O gas fluxes by up to 13% in the North Atlantic.
Accounting for the impact of rain on air-sea gas fluxes	Users can investigate methods that include the different influences that rain can have on air-sea gas fluxes.	Ashton <i>et al.</i> (2016) estimated that rain driven gas transfer and wet deposition of carbon increases the annual oceanic integrated net sink of CO ₂ by up to 6%.
Flexible input data specification and support for <i>in situ</i> data	Tools are provided to support user-specified grid size, temporal resolution, naming conventions and directory structure, automatic unit conversion and conversion between text (ASCII) and netCDF formatted data files.	Allows a wide range of data to be easily used and analysed by the user and the FluxEngine outputs can be easily incorporated into the users original <i>in situ</i> dataset.
Calculate integrated net gas fluxes	A tool for calculating global or regional integrated net gas fluxes (e.g. CO ₂ sink) from netCDF air-sea gas flux data is provided. This enables user defined land, ice and region of interest masks to be used and there are multiple options for handling the impact of sea ice.	Shutler <i>et al.</i> (2016) showed that the calculated net CO ₂ fluxes can vary by 14% for the European shelf sea simply due to differing shelf sea masks, highlighting the need for traceable methods and masks for net flux calculations.
Input data uncertainty analysis	Users can add random noise (with user defined variance and bias) to any input dataset. This enables the users to investigate the impact of input data uncertainties on their air-sea gas flux calculation (e.g. through using an ensemble approach)	Ashton <i>et al.</i> (2016) identified that known uncertainties due to random fluctuations in the input data resulted in a ±1% variation in the monthly net integrated CO ₂ sink. Land <i>et al.</i> (2013) identified that the dominant source of uncertainty in Arctic air-sea gas flux calculations was due to bias in wind speed data (and its impact on the wind speed based gas transfer velocity).

Revision 5/11/2019 10:49
Formatted: Font:Italic

Revision 5/11/2019 10:49
Deleted: .,

Revision 5/11/2019 10:49
Formatted: Font:Italic

Revision 5/11/2019 10:49
Formatted: Font:Italic

Table 4: An overview of the key features provided by the FluxEngine software toolkit and their relevance or use for atmosphere-ocean gas exchange.

10. Appendix D: Installation, verification and benchmarking

855 Installation tools or instructions are provided in the root FluxEngine root directory for the following
operating systems: Ubuntu/Debian based Linux ([install dependencies ubuntu.sh](#)), Apple Mac
([install dependencies macos.sh](#)) and Windows (instructions are within
[FluxEngineV3_instructions.pdf](#)). Two verification utilities (also in located in the root directory) are
provided ([verify_takahashi09.py](#) and [verify_socatv4_sst_salinity_gradients_N00.py](#)). These can be used
860 to verify the successful installation of FluxEngine by running standard global sea-to-air CO₂ gas flux
calculations and net integrated fluxes using the (Takahashi *et al.*, 2009) sea-to-air CO₂ flux climatology
(for year 2000) and the Woolf *et al.* (2019) Surface Ocean CO₂ Atlas (SOCAT, Bakker *et al.*, 2016)
derived sea-to-air CO₂ flux reference dataset for year 2010. Both of these datasets are contained within
Holding *et al.* (2018) and the verification process compares the output from a test run of the toolbox
with the reference data published in Holding *et al.* (2018). The installation is deemed successful if all
865 results are identical to the reference dataset within a precision of 5 decimal places. An additional utility
([run_full_verification.py](#)) enables the user to perform a more detailed verification of different user
defined options that exploit the Woolf *et al.* (2019) reference dataset. This executes a suite of 12
different configurations and scenarios, the justification for which are described within Woolf *et al.*
(2019). Owing to the large volume of data required to execute and verify all of these scenarios, the
870 verification data are not packaged with the standard FluxEngine download, but are all freely available
and contained within Holding *et al.* (2018).

▼
To provide an indication of the execution time a benchmarking analysis was performed using an Intel
875 Core i5 2.7 GHz laptop processor with 8GB RAM running MacOS El Capitan. The automatic
installation took ~3 minutes to complete and the basic verification script using the Woolf *et al.* (2019)
reference dataset (involving a global one year analysis of the gas fluxes for 2010, monthly temporal
resolution and 1° × 1° spatial resolution) took approximately 6 minutes to complete. As the flux
880 calculation is sequential for each grid cell the execution time scales approximately linearly with
number of grid points and number of time steps. Hence, doubling the temporal resolution will
approximately double the execution time, whilst doubling the resolution of both spatial dimensions will
lead to a factor of four increase in execution time.

▲ Author contributions

885 Design and analysis performed by T. Holding, I. Ashton and J. Shutler. Software engineering
performed by T. Holding and I. Ashton. Pre-processing of nitrous oxide data performed by A. Kock.
All authors contributed to the preparation of the manuscript.

Acknowledgements

890 This work was partially funded by the European Space Agency (ESA) Support to Science Element
(STSE) through the OceanFlux Greenhouse Gases project (contract 4000104762/11/I-AM), the
OceanFlux Greenhouse Gases Evolution project (contract 4000112091/14/I-LG), and by the European
Space Agency (ESA) through the Sea surface Kinematics Multiscale monitoring (SKIM) Mission
Science study (contract 4000124734/18/NL/CT/gp) and the ESA SKIM Scientific Performance
895 Evaluation study (contract 4000124521/18/NL/CT/gp), as well as through the NERC RAGNARoCC
project, (grant ref. NE/K002473/1). Further development of FluxEngine was funded by the European

Revision 5/11/2019 10:49
Moved (insertion) [1]

Revision 5/11/2019 10:49
Moved (insertion) [2]

Revision 5/11/2019 10:49
Deleted: .

Revision 5/11/2019 10:49
Moved (insertion) [3]

Revision 5/11/2019 10:49
Moved (insertion) [4]

Revision 5/11/2019 10:49
Moved (insertion) [5]

Revision 5/11/2019 10:49
Formatted: Font:Bold

900 The Surface Ocean CO₂ Atlas (SOCAT) is an international effort, endorsed by the International Ocean Carbon Coordination Project (IOCCP), the Surface Ocean Lower Atmosphere Study (SOLAS) and the Integrated Marine Biosphere Research (IMBeR) program, to deliver a uniformly quality-controlled surface ocean CO₂ database. The many researchers and funding agencies responsible for the collection of data and quality control are thanked for their contributions to SOCAT.

905 CCMP Version-2.0 vector wind analyses are produced by Remote Sensing Systems (<http://www.remss.com>). NCEP Reanalysis data provided by the NOAA/OAR/ESRL PSD, Boulder, Colorado, USA, from their web site at <https://www.esrl.noaa.gov/psd/>.

910 MEMENTO (<https://memento.geomar.de/>) is currently supported by the Kiel Data Management Team at GEOMAR and the BONUS INTEGRAL Project.

This study is a contribution to the international IMBeR project and was supported by the UK Natural Environment Research Council National Capability (CLASS Theme 1.2) funding to Plymouth Marine Laboratory. This is contribution number 330 of the AMT programme.

915 BONUS INTEGRAL receives funding from BONUS (Art 185), funded jointly by the EU, the German Federal Ministry of Education and Research, the Swedish Research Council Formas, the Academy of Finland, the Polish National Centre for Research and Development, and the Estonian Research Council.

920 **Competing interests**

The authors declare that they have no conflict of interest.

925 **References**

- Ashton, I. G., Shutler, J. D., Land, P. E., Woolf, D. K. and Quartly, G. D.: A Sensitivity Analysis of the Impact of Rain on Regional and Global Sea-Air Fluxes of CO₂, edited by M. deCastro, PLoS One, 11(9), e0161105, doi:10.1371/journal.pone.0161105, 2016.
- 930 Atlas, R., Hoffman, R. N., Ardizzone, J., Leidner, S. M., Jusem, J. C., Smith, D. K. and Gombos, D.: A Cross-calibrated, Multiplatform Ocean Surface Wind Velocity Product for Meteorological and Oceanographic Applications, *Bull. Am. Meteorol. Soc.*, 92(2), 157–174, doi:10.1175/2010BAMS2946.1, 2011.
- 935 Bakker, D. C. E., Bange, H. W., Gruber, N., Johannessen, T., Upstill-Goddard, R. C., Borges, A. V., Delille, B., Löscher, C. R., Naqvi, S. W. A., Omar, A. M. and Santana-Casiano, J. M.: Air-Sea Interactions of Natural Long-Lived Greenhouse Gases (CO₂, N₂O, CH₄) in a Changing Climate, pp. 113–169, Springer, Berlin, Heidelberg., 2014.
- 940 Bakker, D. C. E., Pfeil, B., Landa, C. S., Metzl, N. O., Brien, K. M., Olsen, A., Smith, K., Cosca, C., Harasawa, S., Jones, S. D., Nakaoka, S., Nojiri, Y., Schuster, U., Steinhoff, T., Sweeney, C., Takahashi, T., Tilbrook, B., Wada, C., Wanninkhof, R., Alin, S. R., Balestrini, C. F., Barbero, L., Bates, N. R., Bianchi, A. A., Bonou, F., Boutin, J., Bozec, Y., Burger, E. F., Cai, W.-J., Castle, R. D., Chen, L., Chierici, M., Currie, K., Evans, W., Featherstone, C., Feely, R. A., Fransson, A., Goyet, C., Greenwood, N., Gregor, L., Hankin, S., Hardman-Mountford, N. J., Harlay, J., Hauck, J., Hoppema, M., Humphreys, M. P., Hunt, C. W., Huss, B., Ibáñez, J. S. P., Johannessen, T., Keeling, R., Kitidis, V., Körtzinger, A., Kozyr, A., Krasakopoulou, E., Kuwata, A., Landschützer, P., Lauvset, S. K.,

Revision 5/11/2019 10:49

Deleted: Arduin, F., Aksenov, Y., Benetazzo, A., Bertino, L., Brandt, P., Caubet, E., Chapron, B., Collard, F., Cravatte, S., Delouis, J.-M., Dias, F., Dibarboure, G., Gaultier, L., Johannessen, J., Korosov, A., Manucharyan, G., Menemenlis, D., Menendez, M., Monnier, G., Mouche, A., Nouguier, F., Nurser, G., Rampal, P., Reniers, A., Rodriguez, E., Stopa, J., Tison, C., Ubelmann, C., van Sebille, E. and Xie, J.: Measuring currents, ice drift, and waves from space: the Sea surface Kinematics Multiscale monitoring (SKIM) concept, *Ocean Sci.*, 14(3), 337–354, doi:10.5194/os-14-337-2018, 2018. ... [8]

- 965 Lefèvre, N., Lo Monaco, C., Manke, A., Mathis, J. T., Merlivat, L., Millero, F. J., Monteiro, P. M. S., Munro, D. R., Murata, A., Newberger, T., Omar, A. M., Ono, T., Paterson, K., Pearce, D., Pierrot, D., Robbins, L. L., Saito, S., Salisbury, J., Schlitzer, R., Schneider, B., Schweitzer, R., Sieger, R., Skjelvan, I., Sullivan, K. F., Sutherland, S. C., Sutton, A. J., Tadokoro, K., Telszewski, M., Tuma, M., van Heuven, S. M. A. C., Vandemark, D., Ward, B., Watson, A. J. and Xu, S.: A multi-decade record of high-quality fCO₂ data in version 3 of the Surface Ocean CO₂ Atlas (SOCAT), *Earth Syst. Sci. Data*, 8(2), 383–413, doi:10.5194/essd-8-383-2016, 2016.
- 970 Boyer, T.P., J. I. Antonov, O. K. Baranova, C. Coleman, H. E. Garcia, A. Grodsky, D. R. Johnson, R. A. Locarnini, A. V. Mishonov, T.D. O'Brien, C.R. Paver, J.R. Reagan, D. Seidov, I. V. Smolyar, and M. M. Z.: World Ocean Database 2013, NOAA Atlas NESDIF, 72, 209, doi:10.7289/V5NZ85MT, 2013.
- 975 Brown, I. and Rees, A.: Nitrous Oxide measurements from CTD collected depth profiles along a North-South transect in the Atlantic Ocean on cruise JR303/AMT24/JR20140922, *Br. Oceanogr. Data Cent. - Nat. Environ. Res. Counc. UK*, doi:10.5285/7cbcd206-c122-2777-e053-6c86abc041f9, 2018.
- 980 Craig, P. D., Banner, M. L. and Craig, P. D.: Modeling Wave-Enhanced Turbulence in the Ocean Surface Layer, *J. Phys. Oceanogr.*, 24(12), 2546–2559, doi:10.1175/1520-0485(1994)024<2546:MWETIT>2.0.CO;2, 1994.
- 985 Donlon, C., Robinson, I. S., Wimmer, W., Fisher, G., Reynolds, M., Edwards, R. and Nightingale, T. J.: An Infrared Sea Surface Temperature Autonomous Radiometer (ISAR) for Deployment aboard Volunteer Observing Ships (VOS), *J. Atmos. Ocean. Technol.*, 25(1), 93–113, doi:10.1175/2007JTECHO505.1, 2008.
- 990 Fairall, C. W., Bradley, E. F., Rogers, D. P., Edson, J. B. and Young, G. S.: Bulk parameterization of air-sea fluxes for Tropical Ocean-Global Atmosphere Coupled-Ocean Atmosphere Response Experiment, *J. Geophys. Res. Ocean.*, 101(C2), 3747–3764, doi:10.1029/95JC03205, 1996.
- 995 GEBCO: The GEBCO Digital Atlas published by the British Oceanographic Data Centre on behalf of IOC and IHO, 2003.
- 1000 GLOBALVIEW-CO₂: Cooperative Global Atmospheric Data Integration Project. 2013, updated annually. Multi-laboratory compilation of synchronized and gap-filled atmospheric carbon dioxide records for the period 1979-2012 (obspack_co2_1_GLOBALVIEW-CO2_2013_v1.0.4_2013-12-23), Compil. by NOAA Glob. Monit. Division, doi:10.3334/OBSPACK/1002, 2013.
- 1005 Goddijn-Murphy, L. M., Woolf, D. K., Land, P. E., Shutler, J. D. and Donlon, C.: The OceanFlux Greenhouse Gases methodology for deriving a sea surface climatology of CO₂ fugacity in support of air-sea gas flux studies, *Ocean Sci.*, 11(4), 519–541, doi:10.5194/os-11-519-2015, 2015.
- 1010 Henson, S. A., Humphreys, M. P., Land, P. E., Shutler, J. D., Goddijn-Murphy, L. and Warren, M.: Controls on open-ocean North Atlantic ΔpCO₂ at seasonal and interannual timescales are different, *Geophys. Res. Lett.*, 45(17), 9067–9076, doi:10.1029/2018GL078797, 2018.
- 1015 Ho, D. T., Law, C. S., Smith, M. J., Schlosser, P., Harvey, M. and Hill, P.: Measurements of air-sea gas exchange at high wind speeds in the Southern Ocean: Implications for global parameterizations, *Geophys. Res. Lett.*, 33(16), L16611, doi:10.1029/2006GL026817, 2006.
- 1020 Ho, D. T., Veron, F., Harrison, E., Bliven, L. F., Scott, N. and McGillis, W. R.: The combined effect of rain and wind on air-water gas exchange: A feasibility study, *J. Mar. Syst.*, 66(1–4), 150–160, doi:10.1016/J.JMARSYS.2006.02.012, 2007.
- 1025 Holding, J., Ashton, J., Woolf, D. K. and Shutler, J. D.: FluxEngine v2.0 and v3.0 reference and verification data, PANGAEA, doi:10.1594/PANGAEA.890118, 2018.
- 1025 IPCC: Climate Change 2013: The Physical Science Basis. Contribution of Working Group I to the Fifth Assessment Report of the Intergovernmental Panel on Climate Change, edited by V. B. and P. M. M. Stocker, T.F., D. Qin, G.-K. Plattner, M. Tignor, S.K. Allen, J. Boschung, A. Nauels, Y. Xia, Cambridge University Press, Cambridge, United Kingdom and New York, NY, USA, 1535 pp. [online] Available from: <https://www.ipcc.ch/report/ar5/wg1/>, 2013.
- 1025 Jähne, B., Münnich, K. O., Börsinger, R., Dutzi, A., Huber, W. and Libner, P.: On the parameters influencing air-water gas exchange, *J. Geophys. Res.*, 92(C2), 1937–1949,

Revision 5/11/2019 10:49

Deleted: Thomas;

Revision 5/11/2019 10:49

Deleted: Ian;

Revision 5/11/2019 10:49

Deleted: David

Revision 5/11/2019 10:49

Deleted: ;

- 1035 Kalnay, E., Kanamitsu, M., Kistler, R., Collins, W., Deaven, D., Gandin, L., Iredell, M., Saha, S., White, G., Woollen, J., Zhu, Y., Leetmaa, A., Reynolds, R., Chelliah, M., Ebisuzaki, W., Higgins, W., Janowiak, J., Mo, K. C., Ropelewski, C., Wang, J., Jenne, R., Joseph, D., Kalnay, E., Kanamitsu, M., Kistler, R., Collins, W., Deaven, D., Gandin, L., Iredell, M., Saha, S., White, G., Woollen, J., Zhu, Y., Chelliah, M., Ebisuzaki, W., Higgins, W., Janowiak, J., Mo, K. C., Ropelewski, C., Wang, J., Leetmaa, A., Reynolds, R., Jenne, R. and Joseph, D.: The NCEP/NCAR 40-Year Reanalysis Project, *Bull. Am. Meteorol. Soc.*, 77(3), 437–471, doi:10.1175/1520-0477(1996)077<0437:TNYRP>2.0.CO;2, 1996.
- 1040 Kitidis, Vassilis; Brown, I.: Underway physical oceanography and carbon dioxide measurements during James Clark Ross cruise 74JC20131009, PANGAEA, doi:10.1594/PANGAEA.878492, 2017.
- 1045 Kock, A. and Bange, H.: Counting the Ocean's Greenhouse Gas Emissions, *Earth Sp. Sci. News*, 96, doi:10.1029/2015EO023665, 2015.
- 1050 Kock, A., Schafstall, J., Dengler, M., Brandt, P. and Bange, H. W.: Sea-to-air and diapycnal nitrous oxide fluxes in the eastern tropical North Atlantic Ocean, *Biogeosciences*, 9(3), 957–964, doi:10.5194/bg-9-957-2012, 2012.
- 1055 Laruelle, G. G., Cai, W.-J., Hu, X., Gruber, N., Mackenzie, F. T. and Regnier, P.: Continental shelves as a variable but increasing global sink for atmospheric carbon dioxide., *Nat. Commun.*, 9(1), 454, doi:10.1038/s41467-017-02738-z, 2018.
- 1060 M. M. Zweng, Reagan, J. R., Seidov, D., Boyer, T. P., Locarnini, R. A., Garcia, H. E., Mishonov, A. V., Baranova, O. K., Weathers, K., Paver, C. R. and Smolyar, I.: WORLD OCEAN ATLAS 2018 Volume 2: Salinity (pre-release). [online] Available from: <http://www.nodc.noaa.gov/> (Accessed 26 March 2019), 2018.
- 1065 McKenna, S. P. and Bock, E. J.: Physicochemical effects of the marine microlayer on air-sea gas transport, in *Marine Surface Films*, pp. 77–91, Springer-Verlag, Berlin/Heidelberg., 2006.
- 1070 Mesarchaki, E., Kräuter, C., Krall, K. E., Bopp, M., Helleis, F., Williams, J. and Jähne, B.: Measuring air–sea gas-exchange velocities in a large-scale annular wind–wave tank, *Ocean Sci.*, 11(1), 121–138, doi:10.5194/os-11-121-2015, 2015.
- 1075 Nightingale, P. D., Malin, G., Law, C. S., Watson, A. J., Liss, P. S., Liddicoat, M. I., Boutin, J. and Upstill-Goddard, R. C.: In situ evaluation of air-sea gas exchange parameterizations using novel conservative and volatile tracers, *Global Biogeochem. Cycles*, 14(1), 373–387, doi:10.1029/1999GB900091, 2000.
- 1075 Pereira, R., Schneider-Zapp, K. and Upstill-Goddard, R. C.: Surfactant control of gas transfer velocity along an offshore coastal transect: results from a laboratory gas exchange tank, *Biogeosciences*, 13(13), 3981–3989, doi:10.5194/bg-13-3981-2016, 2016.
- 1080 Pereira, R., Ashton, I., Sabbaghzadeh, B., Shutler, J. D. and Upstill-Goddard, R. C.: Reduced air–sea CO₂ exchange in the Atlantic Ocean due to biological surfactants, *Nat. Geosci.*, 11(7), 492–496, doi:10.1038/s41561-018-0136-2, 2018.
- 1085 Ravishankara, A. R., Daniel, J. S. and Portmann, R. W.: Nitrous oxide (N₂O): the dominant ozone-depleting substance emitted in the 21st century., *Science*, 326(5949), 123–5, doi:10.1126/science.1176985, 2009.
- 1085 Reynolds, R. W., Smith, T. M., Liu, C., Chelton, D. B., Casey, K. S. and Schlax, M. G.: Daily High-Resolution-Blended Analyses for Sea Surface Temperature, *J. Clim.*, 20(22), 5473–5496, doi:10.1175/2007JCLI1824.1, 2007.
- 1090 Rödenbeck, C., Bakker, D. C. E., Gruber, N., Iida, Y., Jacobson, A. R., Jones, S., Landschützer, P., Metzl, N., Nakaoka, S., Olsen, A., Park, G.-H., Peylin, P., Rodgers, K. B., Sasse, T. P., Schuster, U., Shutler, J. D., Valsala, V., Wanninkhof, R. and Zeng, J.: Data-based estimates of the ocean carbon sink variability - First results of the Surface Ocean pCO₂ Mapping intercomparison (SOCOM), *Biogeosciences*, 12(23), 7251–7278, doi:10.5194/bg-12-7251-2015, 2015.
- 1095 Rutgersson, A.: Time series of physical oceanography and carbon dioxide measurements at mooring site OSTERGARNSHOLM - 77FS20150128, PANGAEA, doi:10.1594/PANGAEA.878531, 2017.

- 1100 | Salter, M. E., Upstill-Goddard, R. C., Nightingale, P. D., Archer, S. D., Blomquist, B., Ho, D. T., Huebert, B., Schlosser, P. and Yang, M.: Impact of an artificial surfactant release on air-sea gas fluxes during Deep Ocean Gas Exchange Experiment II, *J. Geophys. Res.*, 116(C11), C11016, doi:10.1029/2011JC007023, 2011.
- Schuster, U.: Underway physical oceanography and carbon dioxide measurements during Benguela Stream cruise 642B20131005, PANGAEA, doi:10.1594/PANGAEA.852980, 2016.
- 1105 | Shutler, J. D., Land, P. E., Piolle, J. F., Woolf, D. K., Goddijn-Murphy, L., Paul, F., Girard-Arduin, F., Chapron, B. and Donlon, C. J.: FluxEngine: A flexible processing system for calculating atmosphere-ocean carbon dioxide gas fluxes and climatologies, *J. Atmos. Ocean. Technol.*, 33(4), 741–756, doi:10.1175/JTECH-D-14-00204.1, 2016.
- 1110 | [Shutler, J. D., Wanninkhof, R., Nightingale, P. D., Woolf, D. K., Bakker, D. C., Watson, A., Ashton, I., Holding, T., Chapron, B., Quilfen, Y., Fairall, C., Schuster, U., Nakajima, M. and Donlon, C. J.: Satellites will address critical science priorities for quantifying ocean carbon, *Front. Ecol. Environ.*, fee.2129, doi:10.1002/fee.2129, 2019.](#)
- 1115 | Steinhoff, Tobias; Becker, Meike; Körtzinger, A.: Underway physical oceanography and carbon dioxide measurements during Atlantic Companion cruise 77CN20131004, PANGAEA, doi:10.1594/PANGAEA.852786, 2016.
- 1120 | Takahashi, T., Sutherland, S. C., Wanninkhof, R., Sweeney, C., Feely, R. A., Chipman, D. W., Hales, B., Friederich, G., Chavez, F., Sabine, C., Watson, A., Bakker, D. C. E., Schuster, U., Yoshikawa-Inoue, H., Ishii, M., Midorikawa, T., Nojiri, Y., Körtzinger, A., Steinhoff, T., Hoppema, M., Olafsson, J., Arnarson, T. S., Johannessen, T., Olsen, A., Bellerby, R., Wong, C. S., Delille, B., Bates, N. R. and de Baar, H. J. W.: Climatological mean and decadal change in surface ocean pCO₂, and net sea-air CO₂ flux over the global oceans, *Deep Sea Res. Part II Top. Stud. Oceanogr.*, 56(8–10), 554–577, doi:10.1016/J.DSR2.2008.12.009, 2009.
- 1125 | Tarran, G.: AMT 28 Cruise Report. [online] Available from: https://amt-uk.org/getattachment/Cruises/AMT28/AMT_28_CRUISE_REPORT_RS.pdf, 2018.
- 1130 | Wanninkhof, Rik; Pierrot, D.: Underway physical oceanography and carbon dioxide measurements during REYKJAFLOSS cruise 64RJ20131017, PANGAEA, doi:10.1594/PANGAEA.866092, 2016.
- 1135 | Wanninkhof, R.: Relationship between wind speed and gas exchange over the ocean, *J. Geophys. Res.*, 97(C5), 7373, doi:10.1029/92JC00188, 1992.
- Wanninkhof, R.: Relationship between wind speed and gas exchange over the ocean revisited, *Limnol. Oceanogr. Methods*, 12(6), 351–362, doi:10.4319/lom.2014.12.351, 2014.
- 1140 | WAVEWATCH III development group: User manual and system documentation of WAVEWATCH III version 5.16, Technical Note 329., 2016.
- 1145 | Woolf, D. K., Land, P. E., Shutler, J. D., Goddijn-Murphy, L. M. and Donlon, C. J.: On the calculation of air-sea fluxes of CO₂ in the presence of temperature and salinity gradients, *J. Geophys. Res. Ocean.*, 121(2), 1229–1248, doi:10.1002/2015JC011427, 2016.
- 1150 | Woolf, D. K., Shutler, J. D., Goddijn-Murphy, L., Watson, A. J., Chapron, B., Nightingale, P. D., Donlon, C. J., Piskozub, J., Yelland, M. J., Ashton, I., Holding, T., Schuster, U., Girard-Arduin, F., Grouazel, A., Piolle, J. -F., Warren, M., Wrobel-Niedzwiecka, I., Land, P. E., Torres, R., Prytherch, J., Moat, B., Hanafin, J., Arduin, F. and Paul, F.: Key Uncertainties in the Recent Air-Sea Flux of CO₂, *Global Biogeochem. Cycles*, 0–3, doi:10.1029/2018gb006041, 2019.
- 1155 | Wrobel, I.: Monthly dynamics of carbon dioxide exchange across the sea surface of the Arctic Ocean in response to changes in gas transfer velocity and partial pressure of CO₂ in 2010, *Oceanologia*, 59(4), 445–459, doi:10.1016/J.OCEANO.2017.05.001, 2017.
- Wrobel, I. and Piskozub, J.: Effect of gas-transfer velocity parameterization choice on air-sea CO₂ fluxes in the North Atlantic Ocean and the European Arctic, *Ocean Sci.*, 12(5), 1091–1091, 2016.
- 1160 | Zappa, C. J., McGillis, W. R., Raymond, P. A., Edson, J. B., Hints, E. J., Zemmellink, H. J., Dacey, J. W. H. and Ho, D. T.: Environmental turbulent mixing controls on air-water gas exchange in marine and aquatic systems, *Geophys. Res. Lett.*, 34(10), L10601, doi:10.1029/2006GL028790, 2007.

The FluxEngine air-sea gas flux toolbox: simplified interface and extensions for *in situ* analyses and multiple sparingly soluble gases

Thomas Holding¹, Ian G. Ashton¹, Jamie D. Shutler¹, Peter E. Land², Philip D. Nightingale², Andrew P. Rees², Ian Brown², Jean-Francois Piolle³, Annette Kock⁴, Hermann W Bange⁴, David K. Woolf⁵, Lonneke Goddijn-Murphy⁶, Ryan Pereira⁷, Frederic Paul³, Fanny Girard-Ardhuin³, Bertrand Chapron³, Gregor Rehder⁸, Fabrice Ardhuin³, Craig J. Donlon⁹

¹University of Exeter, Penryn Campus, Cornwall, TR10 9EZ, UK.

²Plymouth Marine Laboratory, Prospect Place, Plymouth, PL1 3DH, UK.

³Ifremer, Univ. Brest, CNRS, IRD, Laboratoire d’Oceanographie Physique et Spatiale (LOPS), IUEM, Brest, France.

⁴GEOMAR Helmholtz Centre for Ocean Research Kiel, Marine Biogeochemistry Research Division, 24105 Kiel, Germany.

⁵International Centre for Island Technology, Heriot-Watt University, Stromness, Orkney, KW16 3AW, UK.

⁶Environmental Research Institute, University of the Highlands and Islands, Thurso, KW14 7EE, UK

⁷The Lyell Centre, Heriot-Watt University, Research Avenue South, Edinburgh, EH14 4AS, UK.

⁸Leibniz-Institute for Baltic Sea Research Warnemünde, 18119 Rostock, Germany.

⁹European Space Agency, Noordwijk, The Netherlands.

Correspondence to: Thomas Holding (t.m.holding@exeter.ac.uk)

Abstract. The flow (flux) of climate critical gases, such as carbon dioxide (CO₂), between the ocean and the atmosphere is a fundamental component of our climate and an important driver of the biogeochemical systems within the oceans. Therefore, the accurate calculation of these air-sea gas fluxes is critical if we are to monitor the oceans and assess the impact that these gases are having on Earth’s climate and ecosystems. FluxEngine is an open source software toolbox that allows users to easily perform calculations of air-sea gas fluxes from model, *in-situ* and Earth observation data. The original development and verification of the toolbox was described in a previous publication. The toolbox has now been considerably updated to allow its use as a Python library, to enable simplified installation, verification of its installation, to enable the handling of multiple sparingly soluble gases and greatly expanded functionality for supporting *in situ* dataset analyses. This new functionality for supporting *in situ* analyses includes user-defined grids, time periods and projections, the ability to re-analyse *in situ* CO₂ data to a common temperature dataset and the ability to easily calculate gas fluxes using *in situ* data from drifting buoys, fixed moorings and research cruises. Here we describe these new capabilities and then demonstrate their application through illustrative case studies. The first case study demonstrates the workflow for accurately calculating CO₂ fluxes using *in situ* data from four research cruises from the Surface Ocean CO₂ Atlas (SOCAT) database. The second case study calculates air-sea CO₂ fluxes using *in situ* data from a fixed monitoring station in the Baltic Sea. The third case study focuses on nitrous oxide (N₂O) and through a user defined gas transfer parameterisation identifies that

biological surfactants in the North Atlantic could suppress individual N₂O sea-air gas fluxes by up to 13%. The fourth and final case study illustrates how a dissipation-based gas transfer parameterisation can be implemented and used. The updated version of the toolbox (version 3) and all documentation is now freely available.

1. Introduction

The exchange of climate relevant gases between the oceans and atmosphere including that of carbon dioxide (CO₂), nitrous oxide (N₂O) and methane (CH₄) is a major component of the climate system, and the ability of the oceans to absorb and desorb these gases varies both temporally and spatially. The need to monitor this exchange has been the driver for international data collation initiatives such as the Surface Ocean CO₂ ATlas (SOCAT, (Bakker *et al.*, 2016)) and the MarinE MethanE and NiTrous Oxide database (MEMENTO, (Kock and Bange, 2015)). These collaborative efforts are now routinely collecting, quality controlling and collating over a million new *in situ* data points each year. FluxEngine complements these initiatives by providing a standardised tool, which can robustly calculate air-sea gas fluxes from such *in situ* data, with the flexibility to incorporate new data sources and methodologies. The use of common tools and methods simplifies collaborations and accelerates advancements, both within and between scientific disciplines, through eliminating methodological or implementation-driven differences and the duplication of effort.

1.0 Overview of FluxEngine

FluxEngine is a flexible open source toolbox that allows users to easily exploit Earth observation and model data, in combination with *in situ* data, to calculate air-sea gas fluxes (Shutler *et al.*, 2016). It is available to download from <http://github.com/oceanflux-ghg/FluxEngine>. The toolbox uses plain text-format configuration files allowing the user to configure the input data sources, random noise or bias on input data, the temporal period for the analysis, the structure of the air-sea gas flux calculation and user-defined gas transfer velocity parameterisations. The calculation itself can be performed using fugacity, partial pressure or concentration data, via a user defined bulk formulation, including formulations that can account for vertical temperature gradients across the mass boundary layer, the very small layer at the surface over which gas exchange occurs. A full description of the differences between the different flux formulations is provided in Shutler *et al.* (2016) and Woolf *et al.* (2016). The formulation that enables vertical temperature and salinity gradients to be included allowing a more accurate gas flux calculation is described in detail by Woolf *et al.* (2016) and takes the generalised form of

$$F = k(\alpha_w f_{G_w} - \alpha_s f_{G_a}) \quad (1)$$

where F is the sea-to-air flux of a sparingly soluble gas G , k is the gas transfer velocity, α_s and α_w are the solubilities of the gas above and below the surface water interface and f_{G_a} and f_{G_w} are the respective fugacities. Here we use ‘p’ and ‘f’ prefixes to refer to partial pressure and fugacity of a gas, respectively. Gas transfer velocity is driven by turbulence at ocean surface, caused by wind stress and wave breaking, amongst other processes. Because of the wide availability of high quality wind data products and the relative difficulty of directly measuring turbulence, it is commonplace to estimate k

using a statistical relationship with wind speed, (e.g. Ho *et al.*, 2006; Nightingale *et al.*, 2000; Wanninkhof, 2014).

90 Concentration of the gas is determined by its solubility and fugacity (or partial pressure). Equation (1) can therefore be rewritten as a product of the gas transfer velocity and the difference in gas concentrations,

$$F = k(G_W - G_S) \quad (2)$$

95 where G_S and G_W are the concentration of the gas above and below the interface. The FluxEngine configuration file allows users to choose the structure of the gas flux calculation, the inputs and the gas transfer velocity (either by choosing an already implemented published algorithm or through parameterising their own). The user can then perform calculations across their chosen input data and the outputs are Climate Forecast (CF) standard netCDF 4.0 files that contain data layers for each of the stages of the calculation, along with process indicator layers to aid the interpretation of the calculated gas fluxes (such as surface chlorophyll-a concentrations, the climatological position of temperature fronts and error indicator layers). A summary of the main features of the toolbox is given in Table 4 (appendix C).

105 Version 1.0 of FluxEngine was introduced and described by (Shutler *et al.*, 2016), which included a full description of the calculations, the flexibility of the toolbox, and the extensive verification of the different calculations along with examples of its use. With the aim to provide a standardised community tool, development has continued since its original release. Feedback from the user communities and the needs of specific scientific studies (e.g. Ashton *et al.*, 2016) have guided these developments and considerable extended the functionality and range of possible applications.

115 At the time of writing, the toolbox and resulting data have been used to quantify regional and global uncertainties (e.g. Wrobel and Piskozub, 2016; Wrobel, 2017; Woolf *et al.*, 2019; Shutler *et al.*, 2019), evaluate the impact of gas transfer processes on regional and global gas exchange (e.g. Ashton *et al.*, 2016; Pereira *et al.*, 2018), evaluate the European shelf sea CO₂ gas-fluxes and sink (Shutler *et al.*, 2016) and investigate biological and physical controls of air-sea exchange (Henson *et al.*, 2018). FluxEngine has also been used to identify shortfalls of current modelling approaches through the inclusion of FluxEngine outputs within an international inter-comparison (Rödenbeck *et al.*, 2015). The toolbox has also been incorporated within undergraduate and postgraduate teaching at the University of Exeter within geography, environmental science and marine biology degrees, and at Utrecht University for computer science.

125 This paper uses four case studies to illustrate key developments and the extended capabilities now contained within version 3.0 of the FluxEngine toolbox. Collectively, the case studies illustrate user selectable grids, support for calculating sea-to-air gas fluxes from time series data collected by fixed monitoring stations and research cruises (and how to incorporate the flux outputs into the original dataset to create a coherent time series), and the ability to calculate nitrous oxide (N₂O) sea-to-air gas fluxes, the addition of a new forcing variable (kinetic energy dissipation rate). The extensive support for *in situ* data contained within version 3 of FluxEngine means that it can now be fully exploited by

130 three different scientific communities in isolation: *in situ*, model and Earth observation; whilst the
original capability to enable gas fluxes to be calculated from combinations of *in situ*, model and Earth
observation data is retained.

135 Section 2 of this paper describes the structural extensions and changes and explains how the toolbox
can now be used as a command line tool or as a Python library. Section 3 then presents the case studies,
while section 4 outlines the future direction and developments for the toolbox and section 5 gives
conclusions. To aid the user the Appendices of this paper provide a list all of the toolbox utilities (Sect.
140 7), details of all data sets used in the case studies (Sect. 8), an overview of the main toolbox features
and options (Sect. 9) and a description of the automatic software installers and verification tools (Sect.
10).

2. New capabilities

The following sections describe the extensions to the FluxEngine toolbox that are now contained within
version 3.

145

2.1. Installation, verification and use

FluxEngine has now been optimised for use on a standalone desktop or laptop computer, removing the
previous requirement for specialist computing facilities. Installation tools or instructions are provided
for Microsoft Windows, Apple MacOS and Ubuntu/Debian based Linux operating systems. Separate
150 utilities can then be used to verify that FluxEngine has been successfully installed. Details of the
installation, verification process and execution times are provided in Sect. 10.

FluxEngine is now implemented as a Python module, which means that FluxEngine and its
accompanying utilities can be imported as a Python module and easily integrated with other software or
155 used as stand-alone tools that are called from the command line. This approach offers a larger degree of
flexibility than offered by version 1 of the toolbox and supports advanced exploitation. For example, a
simple Python script can be written to run a sensitivity analysis where ensembles of flux calculations
are required without any need to modify the underlying FluxEngine software.

2.2. Flexible input data specification

Previous versions of FluxEngine required the user to make changes to the underlying software in order
to use new or differently formatted sources of input data. This required additional (and time
consuming) testing and verification after modifications were made, making FluxEngine less accessible
to those unfamiliar to Python programming. Two features have been added in version 3.0 to address
165 this issue: i) file pattern matching (through standard Unix glob patterns and custom date/time tokens,
described fully in *FluxEngineV3_instructions.pdf*) allows input file name format and directory structure
to be customised using the plain text configuration file, ii) optional pre-processing functions can be
used to manipulate input data after the data have been read into memory. These features can be
specified for each input variable in the configuration file and FluxEngine contains a selection of
170 common pre-processing functions, such as unit conversions or matrix transformation of the input data.
Additional custom pre-processing functions can be added and tested easily by the user without the need
to modify the core FluxEngine software, through copying and then completing the Python template
function provided within the source code (*data_preprocessing.py*). Storing the completed function into

175 the `data_preprocessing.py` file will then result in the custom pre-processing function being automatically available for use in any configuration files.

These features make it possible to use any observational netCDF dataset by specifying the file path and, if required, appropriate pre-processing functions. For example a custom pre-processing function could resample the input files, followed by a transformation to change the projection. This flexibility is conceptualised by the diagram in Fig. 1.

180

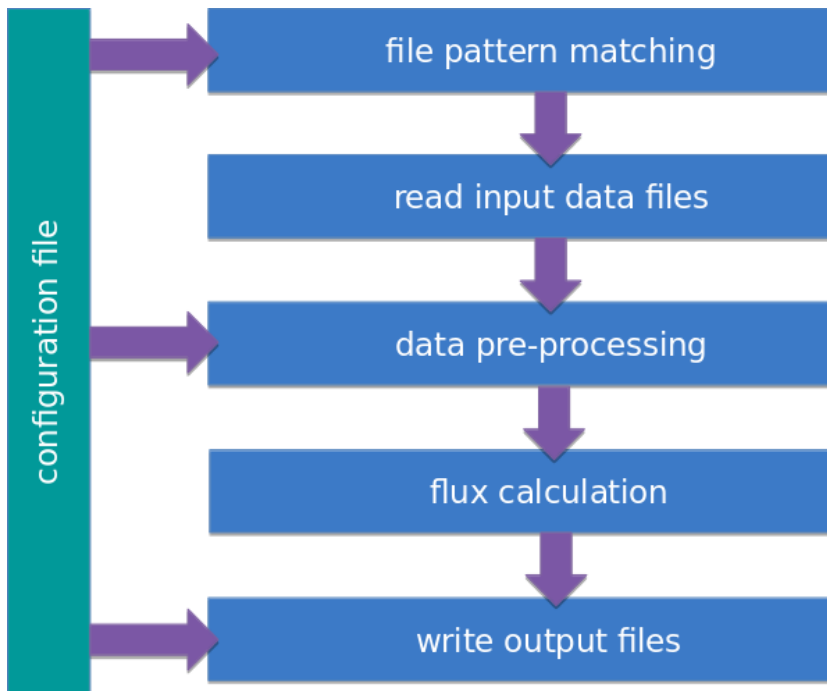


Figure 1: Conceptual diagram showing the way that input data are imported and used by FluxEngine. Single or groups of files are specified using a plain text configuration file. File names are interpreted using a subset of regular expression matching syntax (Unix glob patterns) and additional tokens are used to substitute time and date. The data pre-processing steps occur after input files are read into memory. Pre-processing functions are specified in the configuration file. Finally, the netCDF output files follow a user-specified filename and directory structure (as specified in the configuration file).

2.3. Extensive support for *in situ* data analyses

185 Version 1 of FluxEngine required that all input data be supplied as monthly $1^\circ \times 1^\circ$ global grids. These constraints restricted its relevance to regional analyses and *in situ* analyses, where sub-daily or sub-km resolutions are often more appropriate. The spatial resolution and extent can now be fully specified by the user and regional masks can be used in conjunction with the `ofluxghg_flux_budgets.py` tool to calculate regional net integrated fluxes. In addition, flexible start and stop times and user-specified

190 temporal resolution allows gas fluxes to be calculated for specific time intervals, e.g. the calculation can be configured to match the temporal resolution of the *in situ* data. Furthermore, a new

configuration option allows output from multiple time points to be grouped into a single netCDF file (rather than multiple files, one for each time point). This enables the calculation of gas fluxes from fixed research stations and other scenarios in which it is more convenient to provide results as a time-series.

195

Improvements have been made to the bundled file conversion utilities, which convert between plain text data formats and the netCDF format used by FluxEngine. By default, these tools use the SOCAT format (Bakker *et al.*, 2016) for convenience, but now offer a high degree of flexibility to reflect the variety of data formats and conventions used for storing *in situ* data. This means that the tools can be used with virtually any text formatted *in situ* data files, avoiding the need for the user to convert their data to a fixed format with predefined column names.

200

The new utility, *append2insitu.py*, is designed specifically for use with *in situ* data and appends FluxEngine output as new columns within the original *in situ* data (achieved by matching spatial and temporal coordinates). For example, this means that users can use SOCAT (or custom) formatted *in situ* data as input to FluxEngine and then the results can be placed into a copy of the original input file, allowing the user to study the calculated fluxes, gas transfer rates, gas concentrations etc. alongside (and aligned with) their original *in situ* data. This functionality is demonstrated in case studies one and three within this paper.

205

210

2.4. Reanalysis of *in situ* CO₂ fugacity data to a consistent temperature and depth

A new utility, *reanalyse_socat_driver.py*, is CO₂ specific and exploits a reference SST dataset (e.g. climate quality Earth observation SST data) and the original paired *in situ* measurements of CO₂ fugacity (fCO₂) and temperature to re-calculate the fCO₂ for the reference temperature dataset (and thus a consistent depth). The reasoning for the reanalysis is to reduce uncertainty and unknown biases that arise due to the fCO₂ measurements being collected using different instrumentation at some unknown and potentially variable depth below the surface. A detailed justification of the method and a full description of the approach are described in Goddijn-Murphy *et al.* (2015).

215

220

The reanalysis step is especially important if *in situ* data consisting of a collated dataset (originating from different instruments, sampling strategies or sources) is being used to calculate temporally averaged gas fluxes (e.g. monthly mean values). In this situation the *in situ* measurements are highly likely to be collected from a range of different depths and unlikely to fully capture the monthly mean conditions of temperature and fCO₂ (due to aliasing). Whereas temporally averaged (mean) satellite observations are likely to provide a better representation (reference) of the mean temperature conditions. Therefore re-analysing the collated fCO₂ dataset to this reference temperature enables the calculation of the equivalent mean fCO₂ data.

225

230 It is worth noting that ship draught, and thus underway measurement intake depth, can even vary on a
single research cruise due to changes in sea state, ballasting or cargo. So the method can also be
important for data collected during a single research cruise.

For the case studies presented here the satellite observed SST data used for the reanalysis are valid for a
235 depth of ~1 m (Reynolds *et al.* 2007). So the re-calculated $f\text{CO}_2$ are therefore also valid for this depth,
and are used to represent the conditions at the bottom of the mass boundary layer or sub-skin
temperature. The reanalysis to a consistent depth also enables a more accurate calculation of the gas
fluxes, as it is then possible to accurately calculate two solubilities and thus two concentrations, one at
the bottom, and one at the top of the mass boundary layer.

240 The Goddijn-Murphy *et al.* (2015) re-analysis method relies upon variations in $f\text{CO}_2$ being purely
isochemical. This assumes that the total dissolved inorganic carbon is approximately constant
throughout the surface waters over the temporal period and spatial scale being studied, and that
differences in $f\text{CO}_2$ are solely due to temperature differences altering the equilibria of the carbonate
245 system. Therefore caution should be used when applying the reanalysis method to data where these
assumptions are not valid.

The slow re-equilibrium time of CO_2 in seawater (i.e. on the order of months for CO_2 to equilibrate
with the atmosphere) ensure that monthly mean, or rolling monthly mean (centred on the day of
250 interest) skin or sub-skin sea surface temperature (SST) values are suitable for re-analysing the *in situ*
data. Arguably for re-analysing individual *in situ* datasets (e.g. to calculate gas fluxes for a single cruise
dataset) a robust daily skin or sub-skin SST value would be better, even if that is obtained by a seasonal
curve fitted to the monthly values and interpolated to the day of interest. Another solution would be to
collect paired measurements of skin SST, and $f\text{CO}_2$ and SST at depth, all *in situ*, as has been done on a
255 recent research cruise (Tarran, 2018) as ship-ready instruments are available, e.g. the Infrared Sea
surface Autonomous Radiometer (ISAR, Donlon *et al.*, 2008). This enables the paired measurements at
depth to be re-analysed using the *in situ* skin SST. However in the majority of cases ships collecting
 $f\text{CO}_2$ data do not collect skin data. Where *in situ* skin temperature data are not available and satellite
temperature data are not appropriate, a regional model could be used to estimate skin temperature from
260 the SST a few metres below the surface. An example model capable of this is the US National Oceanic
and Atmospheric Administration (NOAA) Coupled Ocean-Atmosphere Response Experiment
(COARE) model (e.g. see Fairall *et al.*, 1996).

265 Whilst the reanalysis method and utility is CO₂ specific, its applicability to alternative gases (including unreactive N₂O and CH₄) is discussed and shown in Table 1 of (Woolf *et al.*, 2016). The impact on the net gas fluxes of not performing this reanalysis on a relatively large time series of CO₂ measurements through the north and south Atlantic is demonstrated within case study one (Sect. 3.1), whereas the impact on global net integrated gas fluxes has been analysed by Woolf *et al.* (2019).

270 A typical workflow for calculating sea-to-air gas fluxes from *in situ* data using FluxEngine, and the tools used at each step, is illustrated in Fig. 2. All of the *in situ* analysis utilities, including the use of the *reanalyse_socat_driver.py* tool, are demonstrated in case studies one to three (Sect. 3).

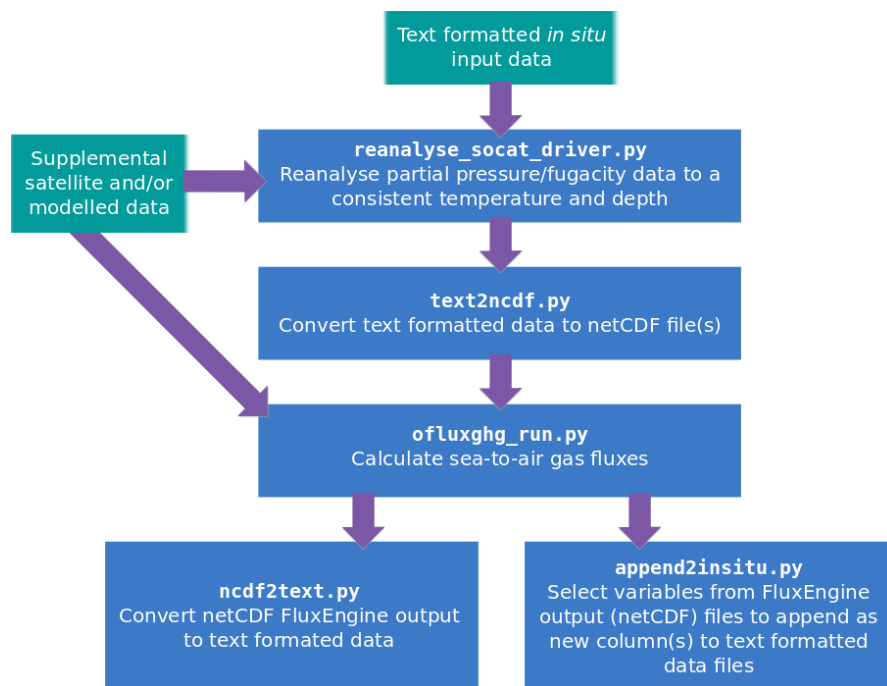


Figure 2: A typical CO₂ workflow for using FluxEngine with *in situ* data, showing the different utilities (blue boxes) and input data (green boxes) used at each stage.

275

2.5. Custom gas transfer velocity parameterisation

The processes that govern exchange, their relative importance and how gas exchange should be parameterised are all active areas of research (e.g. Pereira *et al.* (2018); Wrobel and Piskozub, (2016)).

280

FluxEngine has always allowed users to select or define different gas transfer velocity parameterisations. However, version 3.0 adopts a modular approach to specifying the flux calculation, which makes it simpler for the user to extend the functionality and incorporate new gas transfer parameterisations. Custom parameterisations can be implemented as separate Python classes without

285 modifying the core FluxEngine software. This is achieved by copying and modifying the template class
provided in *rate_parameterisation.py*. Storing the new class within *rate_parameterisation.py* means
that the new parameterisation will be automatically available for inclusion in the configuration file.
These custom parameterisations can define new input variables and therefore make use of additional
input data sources. These custom parameterisations can also produce new data layers in the final
290 netCDF output, such as the results from intermediate calculation steps, which may be useful for testing
or subsequent analysis outside of FluxEngine. Examples of how to use this functionality are provided
in the source code. The toolbox documentation describes the process of, and best practices for,
extending FluxEngine in this way (see Sect. 9.1 and 9.2 within *FluxEngineV3_instructions.pdf*).

This increased flexibility means that users can define and use region-specific gas transfer
295 parameterisations or incorporate new transfer processes into existing gas transfer parameterisations
(such as the impact of biological surfactants as discussed by Pereira *et al.* (2018). Case studies one
(Sect. 3.1) and two (Sect. 3.2) demonstrate the use of different well known wind speed based gas
transfer parameterisations, while case study three (Sect. 3.3) demonstrates the use of a custom gas
transfer velocity parameterisation, which is used to assess the impact of biological surfactants on the
300 N₂O gas fluxes. Case study four (Sect 3.4) utilises a gas transfer velocity parameterisation that is based
on turbulent kinetic energy dissipation and provides an example of using additional input data.

2.6. Extensions for other sparingly soluble gases

The toolbox now supports the handling of two other sparingly soluble gases, (CH₄ and N₂O), and so
305 gas specific data can be substituted into Eq. (1) or Eq. (2) (dependent upon the choice of setup).
FluxEngine can calculate dissolved gas concentration from these gas input data, which can be supplied
as either partial pressure or mean molar fraction of a gas in the dry atmosphere. Alternatively, dissolved
gas concentrations can be provided directly as an input. Gas specific parameterisations for Schmidt
number (Sc) and solubility (α) are automatically chosen from those provided in Wanninkhof, (2014).
310 The option to use the older Sc and α parameterisations from Wanninkhof, (1992) is also included for
compatibility with previous versions and to aid comparative analysis. It is worth noting that both sets of
Sc parameterisations are only valid for saline water, and care should be taken when using them for
analysis of freshwater data, or regions with low salinity (e.g. the Baltic Sea, see case study two, Sect.
3.2). Support for additional and user-defined Schmidt number parameterisations are likely to be added
315 in the future.

3. Case study examples of the new capabilities

The following sections describe the application and results from four case studies that illustrate the new
capabilities. Table 1 summarises the new features that are demonstrated in each case study. These case
320 studies were run using FluxEngine version 3.0 which can be accessed via the GitHub repository (see
code availability in Sect. 6. The configuration files for each case study are included as examples in the
configs sub-directory of the GitHub repository and these will be updated to maintain compatibility as
new versions of the toolbox are released. In addition, interactive iPython Jupyter notebook tutorials for
the first three case studies are included in the *tutorials* sub-directory of the repository. Section 4 of this
325 paper provides more information about these tutorials.

Tom Holding 5/11/2019 10:48

Deleted: -

Tom Holding 5/11/2019 10:48

Deleted:

	New features utilised
Case study 1: Calculating sea to air CO ₂ gas fluxes from ship research cruise data and using SOCAT data.	<p>Flexible input data specification to select <i>in situ</i> data files and unit conversion using pre-processing functions (Sect. 2.2).</p> <p>Utilises new support for <i>in situ</i> data analysis, including the use of the <i>text2ncdf.py</i> and <i>append2insitu.py</i> tools, custom temporal resolution, reanalysis of fCO₂ to a consistent temperature field.</p>
Case study 2: Calculating sea to air CO ₂ gas fluxes from the Östergarnsholm fixed monitoring station data.	<p>Flexible input data specification to select <i>in situ</i> data files and unit conversion using pre-processing functions (Sect. 2.2).</p> <p>Utilises new support for <i>in situ</i> data analysis, including use of <i>text2ncdf.py</i>, daily temporal resolution and output formatted as time-series (Sect. 2.3).</p>
Case study 3: Surfactant suppression of sea to air N ₂ O gas fluxes using the MEMENTO data.	<p>Flexible input data specification and unit conversion using pre-processing functions (Sect 2.2).</p> <p>Utilises new support for <i>in situ</i> data analysis, including use of the <i>text2netcdf.py</i> and <i>append2insit.py</i> tools, custom temporal resolution and cruise-specific time interval (Sect. 2.3).</p> <p>Custom gas transfer parameterisation (Sect. 2.5).</p> <p>Calculation of N₂O gas fluxes (Sect. 2.6).</p>
Case study 4: Gas transfer velocity parameterisation using turbulent kinetic energy dissipation rate.	<p>Unit conversion and use of custom pre-processing functions to calculate the dissipation rate from the input data. This uses the pre-processing functions to perform a non-trivial computation (Sect. 2.2).</p> <p>Use of a custom gas transfer parameterisation which includes the specification of an additional input data layer (Sect. 2.5).</p>

Table 1: Summary of the new functionality demonstrated in each case study.

330 **3.1 Case study 1: Calculating CO₂ fluxes from research cruise data**

Each year over 1 million new *in situ* data points are included within the annual updates to the SOCAT dataset. Field scientists collecting these data often need to calculate the coincident sea-to-air gas fluxes, either using solely *in situ* measurements or through combining them with satellite Earth observation and/or model data.

335

Here we illustrate the procedure for calculating sea-to-air gas fluxes from *in situ* data collected during four different sampling campaigns. These *in situ* data (Kitidis and Brown, 2017; Schuster, 2016; Steinhoff *et al.*, 2016; Wanninkhof *et al.*, 2016) were all collected in the north Atlantic during October 2013. These are hereafter referred to as cruises 1-4, respectively. The *in situ* data were first downloaded from PANGAEA (an open access data publishing and archiving repository, <http://www.pangaea.de>) in tab-delimited format. The datasets follow the standard SOCAT structure and content (see Bakker *et al.*, 2016 table 9).

340

The majority of the measurements needed for the sea-to-air CO₂ gas flux calculation were included within the downloaded datasets. The aqueous fCO₂, salinity, SST and air pressure were measured *in situ* and the molar fraction of CO₂ in dry air (xCO₂) had been extracted from the GLOBALVIEW-CO₂ dataset (GLOBALVIEW-CO₂, 2013). However, wind speed (needed for calculating the gas transfer velocity) was missing in all cases. Therefore, to complement these *in situ* data, multi-sensor merged wind speed data at 10 m were downloaded (Cross-Calibrated Multi-Platform, CCMPv2, 6 hour temporal resolution, 0.25° × 0.25° spatial grid (Atlas, *et al.*, 2011)). These wind speed data were appended to the *in situ* data by matching each *in situ* measurement to the closest temporal and spatial grid point. This same process was used to add columns for the second and third moments of wind speed, which were estimated by taking the second and third power of wind speed, respectively.

345

350

355

Two datasets (Schuster, 2016; Steinhoff *et al.*, 2016) were missing xCO₂ data, and so the same method of matching temporal and spatial grid points was used to fill in these fields using the GLOBALVIEW CO₂ dataset from the US National Oceanic and Atmospheric Administration (NOAA) Earth System Research Laboratory (ESRL) (GLOBALVIEW-CO₂, 2013). For ease, these additional wind speed and xCO₂ data were downloaded, extracted and then inserted into the tab delimited *in situ* file using some simple custom Python scripts but the same process could be performed manually. These scripts are not part of FluxEngine.

360

Collectively the *in situ* data from these cruises were collected from different ships and underway systems, all sampling water at different and unknown depths. These measurements are typically collected from a few metres below the water surface, whereas the CO₂ concentration (combination of fCO₂ and solubility) on either side of the mass boundary layer is required for an accurate gas flux calculation. Before these data from multiple sources can be used for an accurate gas flux calculation, they need to be reanalysed to a common temperature dataset and depth (Goddijn-Murphy *et al.*, 2015; Woolf *et al.*, 2016). Therefore, the *reanalyse_socat_driver.py* tool was first used to reanalyse all fCO₂ data to a consistent temperature and depth.

365

370

Monthly mean sea surface temperatures from the Reynolds Optimally Interpolated Sea Surface Temperature dataset (OISST, Reynolds *et al.*, 2007) were used as the reference sub-skin temperature

375 dataset, resulting in reanalysed $f\text{CO}_2$ that are valid for ~ 1 m and used to represent the bottom of the mass boundary layer (termed sub-skin within Woolf *et al.*, 2016).

The reanalysed $f\text{CO}_2$ were then inserted into the tab-delimited *in situ* dataset producing a single dataset. The tab-delimited file was then converted into a netCDF format file using the *text2ncdf.py* tool. This tool groups all data according to a user-specified spatial sampling grid, calculating the mean value and standard deviation for each cell within the grid as well as the number of data that were used to calculate these statistics. The spatial resolution was defined as $1^\circ \times 1^\circ$ grid and FluxEngine was then configured to use each of the variables in the resulting netCDF file as input, with a pre-processing function applied to convert Reynolds OISST from Celsius to Kelvin (as all SST data within the main flux calculation use Kelvin). In order to produce a single netCDF output file for the entire 35 day period the temporal resolution for the flux calculation was set to 35 days. This allows the cruise tracks from all four cruises (1-4) to be easily visualised at the same time.

390 The sea-to-air CO_2 fluxes were then calculated using the rapid model (see Eq. (1) and Woolf *et al.*, 2016) and was run using a quadratic wind speed based gas transfer velocity parameterisation (Ho *et al.*, 2007). To identify the impact of the $f\text{CO}_2$ reanalysis stage, the sea-to-air CO_2 flux calculation was repeated using the original *in situ* SST and $f\text{CO}_2$.

395 Figure 3a shows the resultant calculated CO_2 flux along each of the cruises (1-4). The southern subtropical part of the cruise track 1 represents an area of the ocean that is a sink of CO_2 (negative sea-to-air flux). The northern sub-tropical section of cruise 1 shows an overall positive CO_2 flux into the atmosphere, while south of 15°N the net fluxes are smaller and in variable direction. Interestingly, there are also examples (e.g. along the equatorial part of cruise track 1 and the western part of cruise track 2) where the direction of the flux has changed as a result of re-analysing the $f\text{CO}_2$ data. The highest magnitude fluxes were seen around the European continental shelf in cruise track 3, with a strong ocean sink west of Ireland and an intermittent source of CO_2 in the North Sea. Figure 3b shows the difference in calculated net flux between use of the original $f\text{CO}_2$ data and the reanalysed $f\text{CO}_2$. Whilst very little difference is seen over large lengths of cruise tracks 1, 2 and 4, there are substantial differences in net flux of up to $0.1 \text{ C m}^{-2} \text{ day}^{-1}$ in some regions, for example within the frontal regions at the edge of the European shelf seas (cruise track 3) or in the southern section of cruise track 1. These are regions where temporally and spatially dynamic temperature gradients can exist that are likely under sampled (aliased) by both the *in situ* measurements and the satellite observations used to re-analyse the $f\text{CO}_2$ data. In this case, reanalysis using an estimated or modelled skin temperature (based on the *in situ* SST at depth) may be more appropriate (see the discussion in Sect 2.4).

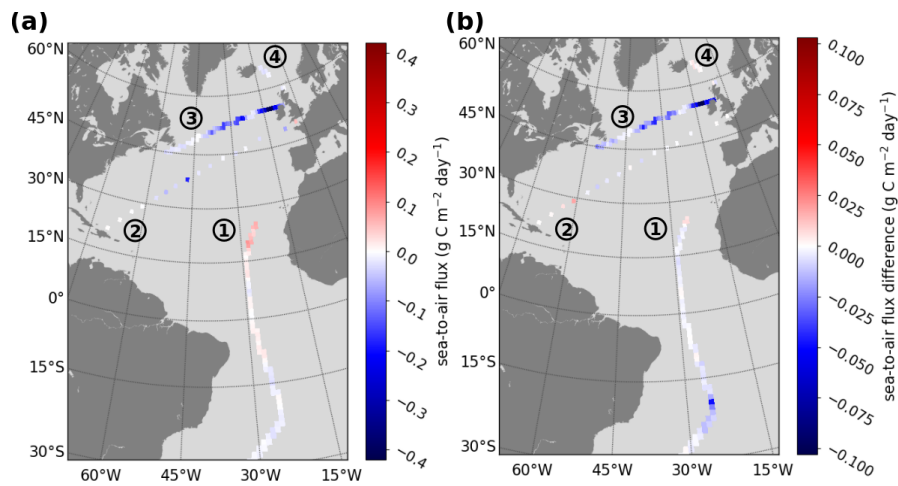


Figure 3: Example sea-to-air CO₂ fluxes calculated using *in situ* data and the gas transfer velocity detailed in Ho *et al.* (2006) (a) fluxes calculated for four sampling cruises in the North Atlantic during October and November 2013 (Kitidis and Brown, 2017; Schuster, 2016; Steinhoff *et al.*, 2016; Wanninkhof *et al.*, 2016) labelled 1-4, respectively. (b) The difference in the calculated flux resulting from using the reanalysed fCO₂ compared to the original *in situ* fCO₂ data (reanalysed minus original).

410

The `append2insitu.py` tool was then used to append FluxEngine output to the original input data file for the Kitidis and Brown (2017) dataset. The output from this tool enables the user to visualise FluxEngine output (including any additional input data such as the CCMP wind speed data) as a time series alongside all other *in situ* data. Figure 4 shows the time series of SST, fCO₂, and xCO₂ (from the downloaded cruise data). Plotted alongside these are the corresponding CCMP wind speed and the calculated concentrations and fluxes using the original and reanalysed fCO₂ data.

415

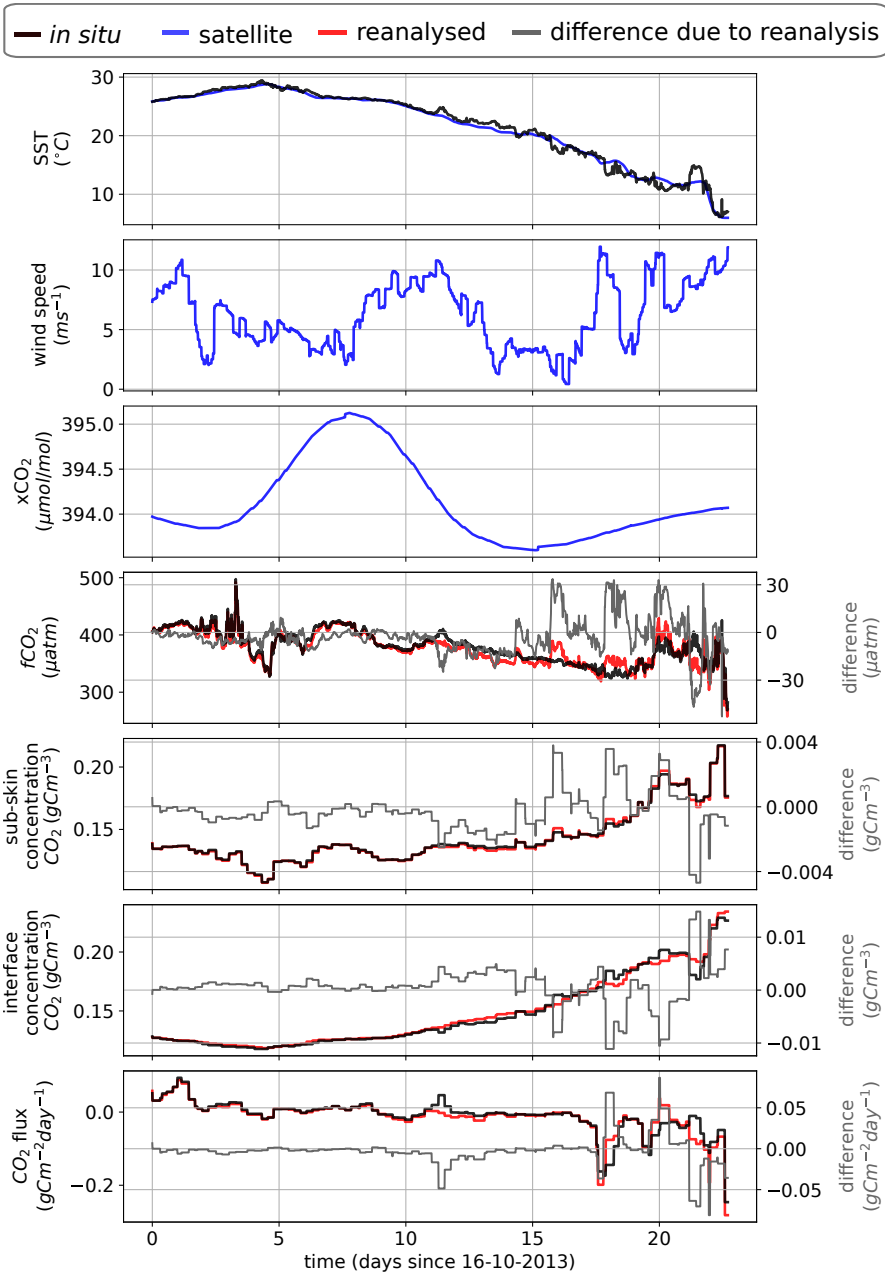


Figure 4: Time series of the (Kitidis and Brown, 2017) *in situ* campaign data with the sea-to-air CO₂ flux as calculated by FluxEngine using the Ho *et al.* (2006) gas transfer velocity parameterisation. The results from the reanalysed fCO₂ values are shown in red to distinguish them from the original data. The differences in fCO₂, sub-skin and interface CO₂ concentration and sea-to-air CO₂ flux, resulting from the reanalysis, are shown in grey (reanalysed minus original).

3.2 Case study 2: Calculating CO₂ fluxes from Östergarnsholm fixed station data

420 In this section the new capabilities for calculating gas fluxes from fixed stations is demonstrated using
data from the long term monitoring station at Östergarnsholm. The Östergarnsholm station is situated
in the Baltic Sea (57.42N, 18.99E) and is part of the Integrated Carbon Observation System (ICOS)
infrastructure. The station was originally established in 1995 with the aim of collecting data on the
marine atmospheric boundary layer to support research on the exchange of heat, momentum and CO₂
425 between the atmosphere and ocean. It is equipped with instruments to measure (amongst other
parameters) profiles of wind speed, water temperature and aqueous fCO₂.

The new FluxEngine support for calculating gas fluxes from fixed stations uses the temporal dimension
of the input files, creating output files of the same dimension that can be easily visualised as a time
430 series. Data for the Östergarnsholm monitoring station covering a period from 28 January 2015 to 9
September 2015 were downloaded from the data repository (Rutgersson, 2017). These data contain *in
situ* measurements for fCO₂, salinity and temperature, model reanalysis air pressure at sea level from
the National Center for Environmental Prediction and National Center for Atmospheric Research
(NCEP/NCAR) dataset (Kalnay *et al.*, 1996), xCO₂ from the NOAA ESRL GLOBALVIEW dataset
435 (GLOBALVIEW-CO2, 2013) and World Ocean Atlas salinity data (Boyer *et al.*, 2013). CCMP wind
speed data were extracted and added to the tab delimited *in situ* dataset using the same method as used
in case study 1 (Sect. 3.1). For gridded input data values were extracted from the single grid point
containing the Östergarnsholm station location was selected from a global 1° × 1° projected grid.

440 The *text2ncdf.py* tool was configured to convert the text formatted data file into a single netCDF file
using a temporal resolution of one day. This produced a netCDF file with a temporal dimension size of
246 (days), containing the daily mean value for each of the 246 days covered by the dataset. For this
case study FluxEngine was configured to use this file as input.

445 The flux calculation used the rapid model (Woolf *et al.*, 2016) with the Nightingale *et al.* (2000) wind
based gas transfer velocity parameterisation and was performed using the original *in situ* fCO₂ and SST
data. The temporal resolution was set to provide daily calculations for each of the 246 days allowing
seasonal variations to be observed. FluxEngine supports arbitrary temporal resolutions to within minute
precision and the choice predominantly depends on the resolution of the available data and the
450 particular research questions to be addressed. FluxEngine was configured to write output into a single
netCDF file as a time series. The *in situ* fCO₂ and SST measurements were assumed to represent the
conditions at the bottom of the mass boundary layer and the concentrations at the top of the mass
boundary layer were estimated by configuring the FluxEngine to estimate the skin temperature using
the *in situ* SST - 0.17 (which is based on the work of Donlon *et al.*, 2002).

455 Figure 5 shows the time series of SST, wind speed, xCO₂, fCO₂, concentration of CO₂ and calculated
sea-to-air CO₂ flux. There is a moderate negative flux (ocean sink of CO₂) throughout most of the
sampled period, which switched to a positive flux (outgassing to the atmosphere) during winter months.
At approximately day 130 there is a local upwelling event which results in an incursion of CO₂ rich
460 cold water. This results in an increase in fCO₂ of approximately 250 µatm, however coincident low
wind speed means that there was little change in the flux during this event.

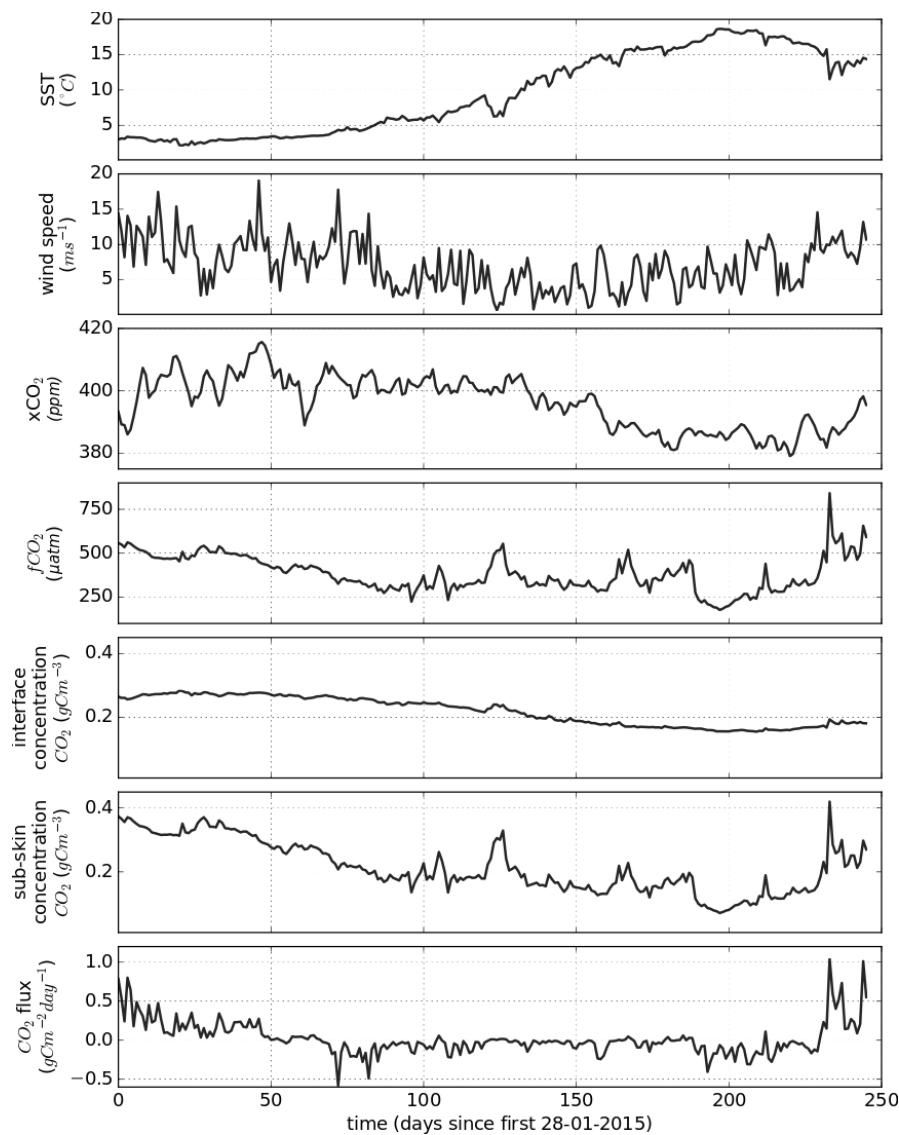


Figure 5: FluxEngine output file using data from Östergarnsholm station over the 246 day period. Example components of the sea-to-air flux calculation are shown alongside the calculated CO₂ flux.

3.3 Case study 3: Surfactant suppression of N₂O gas fluxes using the MEMENTO database

465 Nitrous oxide (N₂O) and methane (CH₄) are both climatically important gases. In the troposphere, they act as greenhouse gases (IPCC, 2013), whereas stratospheric N₂O is the major source for nitric oxide radicals which are involved in one of the main ozone reaction cycles (Ravishankara *et al.*, 2009). Source estimates indicate that the world's oceans play a major role in the global budget of atmospheric N₂O and a minor role in the case of CH₄ (IPCC, 2013). Oligotrophic ocean areas are near equilibrium with the atmosphere and, consequently, make only a relatively small contribution to overall oceanic emissions, whereas biologically productive regions (e.g., estuaries, shelf and coastal upwelling areas) appear to be responsible for the major fraction of the N₂O and CH₄ emissions (Bakker *et al.*, 2014).

470

475 Surfactants are surface-active compounds that can suppress turbulence at the sea surface thus altering
air-sea gas exchange (McKenna and Bock, 2006; Pereira *et al.*, 2016; Salter *et al.*, 2011). There is
growing evidence from field and laboratory studies that naturally occurring surfactants can
significantly reduce the flux of N₂O across the water/atmosphere interface (Kock *et al.*, 2012;
Mesarchaki *et al.*, 2015).

480 Previous work, which studied CO₂ fluxes, found that surfactants potentially reduce the annual net
integrated CO₂ flux by up to 9% in the Atlantic Ocean (Pereira *et al.*, 2018). Here, we use FluxEngine
to apply the methodology of Pereira *et al.* (2018) to *in situ* data from the MEMENTO (MarinE
MethanE and NiTrous Oxide) database (Kock and Bange, 2015) in order to estimate the equivalent
suppression effect on the exchange of N₂O between ocean and atmosphere.

485 While FluxEngine is able to calculate sea-to-air fluxes of both N₂O and CH₄, we confined our analysis
to N₂O because of the sparsity of CH₄ data. *In situ* and 1° x 1° gridded monthly mean atmospheric and
ocean partial pressure of N₂O, sea surface temperature and salinity were obtained from the MEMENTO
database for the Atlantic Meridional Transect (AMT) cruise (AMT-24, JR303), which took place
490 between September and November 2014 (Brown and Rees, 2018). These data were supplemented with
Earth observation wind speed, U_{10} , from the CCMP dataset and modelled air pressure from the
European Centre for Medium-Range Weather Forecasts (ECMWF). All input data were gridded to
monthly means with a 1° x 1° resolution.

495 A custom gas transfer velocity parameterisation was implemented following the template provided in
the toolbox to calculate the gas transfer suppression due to biological surfactants in surface waters. This
parameterisation uses the gas transfer velocity of Nightingale *et al.* (2000) combined with an estimate
of the degree of surfactant suppression from (Pereira *et al.*, 2018). The method described by Pereira
et al. (2018) used sea surface temperature to estimate surfactant suppression meaning that no additional
500 input data fields were needed. FluxEngine was configured to use the rapid flux model (Woolf *et al.*,
2016) and run once with the standard Nightingale *et al.* (2000) gas transfer parameterisation (no
suppression case) and then again using the Pereira *et al.* (2018) parameterisation (suppression case).
This new gas transfer parameterisation is now freely available within the FluxEngine (and can be
selected by specifying `k_Nightingale2000_with_surfactant_suppression` for the `k_parameterisation`
505 option).

After calculating the air-to-sea N₂O fluxes we removed negative (atmosphere to ocean) fluxes. The
fluxes for each grid cell (within which at least one *in situ* measurement exists) are shown in Fig. 6a,
while the difference in sea-to-air flux due to surfactant suppression is shown in Fig. 6b. The largest
510 fluxes occur in the tropics and sub-tropical part of the AMT cruise track (Fig. 6a). Suppression of the
gas transfer reduces the magnitude of the air-sea flux and the largest absolute suppression is also seen
in the tropics and sub-tropical regions (Fig. 6a and Fig. 6b).

The `append2insitu.py` utility was used to combine FluxEngine output with the original *in situ* data. The
515 time series are shown in Fig. 6c for SST, wind speed, atmospheric and aqueous N₂O, and sea-to-air
N₂O flux. The net fluxes along the transect are generally small and in both directions. The overall mean
(and standard deviation) flux was 5.7×10^{-2} ($\pm 5.7 \times 10^{-2}$) g N₂O m⁻² day⁻¹ (no suppression) and 5.0×10^{-2}

($\pm 4.8 \times 10^{-2}$) g N₂O m⁻² day⁻¹ (suppression), indicating in both cases a small net flux into the ocean. There was a mean flux suppression due to surfactants of 13% for the entire dataset.

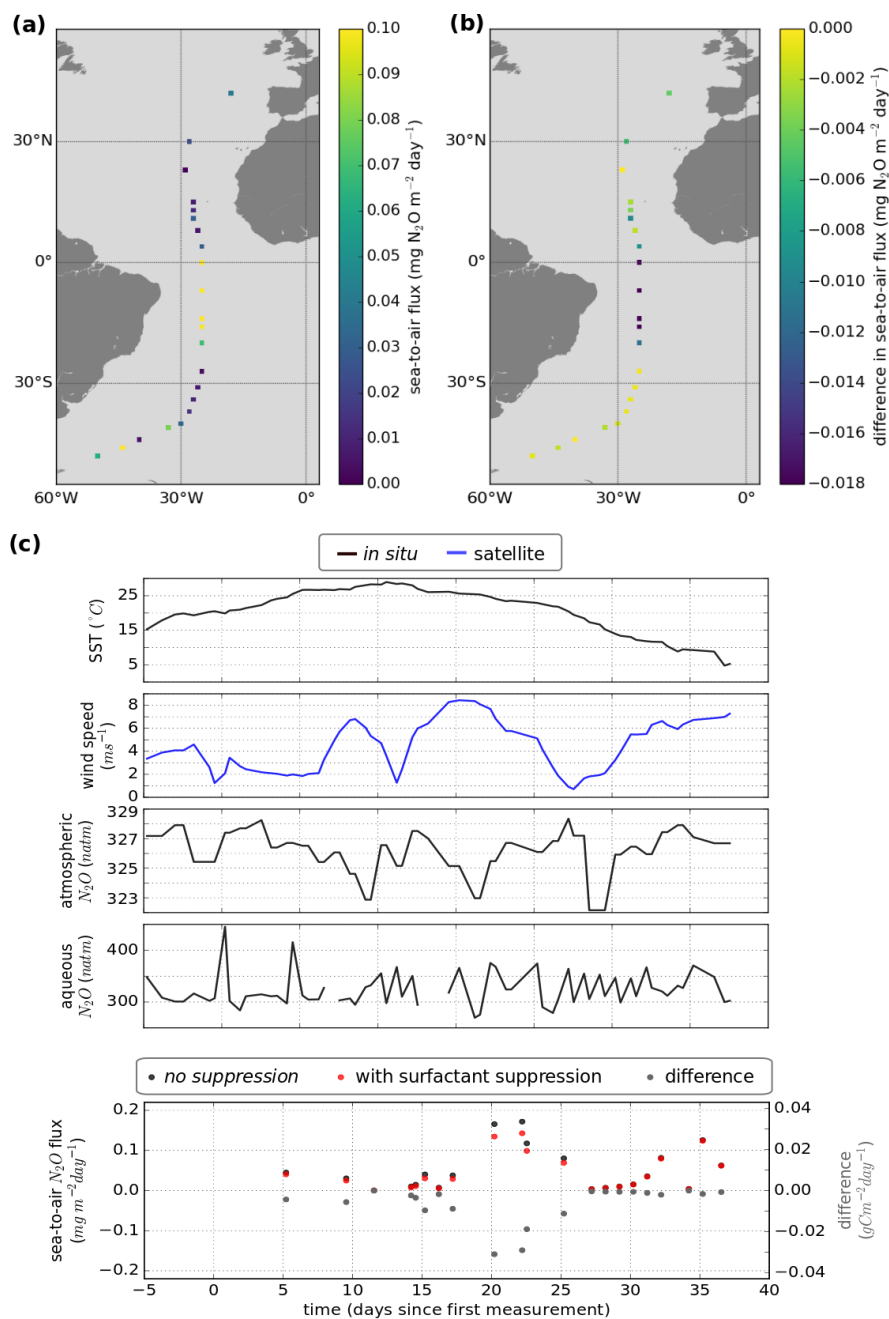


Figure 6: (a) Sea-to-air N₂O flux taking into account surfactant suppression. (b) Change in N₂O flux resulting from surfactant suppression. (c) Time series of SST, wind speed, atmospheric N₂O, aqueous N₂O and sea-to-air flux.

3.4 Case study 4: Gas transfer velocity parameterisation using turbulent kinetic energy dissipation rate

525 The gas transfer velocity, k in equation 1 and 2, is determined by the turbulent mixing near the ocean surface (Jähne *et al.*, 1987). While it is common to estimate gas transfer using a polynomial relationship with wind speed, turbulence in the upper ocean is influenced by additional physical processes that are independent, or not solely dependent, on the wind. These include wave breaking, shear stress due to geostrophic currents, wind-wave-current interactions, bottom-generated turbulence, tidal forces and precipitation (Villas Boas *et al.*, 2019; Zappa *et al.*, 2007; Zhao *et al.*, 2018).

530 In this case study we apply a turbulent kinetic energy dissipation rate (ϵ) based gas transfer velocity parameterisation, as developed by Zappa *et al.* (2007), to quantify the impact of wind- and wave-driven turbulence on sea-to-air CO₂. Zappa *et al.* (2007) used direct measurements of k and ϵ in aquatic and shallow marine regions to derive the following relationship

535
$$k = 0.419Sc^{-0.5}(\epsilon\nu)^{0.25} \quad (3)$$

where k is the gas transfer velocity ($m\ s^{-1}$), Sc is the Schmidt number, ϵ is the turbulent kinetic energy dissipation rate ($W\ kg^{-1}$) and ν is the kinematic viscosity of water ($m^2\ s^{-1}$). We calculate the monthly mean ϵ using the monthly mean wave (swell, secondary swell and wind waves) to ocean turbulent kinetic energy flux (FOC) provided by the WAVEWATCH III model re-analysis (WAVEWATCH III development group, 2016). The mean dissipation rate of turbulent kinetic energy, ϵ_{mean} , is calculated using $\epsilon_{mean} = FOC / (\rho z_{max})$, where ρ is the density of sea water (taken to be $1026\ kg\ m^{-3}$) and z_{max} is the maximum depth over which dissipation is assumed to occur (taken as 10 m from Fig. 8 of Craig and Banner, 1994). This provides the mean total dissipation rate through the volume of water. Equation 3 is valid for ϵ measurements near the surface (of the order of 0.1 to 0.2 m) and ϵ is known to decrease exponentially with depth. To estimate ϵ at a depth of 0.2 m we first fit an exponential function to the curve of ϵ from Fig. 8 of Craig and Banner (1994) which gave:

540
$$\epsilon = \beta \exp(0.20z + 0.78) \quad (4)$$

550 where z is depth and $\beta=1.86\times 10^{-3}$. Normalising this function to have a mean ϵ equal to ϵ_{mean} allows ϵ at any depth to be determined. This was done by fitting β to minimise the difference between ϵ_{mean} calculated from FOC and ϵ_{mean} calculated from equation 4 to produce separate depth relationships with ϵ for each individual grid cell. Finally, the dissipation rate at 0.2 m was calculated by substituting $z=0.2$ into the final depth relationship. The process of fitting of the depth relationship and calculating ϵ at depth $z=0.2$ was implemented using a custom pre-processing function that is included as an example in the FluxEngine download. This demonstrates how pre-processing functions can be used to perform complex data processing.

560 FluxEngine was then used to calculate monthly sea-to-air CO₂ fluxes, globally, for 2010. All inputs to FluxEngine were provided as monthly averages with a $1^\circ \times 1^\circ$ resolution. The additional input data were wind speed data from WAVEWATCH III re-analysis forcing field (WAVEWATCH III development group, 2016), sea surface temperature from Reynolds Optimally Interpolated Sea Surface Temperature dataset (OISST, Reynolds *et al.*, 2007), salinity data from the NOAA World Ocean Atlas

565 (Zweng *et al.*, 2018), $x\text{CO}_2$ from the GLOBALVIEW CO_2 dataset (GLOBALVIEW-CO2, 2013), and
f CO_2 data from the SOCAT derived sea-to-air CO_2 flux reference dataset for 2010 (Woolf *et al.*, 2019).
Since the Zappa *et al.* (2007) relationship was parameterised in low to moderate wind speeds and in
shallow marine environments, a mask was set in the configuration file to constrain the calculation to
570 grid cells with wind speeds less than 10 m s^{-1} and shelf sea water depths between 20 and 200 m,
and then the analysis repeated with depths between 20 and 500 m. These depth ranges were chosen to
be consistent with previous studies (e.g. Laruelle *et al.*, 2018; Shutler *et al.*, 2016), and the General
Bathymetric Chart of the Oceans (GEBCO) Digital Atlas bathymetry was used for this masking
(GEBCO, 2003).

575 The *ofluxghg_flux_budgets.py* tool was used to compute the annual integrated net sea-to-air flux in all
shelf sea regions. Collectively, the global shelf seas result in a net integrated flux into the ocean (sink)
of 0.57 to 0.78 Pg C for 2010, where the range is due to the two shelf definitions. These results are
within the bounds of those determined by previous studies ($0.2 - 1 \text{ PgC yr}^{-1}$ from Laruelle *et al.*, 2018;
Laruelle *et al.*, 2016). However we note that all previous studies have used wind speed for calculating
580 gas exchange. Repeating the analysis with a wind speed based gas transfer velocity (Wanninkhof *et al.*,
2014) instead of equation 4 gives an $\sim 8\%$ smaller net integrated flux of 0.53 to 0.72 Pg C. This result
could suggest that published values of the global shelf sea CO_2 sink (calculated using wind speed gas
transfer) are underestimated, as they do not fully account for wind-wave-current interactions and
whitcapping. Figure 7 shows the resulting mean annual sea-to-air CO_2 flux in 2010 for global shelf
585 seas. The FluxEngine has the capability to use non-wind driven gas transfer parameterisations allowing
more physically based approaches to be evaluated such as the use of ϵ . The first synoptic-scale
observation-based estimates of ϵ could soon be possible from space using Doppler techniques (e.g.
Ardhuin *et al.*, 2019).

590

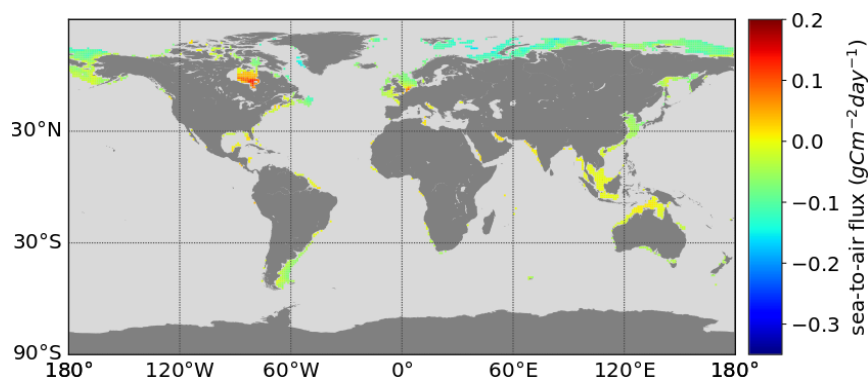


Figure 7: Mean annual sea-to-air CO_2 flux of shelf seas in 2010 using the Zappa *et al.* (2007) gas transfer relationship for all regions and months with wind speeds 0 to 10 m s^{-1} . Shelf regions are defined as having depth between 20 m and 200 m.

4. Future developments

The FluxEngine toolbox will continue to be developed in response to new advances in research and
further user-uptake will be encouraged through the provision of iPython Jupyter notebooks. There are
595 currently four interactive Jupyter notebooks (tutorials) available within the FluxEngine v3.0 download

and these correspond to the first three case studies presented in this paper as well as an additional introductory tutorial. These interactive notebooks allow users to investigate the toolbox without the need to install any additional software. Users are able to modify and re-run the notebook and immediately see the impact of any changes. This approach has been previously used by the authors for supporting collaborative research and summer school teaching. Additional Jupyter notebooks could be written to provide worked examples of: i) driving FluxEngine with a custom Python script to perform a sensitivity or ensemble analysis, ii) using the FluxEngine to study a freshwater environment or iii) using the verification tools module to verify custom changes and extensions to the toolbox. All notebooks will be maintained so that they remain available and relevant to future versions of the FluxEngine.

5. Conclusions

The FluxEngine is an open-source and freely available software toolbox that provides standardised and verified calculations of gas exchange and net integrated fluxes between the ocean and atmosphere, and the toolbox is now being used by *in situ*, Earth observation and modelling scientific communities. The development of the toolbox was driven by the desire to reduce duplication of effort, to facilitate collaboration between different research communities, and thus to accelerate advancements in air-sea gas flux research and monitoring.

Building on Shutler *et al.* (2016), which demonstrated the toolbox and verified the accuracy of the calculations, this paper demonstrates new capabilities that considerably broadens the scope of research questions that can be addressed using FluxEngine. Version 3.0 can now be easily installed and executed on a desktop or laptop computer and does not require specialist hardware or software libraries. It can be used as a Python library or as a set of stand-alone command line utilities. The toolbox now includes an extensive suite of tools for calculating gas fluxes directly from *in situ* data. Collectively, these improvements have streamlined the process for extending the toolbox and will allow users to easily take advantage of newly developed gas transfer velocity parameterisations and/or new sources of input data. These new tools and the toolbox are fully compatible with the internationally established data structures being used by the SOCAT and the MEMENTO communities.

The inclusion of the handling of CH₄ and N₂O sea-air gas fluxes is intended to directly support those communities studying these gases. Significant international research focus and effort is now being directed to collating data on these gases towards monitoring and understanding their spatial distribution and variability.

The FluxEngine toolbox will continue to be updated as new approaches become available. Further development will be guided by the needs of the international research and monitoring communities, and so we welcome feedback from users on all aspects of the toolbox.

6. Code availability

The FluxEngine software is open source and available on a creative commons license via <http://github.com/oceanflux-ghg/FluxEngine>. FluxEngine is in constant development and historic versions are available via GitHub. To access the specific version used to conduct the case studies in

640 section 3, please access the v3.0 release via: <https://github.com/oceanflux-ghg/FluxEngine/releases/tag/v3.0>

7. Appendix A: Utility names and descriptions

645 Several additional utilities are provided as Python scripts to support the installation, verification, execution and processing of output and these are listed in table 2.

Utility	Description
<i>append2insitu.py</i>	Appends netCDF data (e.g. FluxEngine output) to text formatted data files as new columns. Matching rows by longitude, latitude and time.
<i>install_dependencies_macos.py</i> , <i>install_dependencies_ubuntu.py</i>	Installation scripts. Installation instructions are provided for Windows users in <i>FluxEngineV3_instructions.pdf</i>
<i>ncdf2text.py</i>	Converts netCDF output files to text formatted files.
<i>ofluxghg_flux_budgets.py</i>	Calculates total monthly and annual gas flux from FluxEngine output. Supports global and regional analysis.
<i>ofluxghg_run.py</i> <i>reanalyse_socat_driver.py</i>	Commandline tool used to run FluxEngine Uses satellite sea surface temperature to reanalyse CO ₂ fugacity and partial pressure data to a consistent temperature and depth (see Goddijn-Murphy <i>et al.</i> , 2015)
<i>run_full_verification.py</i>	Runs an extended verification procedure. Required additional data from (Holding <i>et al.</i> , 2018)
<i>text2ncdf.py</i>	Converts text formatted data files into FluxEngine compatible netCDF format.
<i>validation_tools.py</i> , <i>compare_net_budgets.py</i>	Contains Python functions to aid verification of FluxEngine output to a reference dataset.
<i>verify_socatv4_sst_salinity_gradients_N00.py</i> , <i>verify_takahashi09.py</i>	Verifies that FluxEngine has been installed correctly by comparing output with a reference data from SOCAT-derived or Takahashi climatologies, respectively.

Table 2: Description of the bundled tools and scripts that are included in FluxEngine. Each tool can be used as a stand-alone command line tool or used as a Python package.

650

8. Appendix B: Datasets used

Table 3 provides details of each of the data sets that were used in the case studies.

Name	Parameter(s)	Reference/source
CCMP v2 (Cross-Calibrated Multi-Platform)	U ₁₀ (wind speed at 10m)	Atlas <i>et al.</i> , 2011 http://www.remss.com/measurements/ccmp/
OISST (Optimally-Interpolated Seas Surface Temperature)	Sea surface temperature (SST)	Reynolds <i>et al.</i> , 2007 https://www.ncdc.noaa.gov/oisst
GLOBALVIEW CO ₂	xCO ₂ (molar fraction of CO ₂ in dry air)	GLOBALVIEW-CO ₂ , 2013 https://www.esrl.noaa.gov/gmd/ccgg/globalview/co2/co2_intro.html
National Centers for Environmental Prediction, National Center for	Air pressure	Kalnay <i>et al.</i> , 1996 https://www.esrl.noaa.gov/psd/data/gridded/data.ncep.reanalysis.pressure.html

Atmospheric Research (NCEP/NCAR)		
Underway data from the James Clark cruise (74JC20131009)	SST, salinity, air pressure, fCO ₂	Kitidis and Brown, 2017 https://doi.pangaea.de/10.1594/PANGAEA.878492
Underway data from the Belguela Stream cruise (642B20131005)	SST, salinity, air pressure, fCO ₂	Schuster, 2016 https://doi.org/10.1594/PANGAEA.852980
Underway data from the Atlantic Companion cruise (77CN20131004)	SST, salinity, air pressure, fCO ₂	Steinhoff <i>et al.</i> , 2016 https://doi.org/10.1594/PANGAEA.852786
Underway data from the REYJAFOSS cruise (64RJ20131017)	SST, salinity, air pressure, fCO ₂ , xCO ₂	Wanninkhof <i>et al.</i> , 2016 https://doi.org/10.1594/PANGAEA.866092
Östergarnsholm station (77FS20150128)	Air pressure, salinity, SST, xCO ₂ (air), fCO ₂ (water)	Rutgersson, 2017 https://doi.pangaea.de/10.1594/PANGAEA.878531
MarinE MethanE and NiTrous Oxide database (MEMENTO)	SST, pN ₂ O _{air} , pN ₂ O _{water}	Kock and Bange, 2015 https://memento.geomar.de/
National Oceanic and Atmospheric Administration, US (NOAA) WAVEWATCH III	U ₁₀ (wind speed at 10m), FOC (wave to turbulent kinetic energy)	WAVEWATCH III development group, 2016
Interpolated and reanalysed fCO ₂ field originating from the SOCAT dataset	fCO ₂ (interpolated)	Dataset methodology: Woolf <i>et al.</i> , 2019 Resultant fCO ₂ data: (Holding <i>et al.</i> , 2018) https://doi.pangaea.de/10.1594/PANGAEA.890118 Original SOCAT dataset: Bakker <i>et al.</i> , 2016 https://www.socat.info/

Table 3: The Earth observation *in situ*, model and climatology data used in this research.

655 9. Appendix C: Summary of main toolbox features

Table 4 lists the main features of the FluxEngine toolbox with summaries of their impact for the accurate calculation of atmosphere-ocean gas fluxes.

Feature or option	Description	Example impact or use
Ability to choose the structure of the bulk gas flux calculation or formulation	The user can choose their bulk formulation, but a formulation based on concentration differences (i.e. containing two solubilities) is advised. This advised formulation enables near-surface temperature and salinity gradients to be included. For reasoning and examples of this advice please see Woolf <i>et al.</i> (2016), Woolf <i>et al.</i> (2019). and Section 1b of Shutler <i>et al.</i> (2016).	Woolf <i>et al.</i> (2019) shows that ignoring vertical temperature and salinity gradients for 2010 results in a 0.35 PgC (12%) bias or underestimate in the oceanic sink of CO ₂ .

User selectable gas transfer velocity parameterisations	The toolbox includes 14 published wind speed parameterisations and one mean square slope parameterisation, along with a generic user-configurable wind speed parameterisation (see section 7 of the FluxEngine manual). Custom user parameterisations can be added using a Python template (section 9.2 of the FluxEngine manual).	Wrobel and Piskozub (2016) showed that the (model) uncertainty due to the choice of quadratic gas transfer parameterisation led to 9% difference in the gas transfer velocity for the North Atlantic and sub polar waters. This uncertainty increased to 65% when all parameterisations were considered.
Reanalyse fCO₂ data to a reference temperature and depth	The user can reanalyse paired <i>in situ</i> fCO ₂ and SST measurements to a consistent depth using a reference temperature dataset as described by Goddijn-Murphy <i>et al.</i> (2015).	This removes unknown biases due to paired data originating from multiple depths. The depth of <i>in situ</i> data can vary during a single research cruise (e.g. due to sea state or ballasting) and measurements from varying depths becomes a more significant problem when using large collated datasets collected using different measurement systems.
User selectable gas input data types	The user can input atmospheric and marine gas data as partial pressures, fugacities or concentrations.	Allows a wider range of poorly soluble gases to be analysed.
Flexibility to calculate air-sea gas fluxes of multiple poorly soluble gases	The toolbox supports user definable sea-to-air gas flux calculations for CO ₂ , CH ₄ and N ₂ O.	This paper estimates that surfactants can suppress N ₂ O gas fluxes by up to 13% in the North Atlantic.
Accounting for the impact of rain on air-sea gas fluxes	Users can investigate methods that include the different influences that rain can have on air-sea gas fluxes.	Ashton <i>et al.</i> (2016) estimated that rain driven gas transfer and wet deposition of carbon increases the annual oceanic integrated net sink of CO ₂ by up to 6%.
Flexible input data specification and support for <i>in situ</i> data	Tools are provided to support user-specified grid size, temporal resolution, naming conventions and directory structure, automatic unit conversion and conversion between text (ASCII) and netCDF formatted data files.	Allows a wide range of data to be easily used and analysed by the user and the FluxEngine outputs can be easily incorporated into the users original <i>in situ</i> dataset.
Calculate integrated net gas fluxes	A tool for calculating global or regional integrated net gas fluxes (e.g. CO ₂ sink) from netCDF air-sea gas flux data is provided. This enables user defined land, ice and region of interest masks to be used and there are multiple options for handling the impact of sea ice.	Shutler <i>et al.</i> (2016) showed that the calculated net CO ₂ fluxes can vary by 14% for the European shelf sea simply due to differing shelf sea masks, highlighting the need for traceable methods and masks for net flux calculations.
Input data uncertainty analysis	Users can add random noise (with user defined variance and bias) to any input dataset. This enables the users to investigate the impact of input data uncertainties on their air-sea gas flux calculation (e.g. through using an ensemble approach)	Ashton <i>et al.</i> (2016) identified that known uncertainties due to random fluctuations in the input data resulted in a ±1% variation in the monthly net integrated CO ₂ sink. Land <i>et al.</i> (2013) identified that the dominant source of uncertainty in Arctic air-sea gas flux calculations was due to bias in wind speed data (and its impact on the wind speed based gas transfer velocity).

Table 4: An overview of the key features provided by the FluxEngine software toolkit and their relevance or use for atmosphere-ocean gas exchange.

660

10. Appendix D: Installation, verification and benchmarking

Installation tools or instructions are provided in the root FluxEngine root directory for the following operating systems: Ubuntu/Debian based Linux (*install_dependencies_ubuntu.sh*), Apple Mac
665 (*install_dependencies_macos.sh*) and Windows (instructions are within *FluxEngineV3_instructions.pdf*). Two verification utilities (also in located in the root directory) are provided (*verify_takahashi09.py* and *verify_socatv4_sst_salinity_gradients_N00.py*). These can be used to verify the successful installation of FluxEngine by running standard global sea-to-air CO₂ gas flux calculations and net integrated fluxes using the (Takahashi *et al.*, 2009) sea-to-air CO₂ flux climatology
670 (for year 2000) and the Woolf *et al.* (2019) Surface Ocean CO₂ Atlas (SOCAT, Bakker *et al.*, 2016) derived sea-to-air CO₂ flux reference dataset for year 2010. Both of these datasets are contained within Holding *et al.* (2018) and the verification process compares the output from a test run of the toolbox with the reference data published in Holding *et al.* (2018). The installation is deemed successful if all results are identical to the reference dataset within a precision of 5 decimal places. An additional utility
675 (*run_full_verification.py*) enables the user to perform a more detailed verification of different user defined options that exploit the Woolf *et al.* (2019) reference dataset. This executes a suite of 12 different configurations and scenarios, the justification for which are described within Woolf *et al.* (2019). Owing to the large volume of data required to execute and verify all of these scenarios, the verification data are not packaged with the standard FluxEngine download, but are all freely available
680 and contained within Holding *et al.* (2018).

To provide an indication of the execution time a benchmarking analysis was performed using an Intel Core i5 2.7 GHz laptop processor with 8GB RAM running MacOS El Capitan. The automatic
685 installation took ~3 minutes to complete and the basic verification script using the Woolf *et al.* (2019) reference dataset (involving a global one year analysis of the gas fluxes for 2010, monthly temporal resolution and 1° × 1° spatial resolution) took approximately 6 minutes to complete. As the flux calculation is sequential for each grid cell the execution time scales approximately linearly with number of grid points and number of time steps. Hence, doubling the temporal resolution will approximately double the execution time, whilst doubling the resolution of both spatial dimensions will
690 lead to a factor of four increase in execution time.

Author contributions

Design and analysis performed by T. Holding, I. Ashton and J. Shutler. Software engineering performed by T. Holding and I. Ashton. Pre-processing of nitrous oxide data performed by A. Kock.
695 All authors contributed to the preparation of the manuscript.

Acknowledgements

This work was partially funded by the European Space Agency (ESA) Support to Science Element (STSE) through the OceanFlux Greenhouse Gases project (contract 4000104762/11/I-AM), the
700 OceanFlux Greenhouse Gases Evolution project (contract 4000112091/14/I-LG), and by the European Space Agency (ESA) through the Sea surface Kinematics Multiscale monitoring (SKIM) Mission Science study (contract 4000124734/18/NL/CT/gp) and the ESA SKIM Scientific Performance Evaluation study (contract 4000124521/18/NL/CT/gp), as well as through the NERC RAGNARoCC project, (grant ref. NE/K002473/1). Further development of FluxEngine was funded by the European

705 Union's Seventh Programme for Research and Technology Development (grant no. 03FO773A (BONUS INTEGRAL) and grant no. 730944 (RINGO)).

The Surface Ocean CO₂ Atlas (SOCAT) is an international effort, endorsed by the International Ocean Carbon Coordination Project (IOCCP), the Surface Ocean Lower Atmosphere Study (SOLAS) and the
710 Integrated Marine Biosphere Research (IMBeR) program, to deliver a uniformly quality-controlled surface ocean CO₂ database. The many researchers and funding agencies responsible for the collection of data and quality control are thanked for their contributions to SOCAT.

CCMP Version-2.0 vector wind analyses are produced by Remote Sensing Systems
715 (<http://www.remss.com>). NCEP Reanalysis data provided by the NOAA/OAR/ESRL PSD, Boulder, Colorado, USA, from their web site at <https://www.esrl.noaa.gov/psd/>.

MEMENTO (<https://memento.geomar.de/>) is currently supported by the Kiel Data Management Team at GEOMAR and the BONUS INTEGRAL Project.

720 This study is a contribution to the international IMBeR project and was supported by the UK Natural Environment Research Council National Capability (CLASS Theme 1.2) funding to Plymouth Marine Laboratory. This is contribution number 330 of the AMT programme.

725 BONUS INTEGRAL receives funding from BONUS (Art 185), funded jointly by the EU, the German Federal Ministry of Education and Research, the Swedish Research Council Formas, the Academy of Finland, the Polish National Centre for Research and Development, and the Estonian Research Council.

Competing interests

730 The authors declare that they have no conflict of interest.

References

735 Ashton, I. G., Shutler, J. D., Land, P. E., Woolf, D. K. and Quartly, G. D.: A Sensitivity Analysis of the Impact of Rain on Regional and Global Sea-Air Fluxes of CO₂, edited by M. deCastro, PLoS One, 11(9), e0161105, doi:10.1371/journal.pone.0161105, 2016.

740 Atlas, R., Hoffman, R. N., Ardizzone, J., Leidner, S. M., Jusem, J. C., Smith, D. K. and Gombos, D.: A Cross-calibrated, Multiplatform Ocean Surface Wind Velocity Product for Meteorological and Oceanographic Applications, Bull. Am. Meteorol. Soc., 92(2), 157–174, doi:10.1175/2010BAMS2946.1, 2011.

745 Bakker, D. C. E., Bange, H. W., Gruber, N., Johannessen, T., Upstill-Goddard, R. C., Borges, A. V., Delille, B., Löscher, C. R., Naqvi, S. W. A., Omar, A. M. and Santana-Casiano, J. M.: Air-Sea Interactions of Natural Long-Lived Greenhouse Gases (CO₂, N₂O, CH₄) in a Changing Climate, pp. 113–169, Springer, Berlin, Heidelberg, 2014.

750 Bakker, D. C. E., Pfeil, B., Landa, C. S., Metzl, N. O., Brien, K. M., Olsen, A., Smith, K., Cosca, C., Harasawa, S., Jones, S. D., Nakaoka, S., Nojiri, Y., Schuster, U., Steinhoff, T., Sweeney, C., Takahashi, T., Tilbrook, B., Wada, C., Wanninkhof, R., Alin, S. R., Balestrini, C. F., Barbero, L., Bates, N. R., Bianchi, A. A., Bonou, F., Boutin, J., Bozec, Y., Burger, E. F., Cai, W.-J., Castle, R. D., Chen, L., Chierici, M., Currie, K., Evans, W., Featherstone, C., Feely, R. A., Fransson, A., Goyet, C., Greenwood, N., Gregor, L., Hankin, S., Hardman-Mountford, N. J., Harlay, J., Hauck, J., Hoppema, M., Humphreys, M. P., Hunt, C. W., Huss, B., Ibáñez, J. S. P., Johannessen, T., Keeling, R., Kitidis, V., Körtzinger, A., Kozyr, A., Krasakopoulou, E., Kuwata, A., Landschützer, P., Lauvset, S. K.,
755

- 760 Lefèvre, N., Lo Monaco, C., Manke, A., Mathis, J. T., Merlivat, L., Millero, F. J., Monteiro, P. M. S., Munro, D. R., Murata, A., Newberger, T., Omar, A. M., Ono, T., Paterson, K., Pearce, D., Pierrot, D., Robbins, L. L., Saito, S., Salisbury, J., Schlitzer, R., Schneider, B., Schweitzer, R., Sieger, R., Skjelvan, I., Sullivan, K. F., Sutherland, S. C., Sutton, A. J., Tadokoro, K., Telszewski, M., Tuma, M., van Heuven, S. M. A. C., Vandemark, D., Ward, B., Watson, A. J. and Xu, S.: A multi-decade record of high-quality fCO₂ data in version 3 of the Surface Ocean CO₂ Atlas (SOCAT), *Earth Syst. Sci. Data*, 8(2), 383–413, doi:10.5194/essd-8-383-2016, 2016.
- 765 Boyer, T.P., J. I. Antonov, O. K. Baranova, C. Coleman, H. E. Garcia, A. Grodsky, D. R. Johnson, R. A. Locarnini, A. V. Mishonov, T.D. O'Brien, C.R. Paver, J.R. Reagan, D. Seidov, I. V. Smolyar, and M. M. Z.: World Ocean Database 2013, NOAA Atlas NESDIF, 72, 209, doi:10.7289/V5NZ85MT, 2013.
- 770 Brown, I. and Rees, A.: Nitrous Oxide measurements from CTD collected depth profiles along a North-South transect in the Atlantic Ocean on cruise JR303/AMT24/JR20140922, *Br. Oceanogr. Data Cent. - Nat. Environ. Res. Counc. UK*, doi:10.5285/7cbcd206-c122-2777-e053-6c86abc041f9, 2018.
- 775 Craig, P. D., Banner, M. L. and Craig, P. D.: Modeling Wave-Enhanced Turbulence in the Ocean Surface Layer, *J. Phys. Oceanogr.*, 24(12), 2546–2559, doi:10.1175/1520-0485(1994)024<2546:MWETIT>2.0.CO;2, 1994.
- 780 Donlon, C., Robinson, I. S., Wimmer, W., Fisher, G., Reynolds, M., Edwards, R. and Nightingale, T. J.: An Infrared Sea Surface Temperature Autonomous Radiometer (ISAR) for Deployment aboard Volunteer Observing Ships (VOS), *J. Atmos. Ocean. Technol.*, 25(1), 93–113, doi:10.1175/2007JTECHO505.1, 2008.
- 785 Fairall, C. W., Bradley, E. F., Rogers, D. P., Edson, J. B. and Young, G. S.: Bulk parameterization of air-sea fluxes for Tropical Ocean-Global Atmosphere Coupled-Ocean Atmosphere Response Experiment, *J. Geophys. Res. Ocean.*, 101(C2), 3747–3764, doi:10.1029/95JC03205, 1996.
- 790 GEBCO: The GEBCO Digital Atlas published by the British Oceanographic Data Centre on behalf of IOC and IHO, 2003.
- 790 GLOBALVIEW-CO₂: Cooperative Global Atmospheric Data Integration Project. 2013, updated annually. Multi-laboratory compilation of synchronized and gap-filled atmospheric carbon dioxide records for the period 1979-2012 (obspack_co2_1_GLOBALVIEW-CO2_2013_v1.0.4_2013-12-23), Compil. by NOAA Glob. Monit. Division, doi:10.3334/OBSPACK/1002, 2013.
- 795 Goddijn-Murphy, L. M., Woolf, D. K., Land, P. E., Shutler, J. D. and Donlon, C.: The OceanFlux Greenhouse Gases methodology for deriving a sea surface climatology of CO₂ fugacity in support of air-sea gas flux studies, *Ocean Sci.*, 11(4), 519–541, doi:10.5194/os-11-519-2015, 2015.
- 800 Henson, S. A., Humphreys, M. P., Land, P. E., Shutler, J. D., Goddijn-Murphy, L. and Warren, M.: Controls on open-ocean North Atlantic ΔpCO₂ at seasonal and interannual timescales are different, *Geophys. Res. Lett.*, 45(17), 9067–9076, doi:10.1029/2018GL078797, 2018.
- 805 Ho, D. T., Law, C. S., Smith, M. J., Schlosser, P., Harvey, M. and Hill, P.: Measurements of air-sea gas exchange at high wind speeds in the Southern Ocean: Implications for global parameterizations, *Geophys. Res. Lett.*, 33(16), L16611, doi:10.1029/2006GL026817, 2006.
- 810 Ho, D. T., Veron, F., Harrison, E., Bliven, L. F., Scott, N. and McGillis, W. R.: The combined effect of rain and wind on air-water gas exchange: A feasibility study, *J. Mar. Syst.*, 66(1–4), 150–160, doi:10.1016/J.JMARSYS.2006.02.012, 2007.
- 815 Holding, T., Ashton, I., Woolf, D. K. and Shutler, J. D.: FluxEngine v2.0 and v3.0 reference and verification data, PANGAEA, doi:10.1594/PANGAEA.890118, 2018.
- 815 IPCC: Climate Change 2013: The Physical Science Basis. Contribution of Working Group I to the Fifth Assessment Report of the Intergovernmental Panel on Climate Change, edited by V. B. and P. M. M. Stocker, T.F., D. Qin, G.-K. Plattner, M. Tignor, S.K. Allen, J. Boschung, A. Nauels, Y. Xia, Cambridge University Press, Cambridge, United Kingdom and New York, NY, USA, 1535 pp. [online] Available from: <https://www.ipcc.ch/report/ar5/wg1/>, 2013.
- 820 Jähne, B., Münnich, K. O., Börsinger, R., Dutzi, A., Huber, W. and Libner, P.: On the parameters influencing air-water gas exchange, *J. Geophys. Res.*, 92(C2), 1937–1949, doi:10.1029/JC092iC02p01937, 1987.

- 825 Kalnay, E., Kanamitsu, M., Kistler, R., Collins, W., Deaven, D., Gandin, L., Iredell, M., Saha, S., White, G., Woollen, J., Zhu, Y., Leetmaa, A., Reynolds, R., Chelliah, M., Ebisuzaki, W., Higgins, W., Janowiak, J., Mo, K. C., Ropelewski, C., Wang, J., Jenne, R., Joseph, D., Kalnay, E., Kanamitsu, M., Kistler, R., Collins, W., Deaven, D., Gandin, L., Iredell, M., Saha, S., White, G., Woollen, J., Zhu, Y., Chelliah, M., Ebisuzaki, W., Higgins, W., Janowiak, J., Mo, K. C., Ropelewski, C., Wang, J., Leetmaa, A., Reynolds, R., Jenne, R. and Joseph, D.: The NCEP/NCAR 40-Year Reanalysis Project, *Bull. Am. Meteorol. Soc.*, 77(3), 437–471, doi:10.1175/1520-0477(1996)077<0437:TNYRP>2.0.CO;2, 1996.
- 830 Kitidis, Vassilis; Brown, I.: Underway physical oceanography and carbon dioxide measurements during James Clark Ross cruise 74JC20131009, PANGAEA, doi:10.1594/PANGAEA.878492, 2017.
- 835 Kock, A. and Bange, H.: Counting the Ocean's Greenhouse Gas Emissions, *Earth Sp. Sci. News*, 96, doi:10.1029/2015EO023665, 2015.
- 840 Kock, A., Schafstall, J., Dengler, M., Brandt, P. and Bange, H. W.: Sea-to-air and diapycnal nitrous oxide fluxes in the eastern tropical North Atlantic Ocean, *Biogeosciences*, 9(3), 957–964, doi:10.5194/bg-9-957-2012, 2012.
- 845 Laruelle, G. G., Cai, W.-J., Hu, X., Gruber, N., Mackenzie, F. T. and Regnier, P.: Continental shelves as a variable but increasing global sink for atmospheric carbon dioxide., *Nat. Commun.*, 9(1), 454, doi:10.1038/s41467-017-02738-z, 2018.
- 845 M. M. Zweng, Reagan, J. R., Seidov, D., Boyer, T. P., Locarnini, R. A., Garcia, H. E., Mishonov, A. V., Baranova, O. K., Weathers, K., Paver, C. R. and Smolyar, I.: WORLD OCEAN ATLAS 2018 Volume 2: Salinity (pre-release). [online] Available from: <http://www.nodc.noaa.gov/> (Accessed 26 March 2019), 2018.
- 850 McKenna, S. P. and Bock, E. J.: Physicochemical effects of the marine microlayer on air-sea gas transport, in *Marine Surface Films*, pp. 77–91, Springer-Verlag, Berlin/Heidelberg., 2006.
- 855 Mesarchaki, E., Kräuter, C., Krall, K. E., Bopp, M., Helleis, F., Williams, J. and Jähne, B.: Measuring air–sea gas-exchange velocities in a large-scale annular wind–wave tank, *Ocean Sci.*, 11(1), 121–138, doi:10.5194/os-11-121-2015, 2015.
- 860 Nightingale, P. D., Malin, G., Law, C. S., Watson, A. J., Liss, P. S., Liddicoat, M. I., Boutin, J. and Upstill-Goddard, R. C.: In situ evaluation of air-sea gas exchange parameterizations using novel conservative and volatile tracers, *Global Biogeochem. Cycles*, 14(1), 373–387, doi:10.1029/1999GB900091, 2000.
- 865 Pereira, R., Schneider-Zapp, K. and Upstill-Goddard, R. C.: Surfactant control of gas transfer velocity along an offshore coastal transect: results from a laboratory gas exchange tank, *Biogeosciences*, 13(13), 3981–3989, doi:10.5194/bg-13-3981-2016, 2016.
- 865 Pereira, R., Ashton, I., Sabbaghzadeh, B., Shutler, J. D. and Upstill-Goddard, R. C.: Reduced air–sea CO₂ exchange in the Atlantic Ocean due to biological surfactants, *Nat. Geosci.*, 11(7), 492–496, doi:10.1038/s41561-018-0136-2, 2018.
- 870 Ravishankara, A. R., Daniel, J. S. and Portmann, R. W.: Nitrous oxide (N₂O): the dominant ozone-depleting substance emitted in the 21st century., *Science*, 326(5949), 123–5, doi:10.1126/science.1176985, 2009.
- 875 Reynolds, R. W., Smith, T. M., Liu, C., Chelton, D. B., Casey, K. S. and Schlax, M. G.: Daily High-Resolution-Blended Analyses for Sea Surface Temperature, *J. Clim.*, 20(22), 5473–5496, doi:10.1175/2007JCLI1824.1, 2007.
- 880 Rödenbeck, C., Bakker, D. C. E., Gruber, N., Iida, Y., Jacobson, A. R., Jones, S., Landschützer, P., Metzl, N., Nakaoka, S., Olsen, A., Park, G.-H., Peylin, P., Rodgers, K. B., Sasse, T. P., Schuster, U., Shutler, J. D., Valsala, V., Wanninkhof, R. and Zeng, J.: Data-based estimates of the ocean carbon sink variability - First results of the Surface Ocean pCO₂ Mapping intercomparison (SOCOM), *Biogeosciences*, 12(23), 7251–7278, doi:10.5194/bg-12-7251-2015, 2015.
- 885 Rutgersson, A.: Time series of physical oceanography and carbon dioxide measurements at mooring site OSTERGARNSHOLM - 77FS20150128, PANGAEA, doi:10.1594/PANGAEA.878531, 2017.
- 885 Salter, M. E., Upstill-Goddard, R. C., Nightingale, P. D., Archer, S. D., Blomquist, B., Ho, D. T., Huebert, B., Schlosser, P. and Yang, M.: Impact of an artificial surfactant release on air-sea gas fluxes

- during Deep Ocean Gas Exchange Experiment II, *J. Geophys. Res.*, 116(C11), C11016, doi:10.1029/2011JC007023, 2011.
- 890 Schuster, U.: Underway physical oceanography and carbon dioxide measurements during Benguela Stream cruise 642B20131005, PANGAEA, doi:10.1594/PANGAEA.852980, 2016.
- 895 Shutler, J. D., Land, P. E., Piolle, J. F., Woolf, D. K., Goddijn-Murphy, L., Paul, F., Girard-Ardhuin, F., Chapron, B. and Donlon, C. J.: FluxEngine: A flexible processing system for calculating atmosphere-ocean carbon dioxide gas fluxes and climatologies, *J. Atmos. Ocean. Technol.*, 33(4), 741–756, doi:10.1175/JTECH-D-14-00204.1, 2016.
- 900 Shutler, J. D., Wanninkhof, R., Nightingale, P. D., Woolf, D. K., Bakker, D. C., Watson, A., Ashton, I., Holding, T., Chapron, B., Quilfen, Y., Fairall, C., Schuster, U., Nakajima, M. and Donlon, C. J.: Satellites will address critical science priorities for quantifying ocean carbon, *Front. Ecol. Environ.*, fee.2129, doi:10.1002/fee.2129, 2019.
- 905 Steinhoff, Tobias; Becker, Meike; Körtzinger, A.: Underway physical oceanography and carbon dioxide measurements during Atlantic Companion cruise 77CN20131004, PANGAEA, doi:10.1594/PANGAEA.852786, 2016.
- 910 Takahashi, T., Sutherland, S. C., Wanninkhof, R., Sweeney, C., Feely, R. A., Chipman, D. W., Hales, B., Friederich, G., Chavez, F., Sabine, C., Watson, A., Bakker, D. C. E., Schuster, U., Yoshikawa-Inoue, H., Ishii, M., Midorikawa, T., Nojiri, Y., Körtzinger, A., Steinhoff, T., Hoppema, M., Olafsson, J., Arnarson, T. S., Johannessen, T., Olsen, A., Bellerby, R., Wong, C. S., Delille, B., Bates, N. R. and de Baar, H. J. W.: Climatological mean and decadal change in surface ocean pCO₂, and net sea-air CO₂ flux over the global oceans, *Deep Sea Res. Part II Top. Stud. Oceanogr.*, 56(8–10), 554–577, doi:10.1016/J.DSR2.2008.12.009, 2009.
- 915 Tarran, G.: AMT 28 Cruise Report. [online] Available from: https://amt-uk.org/getattachment/Cruises/AMT28/AMT_28_CRUISE_REPORT_RS.pdf, 2018.
- 920 Wanninkhof, Rik; Pierrot, D.: Underway physical oceanography and carbon dioxide measurements during REYKJAFLOSS cruise 64RJ20131017, PANGAEA, doi:10.1594/PANGAEA.866092, 2016.
- Wanninkhof, R.: Relationship between wind speed and gas exchange over the ocean, *J. Geophys. Res.*, 97(C5), 7373, doi:10.1029/92JC00188, 1992.
- 925 Wanninkhof, R.: Relationship between wind speed and gas exchange over the ocean revisited, *Limnol. Oceanogr. Methods*, 12(6), 351–362, doi:10.4319/lom.2014.12.351, 2014.
- WAVEWATCH III development group: User manual and system documentation of WAVEWATCH III version 5.16, Technical Note 329., 2016.
- 930 Woolf, D. K., Land, P. E., Shutler, J. D., Goddijn-Murphy, L. M. and Donlon, C. J.: On the calculation of air-sea fluxes of CO₂ in the presence of temperature and salinity gradients, *J. Geophys. Res. Ocean.*, 121(2), 1229–1248, doi:10.1002/2015JC011427, 2016.
- 935 Woolf, D. K., Shutler, J. D., Goddijn-Murphy, L., Watson, A. J., Chapron, B., Nightingale, P. D., Donlon, C. J., Piskozub, J., Yelland, M. J., Ashton, I., Holding, T., Schuster, U., Girard-Ardhuin, F., Grouazel, A., Piolle, J. -F., Warren, M., Wrobel-Niedzwiecka, I., Land, P. E., Torres, R., Prytherch, J., Moat, B., Hanafin, J., Ardhuin, F. and Paul, F.: Key Uncertainties in the Recent Air-Sea Flux of CO₂, *Global Biogeochem. Cycles*, 0–3, doi:10.1029/2018gb006041, 2019.
- 940 Wrobel, I.: Monthly dynamics of carbon dioxide exchange across the sea surface of the Arctic Ocean in response to changes in gas transfer velocity and partial pressure of CO₂ in 2010, *Oceanologia*, 59(4), 445–459, doi:10.1016/J.OCEANO.2017.05.001, 2017.
- 945 Wrobel, I. and Piskozub, J.: Effect of gas-transfer velocity parameterization choice on air-sea CO₂ fluxes in the North Atlantic Ocean and the European Arctic, *Ocean Sci.*, 12(5), 1091–1091, 2016.
- 950 Zappa, C. J., McGillis, W. R., Raymond, P. A., Edson, J. B., Hints, E. J., Zemmleink, H. J., Dacey, J. W. H. and Ho, D. T.: Environmental turbulent mixing controls on air-water gas exchange in marine and aquatic systems, *Geophys. Res. Lett.*, 34(10), L10601, doi:10.1029/2006GL028790, 2007.
- Zhao, D., Jia, N. and Dong, Y.: Relationship between turbulent energy dissipation and gas transfer

